Sampling and Analysis for the Lake Tahoe Atmospheric Deposition Study

Final Report

M.-C. Oliver Chang
Judith C. Chow
Steven Kohl
Hal Voepel
John G. Watson

Presented to:

Research Division, California Air Resources Board
1001 I Street
Sacramento, CA 95814

June 1, 2005

TABLE OF CONTENTS

LIST OF TABLES

LIST OF FIGURES

EXECUTIVE SUMMARY

The Lake Tahoe Atmospheric Deposition Study (LTADS) is a multi-agency sampling effort to improve the quality of the Lake Tahoe by identifying and quantifying the sources that contribute to its decrease in clarity. The California Air Resources Board (CARB) initiated the LTADS in 2002 to quantify the contribution of atmospheric deposition to the declining clarity of Lake Tahoe. The initial study design included two major components: 1) a monitoring network in the Lake Tahoe Basin and 2) special studies, was described in a June 10, 2002 draft work plan by the CARB for LTADS.

CARB designed the monitoring network and measurement matrix for ambient particulate matter (PM) to provide information on the spatial variations around the lake and upwind of the basin for one year. Two types of samplers for PM were deployed in this study. The Two Week Sampler (TWS) for total suspended particulates (TSP), PM_{10}, and $PM_{2.5}$ (particles with aerodynamic diameters less than 10 and 2.5 micrometers [μm], respectively) were installed at five cornerstone sites: Big Hill (BH), Sandy Way (SW), Lake Forest (LF), Thunderbird Lodge (TB), and South Lake Tahoe (SOLA), to avoid problems associated with episodic sampling. In addition, the MiniVol samplers were used to acquire TSP samples at remote/satellite sites with various sampling durations.

During the LTADS, Desert Research Institute (DRI) coordinated the shipping and receiving of sampling media with the CARB site operators. TWS and MiniVol sampling cartridges were sent on a regular schedule to and from the DRI Environmental Analysis Facility (EAF). The DRI field coordinator participated in monthly conference calls with CARB investigators to ensure the smooth operation of field sampling.

Collected TSP, PM_{10}, and $PM_{2.5}$ samples were gravimetrically analyzed for total mass concentration, followed by detailed chemical speciation. A total of 127, 129, and 128 sets of TWS samples were collected for TSP, PM_{10}, and $PM_{2.5}$, respectively; 36 sets of buoy MiniVol TSP samples, and 160 sets of non-buoy MiniVol TSP samples were collected in LTADS. Replicate analysis was performed on 10% of the ambient samples.

Field blanks were applied to subtract passive deposition before, during, and after field sampling; however, field blanks were only collected at SOLA for 10% of the ambient samples and three field blanks were collected for non-buoy MiniVol TSP samples. The limited and site specific field blanks may affect the results of the ambient samples.

The chemical data were evaluated for internal consistency by examining the physical consistency and balance of reconstructed mass, based on chemical species versus measured mass. In general, the samples collected met the criteria of internal physical consistency. A few TWS samples were suspected to be outliers; however, no field flag was noted for these samples (with the exception of one laboratory flag).

The annual average mass concentrations and chemical composition were highest in TSP and lowest in $PM_{2.5}$ at each site; however, such physical consistency was not necessarily observed for TWS samples during the same sampling period. Such sampling bias can be attributed to the low TWS sampling flow rate of 1.3 liters per minute (LPM), low mass concentration of ambient PM,

random bouncing and penetration of particles larger than the 50% cutpoint of the sampling inlet, long sampling duration, and sampling artifacts of semi-volatile species.

Scatter plots showed that MiniVol samples were poorly correlated spatially and temporally; therefore, temporal and spatial variations were only examined for TWS samples. The highest annual average TSP (21.9 $\mu g/m^3$) and PM_{10} (18.8 $\mu g/m^3$) mass concentrations were observed at the SOLA site and the highest annual average $PM_{2.5}$ mass concentration (9.0 $\mu g/m^3$) was observed at the SW site. The lowest TSP, PM_{10}, and $PM_{2.5}$ mass concentration were 6.2, 6.0, and 3.6 $\mu g/m^3$, respectively, at the TB site. Similar annual averages of organic carbon (OC), elemental carbon (EC), ammonium (NH_4NO_3), and sulfate ($SO_4^=$) in TSP, PM_{10}, and $PM_{2.5}$ were observed, suggesting that these species are mainly present in the $PM_{2.5}$ fractions. PM_{10} mass comprised 80-90% of TSP mass and was approximately twice that of $PM_{2.5}$ mass. The most abundant chemical species were OC (16.5-29.8%), silicon (10.8-16.0%), and aluminum (3.9-4.7%) for TSP; OC (16.2-27.8%), silicon (10.0-21.1%), and aluminum (3.5-6.6%) for PM_{10}; and OC (42.1-52.0%), EC (4.9-16.4%), and ammonium (3.1-5.8%) for $PM_{2.5}$.

The lowest TWS TSP, PM_{10}, and $PM_{2.5}$ mass concentrations were observed from March to April 2003 at all five sites. TWS TSP, PM_{10}, and $PM_{2.5}$ mass concentrations observed at the BH, LF and TB sites from May to October 2003 were twice as high as those observed from November 2002 to February 2003; however, TWS TSP, PM_{10}, and $PM_{2.5}$ mass concentrations were comparable during these two periods at the SW and SOLA sites. The elevated TWS TSP, PM_{10}, and $PM_{2.5}$ mass concentrations at the SW and SOLA sites from November 2002 to February 2003 were due to elevated OC and EC concentrations, which were likely the result of increased traffic, sanding, and woodburning associated with winter activities in the Lake Tahoe region.

1. INTRODUCTION

The Lake Tahoe Atmospheric Deposition Study (LTADS) is a multi-agency sampling effort to improve the quality of the Lake Tahoe by identifying and quantifying the sources that contribute to its decrease in clarity. Improved estimates of atmospheric deposition are needed for input into water quality models that will be used to develop Total Maximum Daily Loads required under the federal Clean Water Act.

The initial study design is described in a draft workplan for the LTADS dated June 10, 2002. To avoid problems associated with episodic sampling contributed from specific sources, the California Air Resources Board (CARB) developed a particulate monitoring program for LTADS using Two Week Samplers (TWS) and Airmetrics MiniVol samplers. TWS provide two week integrated samples of ammonia (NH_3), nitric acid (HNO_3), total suspended particles (TSP), PM_{10}, and $PM_{2.5}$ (particles with aerodynamic diameters less than 10 and 2.5 micrometers [µm], respectively) at "cornerstone" sites for one year. MiniVol samplers were used to collect TSP at various remote/satellite sites. Collected TSP, PM_{10}, and $PM_{2.5}$ samples were gravimetrically analyzed for total mass concentration, followed by chemical speciation.

The site locations for the TWS and MiniVol samplers are shown in Figure 1-1 and summarized in Table 1-1. A total of five sites were instrumented with the TWS samplers and twelve sites were instrumented with MiniVol samplers. The TWS site at Big Hill (BH), located southwest of the Lake Tahoe Air Basin, was selected as an indicator site of potential pollutant transport. The remaining TWS sites, Lake Forest (LF), Thunderbird Lodge (TB), South Lake Tahoe (SOLA), and South Lake Tahoe - Sandy Way (SW), were located around the lake and within the Tahoe Basin. Development of site selections and sampling logistics were described in the CARB report (California Environmental Protection Agency, 2005).

In general, SOLA was a shoreline site in South Lake Tahoe proximate to Highway 50. When off-shore winds were in effect, SOLA was substantially affected by emissions from Highway 50 and the surrounding urban regions of South Lake Tahoe. SW was an urban site situated within the urban region south of Highway 50 and roughly 200 meters away from SOLA. When the winds were on-shore, SW was affected by emissions from Highway 50, and when the winds were off-shore, SW was affected by composite emissions of urban South Lake Tahoe. LF was a shoreline site in the northwest Tahoe basin, a short distance from Tahoe City and proximate to Highway 89. When the wind was off-shore, LF was affected by highway emissions, but when the wind was on-shore, LF was affected by lake-wide emissions. Prevailing regional flow is from the southwest and tends to deliver local emissions from South Lake Tahoe across the lake toward the north and northwest. Southwest regional flow may also carry local emissions from LF east towards mid-lake and TB.

Table 1-1. Description of sites for TWS and MiniVol TSP samplers (from the California Air Resource Board)

Lake Tahoe Atmospheric Deposition Study (LTADS) Two Week Sampler (TWS) and Mini Volume Sampler Network Locations

Site Name	Geography	Lakeshore Distance	Network	Size Cuts	Duration
Lake Forest (LF)	Tahoe City North Lake Shore	20 meters S from Hwy 28	TWS	TSP, PM10, PM2.5	14 Days
Thunderbird	East Lake Shore - Distant from Hwy 28	Elephant House 10 meters E	TWS	TSP, PM10, PM2.5	14 Days
SOLA	South Lake Tahoe, South Lake Shore	30 meters N from Hwy 50	TWS	TSP, PM10, PM2.5	14 Days
Sandy Way	South Lake Tahoe, South Lake Inland	40 meters S from Hwy 50	TWS	TSP, PM10, PM2.5	14 Days
Big HIll	Outside the Basin Near Loon Lake	40 kilometers SW of DL Bliss	TWS	TSP, PM10, PM2.5	14 Days
Coast Guard Pier	Tahoe City North Lake Shore	Pier 200 meters SSE from LF	MiniVol	TSP	7 Days
Zephyr Cove	Zephyr Cove Marina, East Lake Shore	Pier 200 meters W from Hwy 50	MiniVol	TSP	7 Days
Bliss State Park	West Lake Shore Inland Mountain	20 meters W from Hwy 89	MiniVol	TSP	7 Days
Wallis Residence Tower	West Lake Shore	20 meters E from Hwy 89	MiniVol	TSP	7 Days
Wallis Residence Pier	West Lake Shore	Pier 50 meters E from Tower	MiniVol	TSP	7 Days
Timber Cove	South Lake Tahoe, South Lake Shore	Pier 200 meters N from SOLA	MiniVol	TSP	2 Days
Buoy TB1 East	Mid Lake North East	-	MiniVol	TSP	1 Day
Buoy TB4 West	Mid Lake North West	-	MiniVol	TSP	1 Day

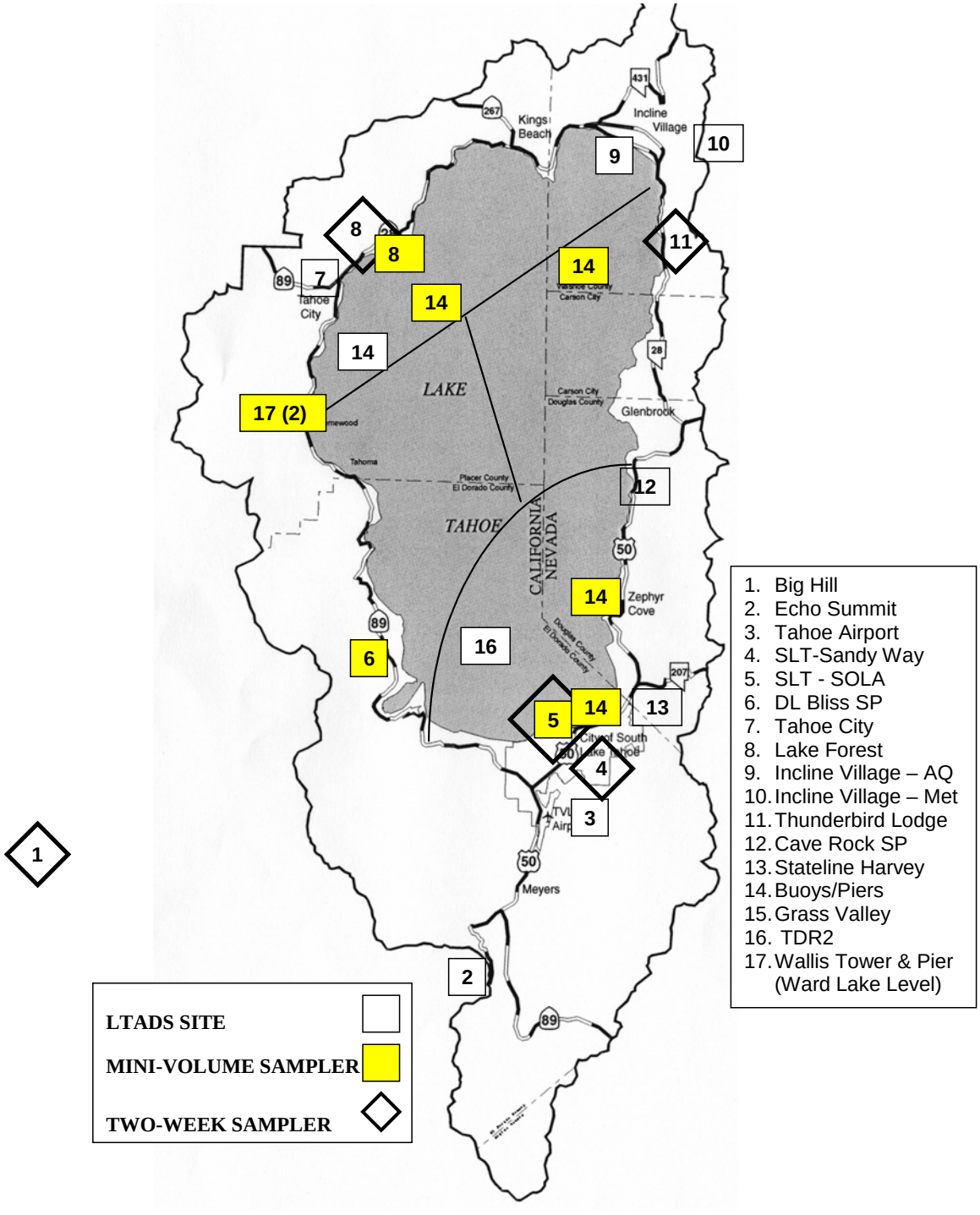

Figure 1-1 Site locations for TWS and MiniVol samplers during the Lake Tahoe Atmospheric Deposition Study (LTADS) (from California Air Resource Board).

During the LTADS, DRI coordinated the shipping and receiving of sampling media with the CARB site operators. TWS and MiniVol sampling cartridges were sent on a regular schedule to and from the DRI Environmental Analysis Facility (EAF). The DRI field logistics coordinator participated in monthly conference calls with CARB investigators to ensure the smooth operation of field sampling.

CARB and the Tahoe Regional Planning Agency (TRPA) selected the sampling locations and provided power and necessary accessories at the sampling sites. The TWS were maintained by CARB personnel and the MiniVol samplers were maintained by CARB, Tahoe Research Group (TRG), and Lahontan Regional Water Quality Control Board (LRWQCB) personnel. Generally, whenever a MiniVol sampler malfunctioned, it was immediately replaced with a spare and the problematic sampler was shipped to the DRI Reno, NV laboratory facilities for repair. This process minimized sampler downtimes and ensured high data recovery. DRI also provided additional MiniVol samplers for use in sampling outside the scope of work for the LTADS (e.g., Bio-available phosphorous sampling). The DRI laboratory coordinator ensured that adequate filter media were available at all times for site operators.

Section 2 describes the preparation, quality assurance, quality control, and chemical analyses methods for TWS and MiniVol samples. The database management and data validation are explained in Section 3. Section 4 presents and discusses the temporal and spatial distributions determined from the TWS data. Section 5 summaries and discusses the findings and observation from the LTADS. References are provided in Section 6. Standard operating procedures (SOPs) for laboratory operations are assembled in Appendix A.

2. SAMPLE PREPARATION, SHIPMENT, RECEIVING, AND ANALYSIS

2.1 Sample Preparation

2.1.1 Configurations of TWS and MiniVol samplers in the Lake Tahoe Atmospheric Deposition Study (LTADS)

Filter-based measurements of atmospheric pollutants were obtained using two types of samplers: Two Week Samplers (TWS) and Airmetrics MiniVol samplers. The TWS were nominally operated for two-week durations and collected integrated samples representing total suspended particulate (TSP), PM_{10} and $PM_{2.5}$, and nitric acid and ammonia via denuder measurements. The TWS were operated at a nominal flow rate of 1.3 liters per minute (LPM) from 11/20/02 to 01/06/04 at five sites chosen by the CARB.

The MiniVol samplers were equipped with TSP inlets and stationed on lake buoys and on land (non-buoys). Buoy samplers operated for the duration of the sampler battery (typically 24 hours) and the duration of the non-buoy sampler operation varied depending on the availability of AC power (~24 hours on batteries and generally ~1 week with an AC power source). The MiniVol samplers were operated at a nominal flow rate of 5.0 LPM from 09/26/02 to 04/26/04.

Each TWS had eight channels: three channels contained Teflon-membrane filters to measure TSP, PM_{10} and $PM_{2.5}$ mass and elements; three channels contained quartz filters to measure TSP, PM_{10}, and $PM_{2.5}$ ions and carbon; and two channels were used to collect ammonia and nitric acid denuder samples. MiniVol samplers were run in pair, where one sampler contained a Teflon-membrane filter and the other contained a quartz-fiber filter. All sampling media collected by the TWS and MiniVol samplers were prepared and chemically analyzed by the DRI/EAF.

2.1.2 Sampling media

Teflon-membrane filters were equilibrated for weighing after passing acceptance testing by X-ray fluorescence (XRF). Initial weights were performed after the filters equilibrated for a minimum of four weeks. A minimum of two filters per lot (approximately 100 filters per lot) received from the manufacturer were analyzed for chemical species to verify that pre-established specifications had been met. The lot was rejected if the verification filters did not pass this acceptance test. Each filter was individually examined over a light table prior to use for discoloration, pinholes, creases, or other defects. In addition to laboratory blanks, 5 to 10% of all filters were designated as field blanks per standard operating procedures (SOP).

Quartz-fiber filters absorb organic gases from ambient air and organic artifacts from the manufacturing process. By pre-firing the quartz-fiber filters, these absorbed gases and artifacts are reduced to constant, insignificant levels. The filters were pre-fired in preparation for thermal/optical reflectance carbon (TOR) analysis, following the Interagency Monitoring of Protected Visual Environments (IMPROVE) protocol (Chow et al., 1993); therefore, the filters were pre-fired at 900 °C to remove all possible TOR analysis interferences. Sets of filters with levels that exceeded 1.5 $\mu g/cm^2$ for organic carbon (OC) and 0.5 $\mu g/cm^2$ for elemental carbon (EC) were re-fired or rejected. Pre-fired filters were sealed and stored in a freezer prior to preparation for field sampling.

Cellulose fiber filters were impregnated with a solution of sodium chloride (5% NaCl, 5% glycerol and 90% distilled deionized water [DDW]) and used for the collection of volatilized nitrate. These filters were prepared in batches and subjected to acceptance testing prior to use in accordance with DRI SOP #2-104.3 (see Appendix A.1).

Filter packs for the TWS were prepared in accordance with the CARB SOP for TWS. Glass denuders were coated and handled according to the CARB SOP for TWS. Filter packs for the MiniVol samplers were prepared in accordance with DRI's SOP # 2-110.4 (see Appendix A.2).

2.1.3 Sample shipping and receiving

The TWS filter packs were packaged and shipped to two locations for deployment. Filter packs for the LF and BH sites were shipped to the CARB in Sacramento, CA; filter packs for the SOLA, TB, and SW sites were shipped to LRWQCB in South Lake Tahoe, CA. Filter packs were sealed in large, recloseable bags (with the site marked on the outside of each bag).

MiniVol sampler filter packs were packaged and shipped to two locations for deployment at the request of the operator. Due to sampler variation, two types of holders were deployed. The filters for use with the CARB MiniVol samplers were loaded into blue cassettes. The buoy filters were shipped to TRG in Tahoe City, CA, and the others were shipped to the CARB Monitoring and Laboratory Division in Sacramento, CA. The filters for use with the DRI MiniVol samplers were loaded into nucleopore holders and shipped to the LRWQCB, South Lake Tahoe, CA, and the CARB Monitoring and Laboratory Division in Sacramento, CA. MiniVol sampler filter packs were sealed in recloseable bags with a field data sheet for each set of filters (paired Teflon-membrane and quartz-fiber filter packs).

All filter packs were placed in coolers refrigerated with blue ice for shipment. The coolers were then shipped by second-day service for arrival by Tuesday of the designated sample change-out week. Entries of the shipment and the sample ID of the filter packs were made in the DRI/EAF shipping logbook.

2.2 Analysis Methods

2.2.1 Mass by gravimetric analysis

Unexposed and exposed Teflon-membrane filters were equilibrated at a temperature of 21.5 ± 1.5 °C and a relative humidity (RH) of 35 ± 5% for a minimum of 24 hours prior to weighing (Chow et al 2005). Weighing was performed on a Mettler MT-5 electro microbalance with ±0.001 mg sensitivity. The charge on each filter was neutralized by exposure to a polonium-210 source for 30 seconds before the filter was placed on the balance pan. The balance was calibrated with a 200 mg Class S weight and the tare was set prior to weighing each batch of filters. After every 10 filters were weighed, the calibration and tare were re-checked. If the results of these performance tests deviated from specifications by more than ±5 (µg), the balance was re-calibrated.

All initial filter weights were checked by an independent technician. Samples were re-weighed if these check-weights did not agree with the original weights within ±0.010 mg. At least 30% of the exposed filter weights were checked by an independent technician. Samples were re-weighed if these check-weights did not agree with the original weights within ±0.015 mg. Pre- and post-

weights, check weights, and re-weights (if required) were recorded on data sheets and directly entered into a data base via an RS232 connection. All weights were entered by filter number into the DRI aerosol data base. Gravimetric analysis is detailed in DRI SOP # 2-102.5 (see Appendix A.3).

2.2.2 Elements by X-ray fluorescence (XRF) analysis

After gravimetric analysis, a Kevex model 700 energy dispersive X-ray fluorescence analyzer (EDXRF) (Watson, et al, 1999) was used to quantify sodium (Na), magnesium (Mg), aluminum (Al), silicon (Si), phosphorus (P), sulfur (S), chlorine (Cl), potassium (K), calcium (Ca), titanium (Ti), vanadium (V), chromium (Cr), manganese (Mn), iron (Fe), cobalt (Co), nickel (Ni), copper (Cu), zinc (Zn), gallium (Ga), arsenic (As), selenium (Se), bromine (Br), rubidium (Rb), strontium (Sr), yttrium (Y), zirconium (Zr), molybdenum (Mo), palladium (Pd), silver (Ag), cadmium (Cd), indium (In), tin (Sn), antimony (Sb), barium (Ba), gold (Au), mercury (Hg), thallium (Tl), lead (Pb), lanthanum (La), and uranium (U) on Teflon-membrane samples.

Calibration was performed using thin film standards from Micromatter Inc. (Deer Harbor, WA). A multi-element thin film standard was analyzed with each run to monitor for calibration drift and was used as the indicator for routine calibrations.

Elemental analysis by EDXRF is detailed in DRI SOP # 2-205.2 (see Appendix A.4).

2.2.3 Organic and elemental carbon by thermal/optical analysis

The thermal/optical reflectance (TOR) method measures total carbon (TC), OC and EC. The TOR method is based on the principle that different types of carbon-containing particles are converted to gases under designated temperature and oxidation conditions. The different carbon fractions from TOR are useful for comparison with other methods that are specific to a single definition for OC and EC. These specific carbon fractions also help to distinguish between seven carbon fractions reported by TOR, following the IMPROVE protocol (Chow, et al, 1993):

- The carbon evolved in a helium (He) atmosphere at temperatures between ambient (~25 °C) and 120 °C (OC1)
- The carbon evolved in a He atmosphere at temperatures between 120 °C and 250 °C (OC2)
- The carbon evolved in a He atmosphere at temperatures between 250 °C and 450 °C (OC3)
- The carbon evolved in a He atmosphere between 450 °C and 550 °C (OC4)
- The carbon evolved in an oxidizing atmosphere at 550 °C (EC1)
- The carbon evolved in an oxidizing atmosphere between 550 °C and 700 °C (EC2)
- The carbon evolved in an oxidizing atmosphere between 700 °C and 800 °C (EC3)

The thermal/optical reflectance carbon analyzer consists of a thermal system and an optical system. The thermal system consists of a quartz tube placed inside a coiled heater. Current through the heater is controlled to attain and maintain pre-set temperatures for given time periods. A portion of a quartz-fiber filter is placed in the heating zone and heated to designated temperatures under non-oxidizing and oxidizing atmospheres. The optical system consists of a He-Ne laser, a fiber optic transmitter and receiver, and a photocell. The filter deposit faces a

quartz light tube so that the intensity of the reflected laser beam can be monitored throughout the analysis.

As the temperature is increased from ambient (~25 °C) to 550 °C in a non-oxidizing He atmosphere, OC compounds are volatilized from the filter while EC is not oxidized. When oxygen (O_2) is added to the He at temperatures greater than 550 °C, the EC burns and enters the sample stream. The evolved gases pass through an oxidizing bed of heated manganese dioxide, where they are oxidized to carbon dioxide (CO_2), and then across a heated nickel catalyst that reduces the CO_2 to methane (CH_4). The CH_4 is then quantified with a flame ionization detector (FID).

The reflected laser light is continuously monitored throughout the analysis cycle. The negative change in reflectance is proportional to the degree of pyrolytic conversion from OC to EC that occurs during OC analysis. After O_2 is introduced, the reflectance increases rapidly as the light-absorbing carbon is burned off of the filter. The carbon measured after the reflectance attains the value it had at the beginning of the analysis cycle is classified as EC. This adjustment for pyrolysis can be as high as 25% of OC or EC and therefore cannot be ignored.

The instrument was calibrated by analyzing samples of known amounts of CH_4, CO_2 and potassium hydrogen phthalate (KHP). The FID response was compared to a reference level of CH_4 injected at the end of each sample analysis. Performance tests of the instrument's calibration were conducted at the beginning and end of each day's operation. Intervening samples were re-analyzed when calibration changes greater than ±10% are found.

Known amounts of American Chemical Society (ACS) certified reagent grade crystal sucrose and KHP were committed to TOR as a verification of the OC fractions. Fifteen different standards were used for each calibration; however, widely accepted primary standards for EC and OC are still lacking. Results of the TOR analysis of each filter were entered into the DRI data base.

Carbon analysis is detailed in DRI SOP # 2-204.6 (see Appendix A.5).

2.2.4 Inorganic ions

Water-soluble chloride, nitrate, sulfate, ammonium, sodium, magnesium, calcium, and potassium were obtained by extracting the quartz-fiber particle filter in 15 ml of DDW. The extraction vials were capped and sonicated for 60 minutes, shaken for 60 minutes, then aged overnight to assure complete extraction of the deposited material in the solvent. The ultrasonic bath water was monitored to prevent temperature increases from the dissipation of ultrasonic energy in the water. After extraction, these solutions were stored under refrigeration prior to analysis. Extraction procedures are detailed in DRI SOP # 2-109.5 (see Appendix A.6).

2.2.4.1 Anions (chloride, nitrate, phosphate, and sulfate) by ion chromatography

Water-soluble chloride (Cl^-), nitrate (NO_3^-), phosphate (PO_4^{3-})and sulfate ($SO_4^{=}$) were measured with the Dionex 2020i (Sunnyvale, CA) ion chromatograph (IC) (Chow and Watson, 1999). The IC uses an ion-exchange column to separate the sample ions in time for individual quantification by a conductivity detector. Prior to detection, the column effluent enters a suppressor column where the chemical composition of the component is altered and results in a matrix of low

conductivity. The ions are identified by their elution/retention times, and are quantified by the conductivity peak area. Approximately 2.0 ml of the filter extract are injected into the IC. The resulting peaks are integrated and the peak integrals are converted to concentrations using calibration curves derived from solution standards. The Dionex system for the analysis of Cl^-, NO_3^-, and $SO_4^=$ contains a guard column (AG4a column, Cat. No. #37042), an anion separator column (AS4a column, Cat. No. #37041) with a strong basic anion exchange resin, and an anion micro-membrane suppressor column (250 x 6 mm ID) with a strong acid ion exchange resin. The anion eluent consists of sodium carbonate (Na_2CO_3) and sodium bicarbonate ($NaHCO_3$) prepared in DDW. The DDW is verified to have a conductivity of less than 1.8 x 10-5 ohm/cm prior to preparation of the eluent. For quantitative determinations, the IC is operated at a flow rate of 2.0 mL per minute.

The primary standard solution containing NaCl, $NaNO_3$, and $(Na)_2SO_4$ were prepared with reagent-grade salts dried in an oven for one hour at 105 °C and then brought to room temperature in a desiccator. The anhydrous salts were weighed to the nearest 0.10 mg on a routinely calibrated analytical balance under controlled temperature (~20 °C) and RH (±30%). The salts were then diluted in precise volumes of DDW. Calibration standards were prepared at least once per month by diluting the primary standard solution to concentrations covering the range expected in the filter extracts. The standards were then stored in a refrigerator. Calibration concentrations of 0.1, 0.2, 0.5, 1.0, and 2.0 mg/ml were prepared or each of the analysis species.

Calibration curves were performed weekly. Chemical compounds were identified by matching the retention time of each peak in the unknown sample with the retention times of peaks in the chromatograms of the standards. A DDW blank was analyzed after every 20 samples and a calibration standard was analyzed after every 10 samples. These quality control checks verified the baseline and the calibration, respectively. Environmental Research Associates (ERA, Arvada, CO) standards were used daily as an independent quality assurance (QA) check. These standards (ERA Wastewater Nutrient and ERA Mineral WW) are traceable to the National Institute of Standards and Technology (NIST) simulated rainwater standards. If the values obtained for these standards did not coincide within a pre-specified uncertainty level (typically three standard deviations of the baseline level, or ±5%), the samples analyzed between that standard and the previous calibration standards were re-analyzed.

After analysis, the printout for each sample in the batch was reviewed for the following: 1) proper operational settings, 2) correct peak shapes and integration windows, 3) peak overlaps, 4) correct background subtraction, and 5) quality control sample comparisons. When values for replicates differed by more than ±10% or values for standards differed by more than ±5%, samples before and after these quality control checks were designated for re-analysis in a subsequent batch. Individual samples with unusual peak shapes, background subtractions, or deviations from standard operating parameters were also designated for re-analysis.

Water soluble nitrate and nitric acid concentrations were obtained from the cellulose backup filter and the nitric acid denuder, respectively, using the same IC analysis procedure. IC analysis procedures are detailed in DRI SOP # 2-203.5 (see Appendix A.7).

2.2.4.2 Ammonium by automated colorimetry

An Astoria 2 Automated Colorimetry (AC) system (Astoria–Pacific, Clackamas, OR) was used to measure ammonium concentrations by the indolphenol method. Each sample was mixed with reagents and subjected to appropriate reaction periods before submission to the colorimeter. Beer's Law relates the liquid's absorbency to the amount of the ion in the sample. A photomultiplier tube measured this absorbency through an interference filter specific to ammonium. Two ml of extract in a sample vial were placed in a computer-controlled autosampler. Calibration curves were produced with each daily batch of samples.

Ammonia concentrations from the citric acid denuders were determined using the same analysis method.

AC analysis procedures are detailed in DRI SOP # 2-207.5 (see Appendix A.8).

2.2.4.3 Soluble sodium and potassium by atomic absorption spectrometry

Soluble sodium, magnesium, potassium and calcium were measured using a Varian Spectra AA-880 atomic absorption spectrophotometer. In atomic absorption spectrophotometry, the sample is aspirated into a flame and atomized. A light beam from a hollow cathode lamp is directed through the flame into a monochromator, and then onto a photoelectric detector that measures the amount of light absorbed by the atomized element in the flame. The cathode of a hollow cathode lamp contains the pure metal which results in a line source emission spectrum. Since each element has its own characteristic absorption wavelength, the source lamp composed of that element is used. The amount of energy of the characteristic wavelength absorbed in the flame is proportional to the concentration of the element in the sample. Calibration curves were produced with each daily batch of samples.

AA analysis procedures are detailed in DRI SOP 2-206.3 (see Appendix A.9).

3. DATABASE MANAGEMENT AND DATA VALIDATION

This section evaluates the precision, accuracy, and validity of sampling and analysis for LTADS. Numerous air quality studies have been conducted over the past decade, but the data are not often available or applicable to analysis and modeling because the databases lack documentation with regard to sampling and analysis methods, quality control/quality assurance procedures, accuracy specifications, precision calculations, and data validity. Lioy et al. (1980), Chow and Watson (1989), Watson and Chow (1992), and Chow and Watson (1994) summarized the requirements, limitations, and current availability of ambient and source databases in the United States. The data sets for LTADS intend to meet these requirements. The data files for this study have the following attributes:

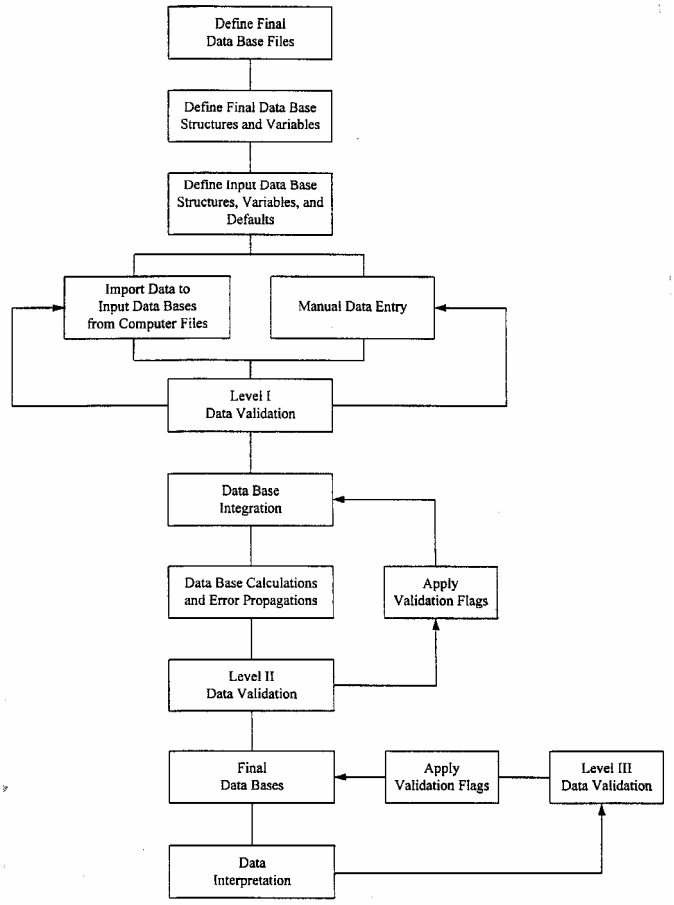

Figure 3-1. Flow diagram of the database management system.

- They contain the ambient observables needed to assess source and receptor relationships.
- They are available in a well-documented, computerized form accessible by personal computers and over the Internet.
- Measurement methods, locations, and schedules are documented.
- Precision and accuracy estimates are reported.
- Validation flags are assigned.

This section introduces the features, data structures, and contents of the LTADS data archive. Figure 3-1 illustrates the approach followed to obtain the final data files. Detailed data processing and data validation procedures are documented in Section 3.2. These data are available in Microsoft Excel format for convenient distribution to data users. The file extension identifies the file type according to the following definitions:

- TXT = ASCII text file
- DOC = Microsoft Word document
- XLS = Microsoft Excel spreadsheet

The assembled aerosol database for filter pack measurements taken during LTADS is fully described in the Microsoft Excel file (see Table 3-1), which documents variable names, descriptions, and measurement units.

Table 3-1. Variable names, descriptions, and measurement units in the assembled aerosol database for filter pack measurements taken during the study.

Field Code	Description	Measurement Unit
SITE	Sampling site	
DATE	Sampling date	
SIZE	Sample particle size cut	µm
DATEI	Sample start date	
DATEF	Sample end date	
TID	Teflon filter pack ID	
QID	Quartz filter pack ID	
TFFLG	Teflon filter pack field flag	
QFFLG	Quartz filter pack field flag	
MSGF	Gravimetry analysis flag	
NHCF	Ammonia analysis flag	
HNIF	Volatilized nitrate analysis flag	
ANIF	Anion analysis flag	
N4CF	Ammonium analysis flag	
KPAF	Soluble potassium analysis flag	
OETF	Carbon analysis flag	
ELXF	XRF analysis flag	
TVOC	Teflon filter volume	m^3
TVOU	Teflon filter volume uncertainty	m^3
QVOC	Quartz filter volume	m^3
QVOU	Quartz filter volume uncertainty	m^3
MSGC	Mass concentration	$\mu g/m^3$
MSGU	Mass concentration uncertainty	$\mu g/m^3$
NHCC	NH3 concentration	$\mu g/m^3$
NHCU	NH3 concentration uncertainty	$\mu g/m^3$
BKN3IC	Volatilized nitrate concentration	$\mu g/m^3$
BKN3IU	Volatilized nitrate concentration uncertainty	$\mu g/m^3$
CLIC	Chloride concentration	$\mu g/m^3$
CLIU	Chloride concentration uncertainty	$\mu g/m^3$
N2IC	Nitrite concentration	$\mu g/m^3$
N2IU	Nitrite concentration uncertainty	$\mu g/m^3$
N3IC	Nitrate concentration	$\mu g/m^3$
N3IU	Nitrate concentration uncertainty	$\mu g/m^3$
P4IC	Phosphate concentration	$\mu g/m^3$
P4IU	Phosphate concentration uncertainty	

Table 3-1. (continued)

Field Code	Description	Measurement Unit
S4IC	Sulfate concentration	µg/m^3
S4IU	Sulfate concentration uncertainty	µg/m^3
N4CC	Ammonium concentration	µg/m^3
N4CU	Ammonium concentration uncertainty	µg/m^3
NAAC	Soluble Sodium concentration	µg/m^3
NAAU	Soluble Sodium concentration uncertainty	µg/m^3
MGAC	Soluble Magnesium concentration	µg/m^3
MGAU	Soluble Magnesium concentration uncertainty	µg/m^3
KPAC	Soluble Potassium concentration	µg/m^3
KPAU	Soluble Potassium concentration uncertainty	µg/m^3
CAAC	Soluble Calcium concentration	µg/m^3
CAAU	Soluble Calcium concentration uncertainty	µg/m^3
O1TC	Organic Carbon fraction one concentration	µg/m^3
O1TU	OC fraction one concentration uncertainty	µg/m^3
O2TC	Organic Carbon fraction two concentration	µg/m^3
O2TU	OC fraction two concentration uncertainty	µg/m^3
O3TC	Organic Carbon fraction three concentration	µg/m^3
O3TU	OC fraction three concentration uncertainty	µg/m^3
O4TC	Organic Carbon fraction four concentration	µg/m^3
O4TU	OC fraction four concentration uncertainty	µg/m^3
OPTC	Pyrolyzed Organic carbon concentration	µg/m^3
OPTU	Pyrolyzed OC concentration uncertainty	µg/m^3
OCTC	Organic Carbon concentration	µg/m^3
OCTU	Organic Carbon concentration uncertainty	µg/m^3
E1TC	Elemental Carbon fraction one concentration	µg/m^3
E1TU	EC fraction one concentration uncertainty	µg/m^3
E2TC	Elemental Carbon fraction two concentration	µg/m^3
E2TU	EC fraction two concentration uncertainty	µg/m^3
E3TC	Elemental Carbon fraction three concentration	µg/m^3
E3TU	EC fraction three concentration uncertainty	µg/m^3
ECTC	Elemental Carbon concentration	µg/m^3
ECTU	Elemental Carbon concentration uncertainty	µg/m^3
TCTC	Total Carbon concentration	µg/m^3
TCTU	Total Carbon concentration uncertainty	µg/m^3
NAXC	Sodium concentration	µg/m^3
NAXU	Sodium concentration uncertainty	µg/m^3
MGXC	Magnesium concentration	µg/m^3
MGXU	Magnesium concentration uncertainty	µg/m^3
ALXC	Aluminum concentration	µg/m^3
ALXU	Aluminum concentration uncertainty	µg/m^3
SIXC	Silicon concentration	µg/m^3
SIXU	Silicon concentration uncertainty	µg/m^3
PHXC	Phosphorous concentration	µg/m^3
PHXU	Phosphorous concentration uncertainty	µg/m^3
SUXC	Sulfur concentration	µg/m^3

Table 3-1. (continued)

Field Code	Description	Measurement Unit
SUXU	Sulfur concentration uncertainty	$\mu g/m^3$
CLXC	Chlorine concentration	$\mu g/m^3$
CLXU	Chlorine concentration uncertainty	$\mu g/m^3$
KPXC	Potassium concentration	$\mu g/m^3$
KPXU	Potassium concentration uncertainty	$\mu g/m^3$
CAXC	Calcium concentration	$\mu g/m^3$
CAXU	Calcium concentration uncertainty	$\mu g/m^3$
TIXC	Titanium concentration	$\mu g/m^3$
TIXU	Titanium concentration uncertainty	$\mu g/m^3$
VAXC	Vanadium concentration	$\mu g/m^3$
VAXU	Vanadium concentration uncertainty	$\mu g/m^3$
CRXC	Chromium concentration	$\mu g/m^3$
CRXU	Chromium concentration uncertainty	$\mu g/m^3$
MNXC	Manganese concentration	$\mu g/m^3$
MNXU	Manganese concentration uncertainty	$\mu g/m^3$
FEXC	Iron concentration	$\mu g/m^3$
FEXU	Iron concentration uncertainty	$\mu g/m^3$
COXC	Cobalt concentration	$\mu g/m^3$
COXU	Cobalt concentration uncertainty	$\mu g/m^3$
NIXC	Nickel concentration	$\mu g/m^3$
NIXU	Nickel concentration uncertainty	$\mu g/m^3$
CUXC	Copper concentration	$\mu g/m^3$
CUXU	Copper concentration uncertainty	$\mu g/m^3$
ZNXC	Zinc concentration	$\mu g/m^3$
ZNXU	Zinc concentration uncertainty	$\mu g/m^3$
GAXC	Gallium concentration	$\mu g/m^3$
GAXU	Gallium concentration uncertainty	$\mu g/m^3$
ASXC	Arsenic concentration	$\mu g/m^3$
ASXU	Arsenic concentration uncertainty	$\mu g/m^3$
SEXC	Selenium concentration	$\mu g/m^3$
SEXU	Selenium concentration uncertainty	$\mu g/m^3$
BRXC	Bromine concentration	$\mu g/m^3$
BRXU	Bromine concentration uncertainty	$\mu g/m^3$
RBXC	Rubidium concentration	$\mu g/m^3$
RBXU	Rubidium concentration uncertainty	$\mu g/m^3$
SRXC	Strontium concentration	$\mu g/m^3$
SRXU	Strontium concentration uncertainty	$\mu g/m^3$
YTXC	Yttrium concentration	$\mu g/m^3$
YTXU	Yttrium concentration uncertainty	$\mu g/m^3$
ZRXC	Zirconium concentration	$\mu g/m^3$
ZRXU	Zirconium concentration uncertainty	$\mu g/m^3$
MOXC	Molybdenum concentration	$\mu g/m^3$
MOXU	Molybdenum concentration uncertainty	$\mu g/m^3$
PDXC	Palladium concentration	$\mu g/m^3$

Table 3-1. (continued)

Field Code	Description	Measurement Unit
PDXU	Palladium concentration uncertainty	$\mu g/m^3$
AGXC	Silver concentration	$\mu g/m^3$
AGXU	Silver concentration uncertainty	$\mu g/m^3$
CDXC	Cadmium concentration	$\mu g/m^3$
CDXU	Cadmium concentration uncertainty	$\mu g/m^3$
INXC	Indium concentration	$\mu g/m^3$
INXU	Indium concentration uncertainty	$\mu g/m^3$
SNXC	Tin concentration	$\mu g/m^3$
SNXU	Tin concentration uncertainty	$\mu g/m^3$
SBXC	Antimony concentration	$\mu g/m^3$
SBXU	Antimony concentration uncertainty	$\mu g/m^3$
BAXC	Barium concentration	$\mu g/m^3$
BAXU	Barium concentration uncertainty	$\mu g/m^3$
LAXC	Lanthanum concentration	$\mu g/m^3$
LAXU	Lanthanum concentration uncertainty	$\mu g/m^3$
AUXC	Gold concentration	$\mu g/m^3$
AUXU	Gold concentration uncertainty	$\mu g/m^3$
HGXC	Mercury concentration	$\mu g/m^3$
HGXU	Mercury concentration uncertainty	$\mu g/m^3$
TLXC	Thallium concentration	$\mu g/m^3$
TLXU	Thallium concentration uncertainty	$\mu g/m^3$
PBXC	Lead concentration	$\mu g/m^3$
PBXU	Lead concentration uncertainty	$\mu g/m^3$
URXC	Uranium concentration	$\mu g/m^3$
URXU	Uranium concentration uncertainty	$\mu g/m^3$
COMMENT	Sampling and/or analysis comments	

3.1 Database Structures and Features

The raw LTADS data were processed with Microsoft FoxPro 2.6 for Windows (Microsoft Corp., 1994), a commercially available relational database management system. FoxPro can accommodate 256 fields of up to 4,000 characters per record and up to one billion records per file. This system can be implemented on most IBM PC-compatible desktop computers. The database files (*.DBF) can also be read directly into a variety of popular statistical, plotting, database, and spreadsheet programs without requiring any specific conversion software. After processing, the final LTADS data were converted from FoxPro to Microsoft Excel format for reporting purposes.

In FoxPro, one of five field types (character, date, numerical, logical, or memo) was assigned to each observable. Sampling sites and particle size fractions were defined as “character” fields, sampling dates were defined as “date” fields, and measured data were defined as “numeric” fields, “logical” fields were used to represent a “yes” or “no” value applied to a variable, and “memo” fields accommodated large blocks of text and were used to document the data validation results.

Data contained in different database files can be linked by indexing on and relating to common attributes in each file. Generally, sampling site, sampling hour, sampling period, particle size, and sampling substrate IDs were the common fields used to relate the data between files.

To assemble the final data files, information was merged from many data files derived from field monitoring and laboratory analyses by relating information on the common fields cited above.

3.2 Measurement and Analytical Specifications

Every measurement consists of: 1) a value; 2) a precision; 3) an accuracy; and 4) a validity (Hidy, 1985; Watson et al., 1989, 1995). The measurement methods described in this section were used to obtain the value. Performance testing via regular submission of standards, blank analysis, and replicate analysis were used to estimate precision. These precisions were reported in the data files described in Section 3.1 so they could be propagated through air quality models and used to evaluate how well different values compare with one another. The submission and evaluation of independent standards through quality audits were used to estimate accuracy. Validity applied to both the measurement method and to each measurement taken with that method. The validity of each measurement was indicated by appropriate flagging within the database and the validity of the methods used in this study have been evaluated by tests described in Section 3.4.

3.2.1 Definitions of measurement attributes

The precision, accuracy, and validity of the LTADS aerosol measurements are defined as follows (Chow et al., 1993):

- A **measurement** is an observation at a specific time and place that possesses: 1) value – the center of the measurement interval; 2) precision – the width of the measurement interval; 3) accuracy – the difference between measured and reference values; and 4) validity – the compliance with assumptions made in the measurement method.
- A **measurement method** is the combination of equipment, reagents, and procedures that provides the value of a measurement. The full description of the measurement method requires substantial documentation. For example, two methods may use the same sampling systems and the same analysis systems; however, they are not identical if one method performs acceptance testing on the filter media and the other does not. Seemingly minor differences between methods can result in major differences in measurement values.
- **Measurement method validity** is the identification of measurement method assumptions, the quantification of the effects of deviations from those assumptions, the evaluation that deviations are within reasonable tolerances for the specific application, and the creation of procedures to quantify and minimize those deviations during a specific application.
- **Sample validation** is accomplished by procedures that identify deviations from measurement assumptions and the assignment of flags to individual measurements to indicate for potential deviations from assumptions.

- The **comparability and equivalence of sampling and analysis methods** are established by the comparison of values and precisions for the same measurement obtained by different measurement methods. Inter-laboratory and intra-laboratory comparisons are usually made to establish this comparability. Simultaneous measurements of the same observable are considered equivalent when more than 90% of the values differ by no more than the sum of two one-sigma precision intervals for each measurement.
- **Completeness** measures how many environmental measurements with specified values, precisions, accuracies, and validities were obtained out of the total number attainable. It measures the practicability of applying the selected measurement processes throughout the measurement period. Databases which have excellent precision, accuracy, and validity may be of little use if they contain so many missing values that data interpretation is impossible.

A database with numerous data points, such as the one used in this study, requires detailed documentation of precision, accuracy, and validity of the measurements. This section addresses the procedures followed to define these quantities and presents the results of those procedures.

3.2.2 Definitions of measurement precision

Measurement precisions were propagated from precisions of the volumetric measurements, the chemical composition measurements, and the field blank variability using the methods of Bevington (1969) and Watson et al. (1995). The following equations calculated the precision associated with filter-based measurements:

$$C_i = (M_i - B_i)/V \quad (3\text{-}1)$$

$$V = F \times t \quad (3\text{-}2)$$

$$B_i = \frac{1}{n}\sum_{j=1}^{n} B_{ij} \quad \text{for } B_i > \sigma_{Bi} \quad (3\text{-}3)$$

$$B_i = 0 \quad \text{for } B_i \le \sigma_{Bi} \quad (3\text{-}4)$$

$$\sigma_{Bi} = STD_{Bi} = \left[\frac{1}{n-1}\sum_{j=1}^{n}(B_{ij} - B_i)^2\right]^{1/2} \quad \text{for } STD_{Bi} > SIG_{Bi} \quad (3\text{-}5)$$

$$\sigma_{Bi} = SIG_{Bi} = \left[\frac{1}{n}\sum_{j=1}^{n}(\sigma_{Bij})^2\right]^{1/2} \quad \text{for } STD_{Bi} \le SIG_{4Bi} \quad (3\text{-}6)$$

$$\sigma_{Ci} = \left[\frac{\sigma_{Mi}^{\ 2} + \sigma_{Bi}^{\ 2}}{V^2} + \frac{\sigma_V^{\ 2}(M_i - B_i)^2}{V^4}\right]^{1/2} \quad (3\text{-}7)$$

$$\sigma_{RMS_i} = \left(\frac{1}{n}\sum_{j=1}^{n}\sigma_{Ci}^{\ 2}\right)^{1/2} \quad (3\text{-}8)$$

$$\sigma_V/V = 0.05 \quad (3\text{-}9)$$

where:

B_i = average amount of species i on field blanks
B_{ij} = the amount of species i found on field blank j
C_i = the ambient concentration of species i

F	=	flow rate throughout sampling period
M_i	=	amount of species i on the substrate
M_{ijf}	=	amount of species i on sample j from original analysis
M_{ijr}	=	amount of species i on sample j from replicate analysis
n	=	total number of samples in the sum
SIG_{Bi}	=	the root mean square error (RMSE), the square root of the averaged sum of the squared of σ_{Bij}.
STD_{Bi}	=	standard deviation of the blank
σ_{Bi}	=	blank precision for species i
σ_{Bij}	=	precision of the species i found on field blank j
σ_{Ci}	=	propagated precision for the concentration of species i
σ_{Mi}	=	precision of amount of species i on the substrate
σ_{RMS_i}	=	root mean square precision for species i
σ_V	=	precision of sample volume
t	=	sample duration
V	=	volume of air sampled

Dynamic field blanks were periodically placed in each sampling system without air being drawn through them to estimate the magnitude of passive deposition for the period of time during which the filter packs remained in a sampler. No statistically significant inter-site differences in field blank concentrations were found for any species after removal of outliers (i.e., concentration exceeding three times the standard deviations of the field blanks). The average field blank concentrations (with outliers removed) were calculated for each species on each substrate (e.g., Teflon-membrane, quartz-fiber), irrespective of the sites.

3.2.3 Analytical Specifications

Blank precisions (σ_{Bi}) are defined as the higher value of the standard deviation of the blank measurements (STD_{Bi}) or the square root of the averaged squared uncertainties of the blank concentrations (SIG_{Bi}). If the average blank for a species was less than its precision, the blank was set to zero (as shown in Equation 3-4). The precisions (σ_{Mi}) for XRF analysis were determined from counting statistics unique to each sample; therefore, the σ_{Mi} is a function of the energy-specific peak area, the background, and the area under the baseline.

3.3 Quality Assurance

Quality control (QC) and quality auditing establish the precision, accuracy, and validity of measured values. Quality assurance (QA) integrates QC, quality auditing, measurement method validation, and sample validation into the measurement process. The results of quality assurance are data values with specified precisions, accuracies, and validities.

For TWS, field blanks were only acquired at SOLA; and three field blanks were acquired for MiniVol samplers, as shown in Table 3-2. Replicate analyses were performed for ~10% of all ambient samples.

Table 3-2. Field blanks collected in the Lake Tahoe Atmospheric Deposition Study (LTADS)

SITE	Start Date	End Date	SIZE	PERIOD	Gravimetric Mass (µg/filter)	Uncertainty of Gravimetric Mass (µg/filter)
Two Week Samplers						
SOLA	12/4/2002	12/18/2002	TSP	2	21.00	4.92
SOLA	12/4/2002	12/18/2002	10	2	9.00	4.92
SOLA	12/4/2002	12/18/2002	2.5	2	1.00	4.92
SOLA	5/21/2003	6/4/2003	TSP	14	30.00	7.40
SOLA	2/21/2003	6/4/2003	10	14	5.00	7.40
SOLA	5/21/2003	6/4/2003	2.5	14	5.00	7.40
SOLA	7/16/2003	7/30/2003	TSP	18	8.00	7.98
SOLA	7/16/2003	7/30/2003	10	18	1.00	7.98
SOLA	7/16/2003	7/30/2003	2.5	18	-13.00	7.98
MiniVol						
Zephyr Cove	7/8/2003	7/15/2003	TSP	7	4.00	7.24
Wallis Tower	7/25/2003	8/1/2003	TSP	7	15.00	7.24
Wallis Residence Platform	8/1/2003	8/8/2003	TSP	7	6.00	7.24

*Field blank samples period 2 and period 14 are used for the background subtraction for two week samplers from 12/4/2002 to 6/4/2003.

**Field blank sample period 18 is used for the background subtraction for two week samplers from period 6/18/2003 to 1/6/2004.

***MiniVol sampler field blank average is used for the background subtraction for all MiniVol sampler samples.

Quality audits of sample flow rates were conducted at the beginning and 3/4 of the way through the study period, and these audits determined that flow rates were within ±10% of specifications. Data were submitted to three levels of data validation (Chow et al., 1994; Watson et al., 2001). Detailed data validation processes are documented in the following subsections.

3.4 Data Validation

Data acquired from the study were submitted to three data validation levels:

- Level 0 sample validation: designates data as they come off the instrument. This process ascertains that the field or laboratory instrument is functioning properly.
- Level I sample validation: 1) flags samples where significant deviation from measurement assumptions have occurred, 2) verifies computer file entries against data sheets, 3) eliminates values for measurements that are known to be invalid because of instrument malfunctions, 4) replaces data from a backup data acquisition system in the event of failure of the primary system, and 5) adjusts values for quantifiable calibration or interference biases.
- Level II sample validation applies consistency tests to the assembled data based on known physical relationships between variables.
- Level III sample validation is part of the data interpretation process. The first assumption upon finding a measurement which is inconsistent with physical expectations is that the unusual value is due to a measurement error. If, upon tracing the path of the measurement, nothing unusual is found, then it may be assumed the value was the result of a valid environmental cause. Unusual values are identified during the data interpretation process as: 1) extreme values, 2) values which would otherwise normally track the values of other variables in a time series, and 3) values

for observables which would normally follow a qualitatively predictable spatial or temporal pattern.

Level I validation flags and comments are included with each data record in the database, as documented in Section 3.2. Level II validation tests and results are described in the following subsections.

Level II tests evaluate the chemical data for internal consistency. In this study, Level II data validations were made for: 1) physical consistency and 2) balance of reconstructed mass based on chemical species versus measured mass. Correlations and linear regression statistics were computed and scatter plots prepared to examine the data. A total of 127, 129, and 128 sets of filter samples were collected for TWS TSP, PM_{10}, and $PM_{2.5}$, respectively. A total of 38 and 161 sets of samples were collected for buoy and non-buoy MiniVol samples, respectively, and only 36 (excluding 30/04/03 and 31/12/03) and 160 (excluding 29/01/03) were examined. Statistical comparisons of chemical species concentrations and analytical uncertainty of the results are shown in Table 3-3.

Table 3-3. Statistical Analysis of comparison between chemical species concentrations above analytical uncertainty in sample number, average of the ratios, and one standard deviation of the ratios for TWS TSP, PM_{10}, $PM_{2.5}$, buoy, and non-buoy MiniVol samples.

	TWS TSP				TWS PM_{10}				TWS $PM_{2.5}$			
Species	C>U	N	Mean	StdDev	C>U	N	Mean	StdDev	C>U	N	Mean	StdDev
Mass	127	127	13.94	4.34	129	129	13.26	4.41	128	128	8.12	3.59
Backup Nitrate	124	127	5.31	2.90	124	129	4.38	2.24	123	127	4.15	2.12
Chloride	34	127	0.85	1.32	31	129	0.62	1.00	9	128	0.28	0.58
Nitrite	0	127	0.00	0.00	2	129	0.29	2.32	2	128	0.17	1.72
Nitrate	124	127	4.97	2.55	126	129	4.34	2.37	99	128	2.63	2.27
Phosphate	0	127	0.00	0.00	2	129	0.14	1.09	2	128	0.08	0.81
Sulfate	126	127	6.52	2.83	127	129	6.89	2.67	125	128	6.34	2.72
Ammonium	126	127	6.51	2.43	125	129	5.93	2.65	128	128	6.25	2.69
Soluble Sodium	117	127	10.30	5.17	124	129	9.55	4.90	75	128	2.98	3.87
Soluble Magnesium	93	127	4.84	3.81	93	129	4.18	3.50	29	128	0.62	1.09
Soluble Potassium	124	127	4.33	2.86	124	129	4.00	2.64	115	128	3.10	2.25
Soluble Calcium	117	127	4.41	2.51	122	129	3.91	1.94	20	128	0.45	0.69
Organic Carbon Fraction 1	94	127	3.25	2.54	121	129	5.81	2.80	125	128	6.66	2.78
Organic Carbon Fraction 2	126	127	6.33	2.51	128	129	6.22	2.58	128	128	5.91	2.56
Organic Carbon Fraction 3	127	127	8.20	2.57	129	129	7.94	2.71	126	128	6.89	2.84
Organic Carbon Fraction 4	127	127	7.32	3.31	128	129	7.23	3.54	124	128	6.21	3.27
Pyrolyzed Organic Carbon	118	127	4.39	1.87	119	129	4.26	1.83	122	128	4.34	1.57
Organic Carbon	127	127	12.58	3.90	129	129	13.07	4.19	127	128	12.47	4.41
Elemental Carbon Fraction 1	127	127	6.38	1.84	129	129	6.34	1.96	126	128	5.98	2.06
Elemental Carbon Fraction 2	127	127	5.72	1.87	129	129	5.92	2.06	126	128	5.74	1.86
Elemental Carbon Fraction 3	54	127	1.52	2.04	68	129	1.89	2.22	76	128	2.55	2.95
Elemental Carbon	125	127	4.96	2.25	129	129	5.24	2.30	126	128	5.04	2.28
Total Carbon	127	127	13.28	4.00	129	129	13.83	4.28	127	128	13.19	4.40
Sodium	23	127	0.42	0.77	24	129	0.44	0.79	19	128	0.49	1.20
Magnesium	36	127	0.61	0.81	28	129	0.60	0.99	15	128	0.31	0.46
Aluminum	127	127	3.22	0.36	129	129	3.14	0.48	99	128	2.04	1.36
Silicon	127	127	3.13	0.06	129	129	3.11	0.12	126	128	8.08	3.92
Phosphorous	4	127	0.08	0.30	5	129	0.08	0.30	0	128	0.02	0.10
Sulfur	127	127	15.86	3.30	130	129	15.65	3.63	127	128	15.14	3.79
Chlorine	67	127	1.52	1.35	62	129	1.39	1.36	9	128	0.22	0.50
Potassium	127	127	4.95	0.15	129	129	4.90	0.34	127	128	10.36	3.54
Calcium	127	127	5.85	0.20	129	129	5.73	0.60	127	128	6.75	2.96
Titanium	101	127	2.95	2.11	92	129	2.27	1.85	0	128	0.14	0.16
Vanadium	0	127	0.12	0.17	1	129	0.11	0.19	0	128	0.04	0.07
Chromium	15	127	0.42	0.45	13	129	0.48	1.19	0	128	0.09	0.16
Manganese	118	127	8.87	4.47	120	129	7.65	4.13	59	128	1.25	1.12
Iron	127	127	18.82	2.52	129	129	18.23	3.66	125	128	12.17	4.45
Cobalt	0	127	0.50	0.21	2	129	0.51	0.28	9	128	0.54	0.44
Nickel	38	127	0.82	0.77	35	129	0.89	1.27	3	128	0.30	0.35
Copper	114	127	4.60	3.36	111	129	4.04	3.30	65	128	1.78	2.96
Zinc	126	127	9.80	5.16	124	129	8.14	5.03	111	128	4.61	3.74
Gallium	0	127	0.03	0.12	1	129	0.06	0.17	0	128	0.03	0.12
Arsenic	3	127	0.16	0.25	1	129	0.13	0.20	1	128	0.10	0.21
Selenium	3	127	0.16	0.25	0	129	0.18	0.24	1	128	0.17	0.25
Bromine	121	127	3.67	1.71	122	129	3.66	1.78	119	128	3.34	1.84
Rubidium	75	127	1.46	1.03	58	129	1.02	0.84	3	128	0.25	0.28
Strontium	108	127	5.57	3.98	105	129	4.52	3.67	15	128	0.48	0.51
Yttrium	7	127	0.40	0.29	6	129	0.36	0.31	1	128	0.22	0.21
Zirconium	66	127	1.20	1.05	58	129	1.08	0.98	0	128	0.09	0.16
Molybdenum	5	127	0.15	0.32	2	129	0.13	0.27	1	128	0.11	0.26
Palladium	1	127	0.10	0.19	0	129	0.07	0.13	0	128	0.07	0.13
Silver	1	127	0.10	0.22	0	129	0.09	0.16	0	128	0.09	0.16
Cadmium	1	127	0.11	0.23	0	129	0.11	0.18	1	128	0.13	0.22
Indium	3	127	0.16	0.26	0	129	0.15	0.19	1	128	0.12	0.21
Tin	4	127	0.28	0.28	5	129	0.32	0.31	5	128	0.24	0.30
Antimony	7	127	0.26	0.36	5	129	0.21	0.31	2	128	0.18	0.26
Barium	26	127	0.55	0.59	19	129	0.43	0.51	7	128	0.25	0.32
Lanthanum	1	127	0.20	0.22	0	129	0.18	0.21	0	128	0.19	0.21
Gold	0	127	0.07	0.17	1	129	0.08	0.17	0	128	0.06	0.15
Mercury	1	127	0.12	0.18	0	129	0.11	0.16	0	128	0.09	0.16
Thallium	0	127	0.08	0.16	0	129	0.04	0.11	0	128	0.04	0.09
Lead	58	127	0.96	0.91	66	129	1.08	1.02	36	128	0.69	1.37
Uranium	0	127	0.10	0.15	0	129	0.11	0.14	0	128	0.09	0.14
Reconstructed Mass*	N/A	127	16.04	9.79	N/A	129	14.27	9.61	N/A	128	6.39	4.03

Table 3-3. cont'd

	Buoy MiniVol**				Non-buoy MiniVol**			
Species	C>U	N	Mean	StdDev	C>U	N	Mean	StdDev
Mass	36	38	8.05	4.11	158	161	16.10	4.99
Backup Nitrate	N/A	N/A	N/A	N/A	N/A	N/A	N/A	N/A
Chloride	35	36	3.98	1.44	137	161	3.11	3.48
Nitrite	N/A	N/A	N/A	N/A	N/A	N/A	N/A	N/A
Nitrate	36	36	7.31	3.89	151	161	5.69	4.27
Phosphate	0	36	0.00	0.00	2	160	0.36	2.62
Sulfate	35	36	5.44	3.66	155	161	6.77	3.75
Ammonium	36	36	4.84	2.35	155	161	7.91	3.91
Soluble Sodium	36	36	15.39	2.26	157	161	9.98	5.17
Soluble Magnesium	34	36	8.01	4.63	150	161	10.33	5.12
Soluble Potassium	36	36	7.59	3.11	160	161	10.52	4.25
Soluble Calcium	36	36	5.98	3.53	161	161	8.00	4.58
Organic Carbon Fraction 1	21	36	1.84	1.90	109	161	1.75	1.52
Organic Carbon Fraction 2	36	36	6.54	2.09	152	161	6.02	3.23
Organic Carbon Fraction 3	36	36	5.82	1.55	157	161	7.74	3.53
Organic Carbon Fraction 4	36	36	4.62	1.59	157	161	8.12	3.37
Pyrolyzed Organic Carbon	24	36	2.25	1.85	138	161	4.56	2.81
Organic Carbon	36	36	8.15	2.23	157	161	9.29	4.43
Elemental Carbon Fraction 1	26	36	2.81	2.24	157	161	6.71	2.74
Elemental Carbon Fraction 2	34	36	3.26	1.83	157	161	5.06	1.96
Elemental Carbon Fraction 3	0	36	0.00	0.00	82	161	1.95	2.30
Elemental Carbon	23	36	2.34	1.85	156	161	7.15	2.63
Total Carbon	36	36	7.34	2.28	158	161	9.69	4.44
Sodium	14	38	2.31	2.73	42	160	0.70	1.08
Magnesium	10	38	1.51	2.21	44	160	0.78	0.98
Aluminum	25	38	2.09	1.25	142	160	2.75	0.94
Silicon	38	38	3.11	0.08	155	160	2.89	0.55
Phosphorous	6	38	0.47	0.77	3	160	0.04	0.20
Sulfur	38	38	14.41	4.19	160	160	17.05	3.77
Chlorine	10	38	0.87	1.13	90	160	1.64	1.34
Potassium	33	38	3.99	1.54	159	160	4.76	0.67
Calcium	35	38	4.85	1.64	159	160	5.30	1.24
Titanium	0	38	0.18	0.24	113	160	3.19	3.57
Vanadium	0	38	0.04	0.07	0	160	0.13	0.18
Chromium	0	38	0.14	0.22	25	160	0.53	0.84
Manganese	16	38	2.95	3.34	143	160	7.93	5.15
Iron	38	38	17.02	3.53	159	160	15.54	5.50
Cobalt	0	38	0.31	0.27	2	160	0.39	0.22
Nickel	4	38	0.70	1.05	65	160	1.36	1.88
Copper	12	38	1.85	2.33	137	160	5.55	4.92
Zinc	21	38	3.85	3.94	154	160	10.84	5.53
Gallium	0	38	0.09	0.24	0	160	0.08	0.16
Arsenic	3	38	0.35	0.88	11	160	0.28	0.36
Selenium	0	38	0.23	0.25	4	160	0.18	0.34
Bromine	11	38	1.56	2.01	131	160	3.42	2.45
Rubidium	0	38	0.12	0.26	57	160	1.33	2.22
Strontium	6	38	0.96	1.47	134	160	6.36	5.36
Yttrium	0	38	0.20	0.26	10	160	0.36	0.51
Zirconium	1	38	0.31	0.64	82	160	1.66	2.16
Molybdenum	5	38	0.77	1.37	9	160	0.24	0.38
Palladium	0	38	0.20	0.27	0	160	0.15	0.21
Silver	0	38	0.36	0.33	5	160	0.24	0.29
Cadmium	0	38	0.19	0.31	1	160	0.17	0.22
Indium	0	38	0.21	0.32	2	160	0.20	0.23
Tin	3	38	0.50	0.91	9	160	0.22	0.33
Antimony	0	38	0.26	0.34	5	160	0.18	0.32
Barium	4	38	0.61	1.10	47	160	0.79	1.14
Lanthanum	0	38	0.17	0.25	1	160	0.14	0.21
Gold	0	38	0.18	0.29	0	160	0.08	0.16
Mercury	0	38	0.15	0.19	0	160	0.09	0.14
Thallium	0	38	0.05	0.14	5	160	0.16	0.36
Lead	7	38	1.01	1.79	55	160	0.90	1.22
Uranium	0	38	0.09	0.15	0	160	0.04	0.08
Reconstructed Mass*	N/A	36	9.14	4.16	N/A	160	13.34	12.93

* Reconstructed Mass = IMPROVE reconstructed mass formula

**Backup nitrate and nitrite were not measured on MiniVols.

3.4.1 Physical consistency

The compositions of chemical species concentrations measured by different chemical analysis methods were examined. Physical consistency was tested for: 1) sum of chemical species vs. measured mass, 2) $SO_4^=$ versus total sulfur (S), 3) Cl^- versus chlorine (Cl), 4) K^+ versus total potassium (K), 5) anion/cation balance, 6) ammonia balance, 7) gas/particle equilibrium of semi-volatile compounds, and 8) reconstructed mass versus measured mass.

3.4.1.1 Sum of chemical species vs. measured mass

Chemical species, including elements, ions, and cations analyzed by XRF, IC, and AA, respectively, and OC and EC, were summed and compared to mass measured by gravimetric analysis. Oxygen was not considered in the form of metal oxides and organic carbon; therefore, it was expected that the slope and ratio of the sum of chemical species to measured mass would be less than 1. The correlation (r^2) and intercept vary by site and sampling period and are dependent on chemical compositions in particulates; therefore, they are not used for data QA/QC. Figure 3-2(a-c) shows that the slopes between the sum of chemical species and measured mass at all five sites for TWS TSP, PM_{10}, and $PM_{2.5}$ were 0.40, 0.54, and 0.65, respectively. The average ratios between the sum of chemical species and measured mass for TWS TSP, PM_{10}, and $PM_{2.5}$ were 0.65, 0.68, and 0.84, respectively. The slopes in the scatter plots of sum of species to measured mass (Figure 3-2d,e) are 0.40 and 0.45, for TSP collected by MiniVol sampler on lake shore (non-buoy MiniVol samplers) and TSP collected by MiniVol sampler on buoys (buoy MiniVol sampler), respectively. The average ratio between the sum of chemical species and measured mass are generally less than one, except that for the buoy TSP MiniVol samplers. The sampling duration for buoy TSP MiniVol sampler is generally less than 24 hours with low TSP mass concentrations. In addition, the samples were left on the buoy until the scheduled collection date may result in high uncertainty of the sample quality. These slopes and ratios met the expected criteria. A lab flag was noted on 12/04/02 for the measured mass (fiber or fuzz observed on filter) at the Lake Forest site, which may explain the high measured mass but low sum of chemical species.

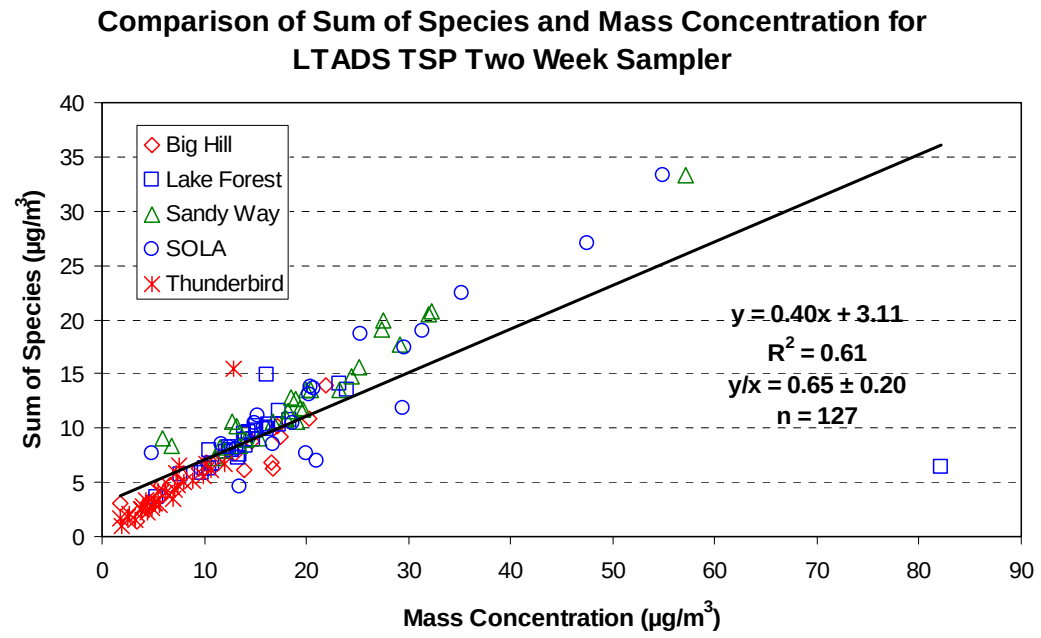

(a)

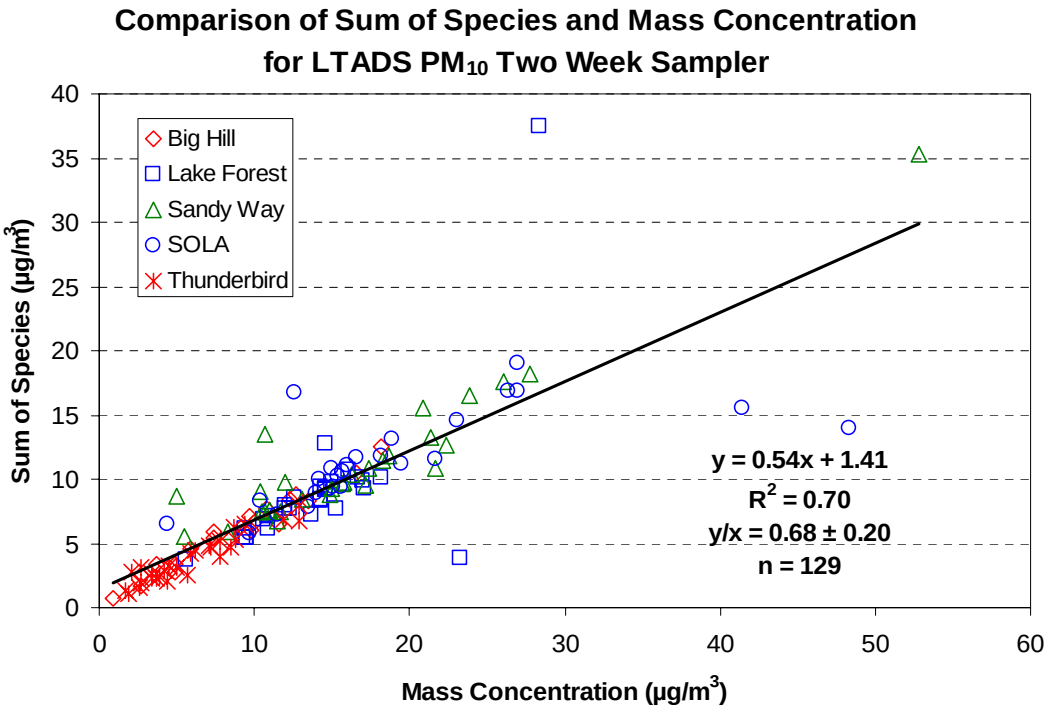

(b)

Figure 3-2. Comparisons of sum of chemical species and measured mass at five site for: (a) TSP, b) PM_{10}, and c) $PM_{2.5}$, d) Buoy MiniVol TSP, and e) non-Buoy MiniVol TSP.

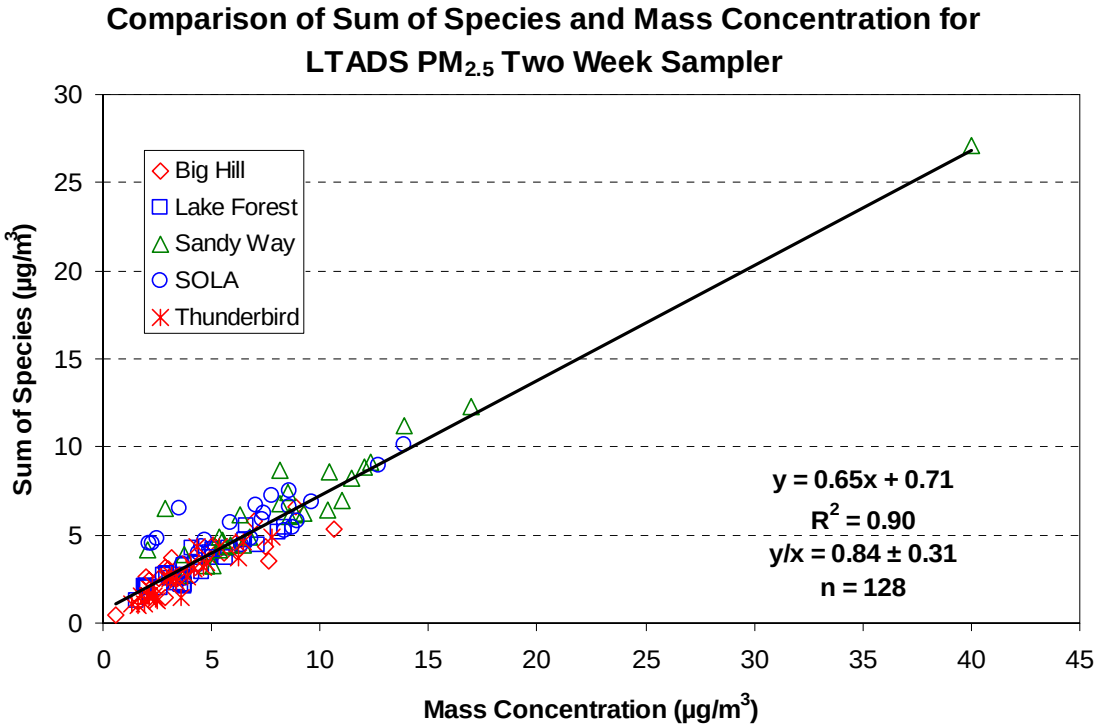

(c)

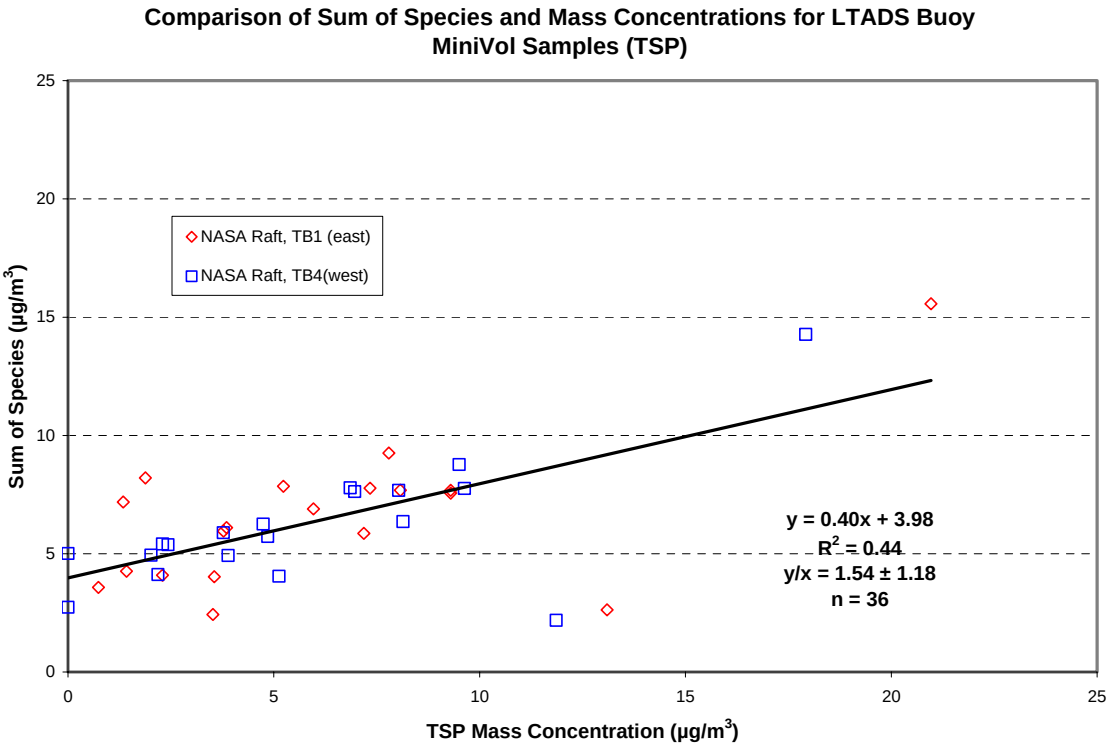

(d)

Figure 3-2, cont'd

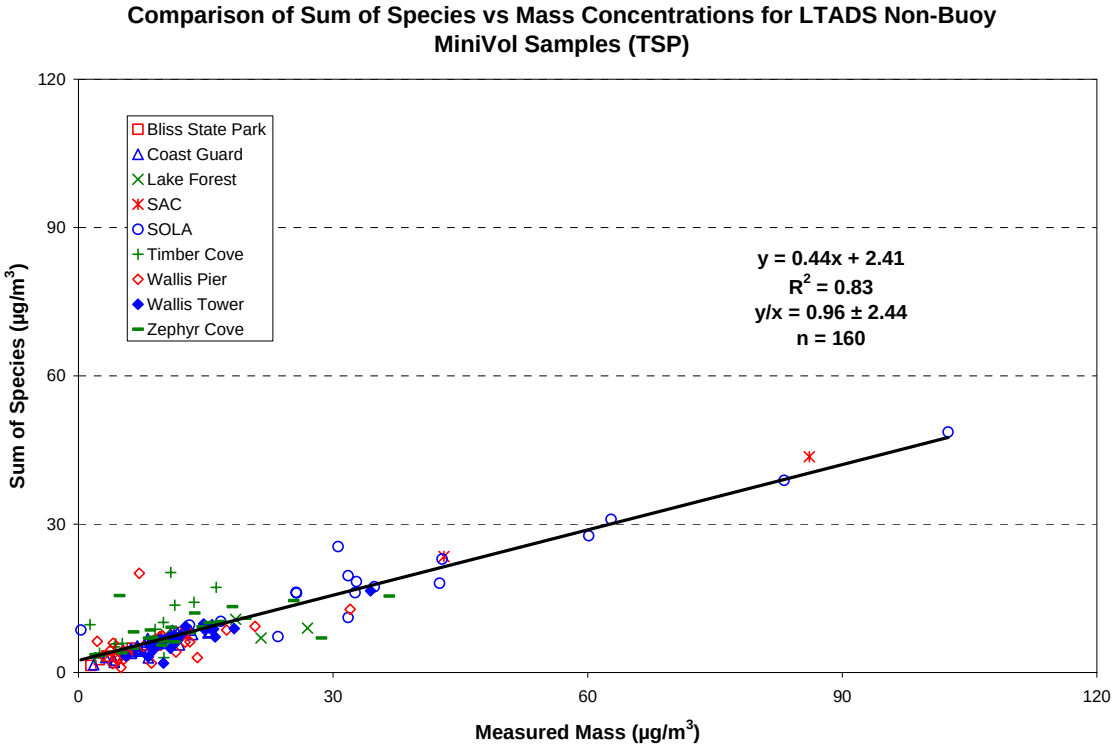

(e)

Figure 3-2, cont'd

3.4.1.2 Sulfate ($SO_4^=$) versus total sulfur (S)

$SO_4^=$ was measured by IC analysis on quartz-fiber filters and S was measured by XRF analysis on Teflon-membrane filters. The ratio of $SO_4^=$:S should equal 3:1 if all S is present as $SO_4^=$. Figure 3-3(a-c) shows scatter plots of $SO_4^=$ versus S concentrations at five sites for TWS TSP, PM_{10}, and $PM_{2.5}$. The average $SO_4^=$:S ratios for TSP, PM_{10}, and $PM_{2.5}$ were 2.1±0.93, 2.3±1.1, and 2.3±1.0, respectively, which were lower than the 3:1 ratio. This suggests that a significant amount of S in particulate matter (PM) consists of non-soluble S compounds. The regression statistics gave slopes of 1.88 with an intercept of 0.033 µg/m^3 for TSW TSP, 1.62 with an intercept of 0.12 µg/m^3 for PM_{10}, and 1.65 with an intercept of 0.10 µg/m^3 for $PM_{2.5}$. The correlation (r^2) between $SO_4^=$ and S increased from 0.60 to 0.76 as particle size range decreased from TSP to $PM_{2.5}$, which agrees with the knowledge that most of the S in $PM_{2.5}$ is in the form of $SO_4^=$ and therefore better correlated.

For the buoy TSP MiniVol samplers, the average $SO_4^=$:S ratio in Figure 3-3d is 3.22±2.36 and the slope is 2.17 with intercept of 0.04µg/m^3 and high r^2 of 0.82; the average ratio is 2.83± 8.44 and the slope is 1.26 with intercept of 0.15µg/m^3 and low r^2 of 0.41 for non-buoy TSP MiniVol samplers. The high standard deviation of the average $SO_4^=$:S ratio for the non-buoy TSP MiniVol samplers is probably due to the various sampling durations and locations. Nevertheless, the slopes of $SO_4^=$:S and average $SO_4^=$:S ratio less than 3:1 can be attributed to either the existence of non-soluble $SO_4^=$ or to flow rate differences between the sampling channels of DTFE and quartz-fiber filters.

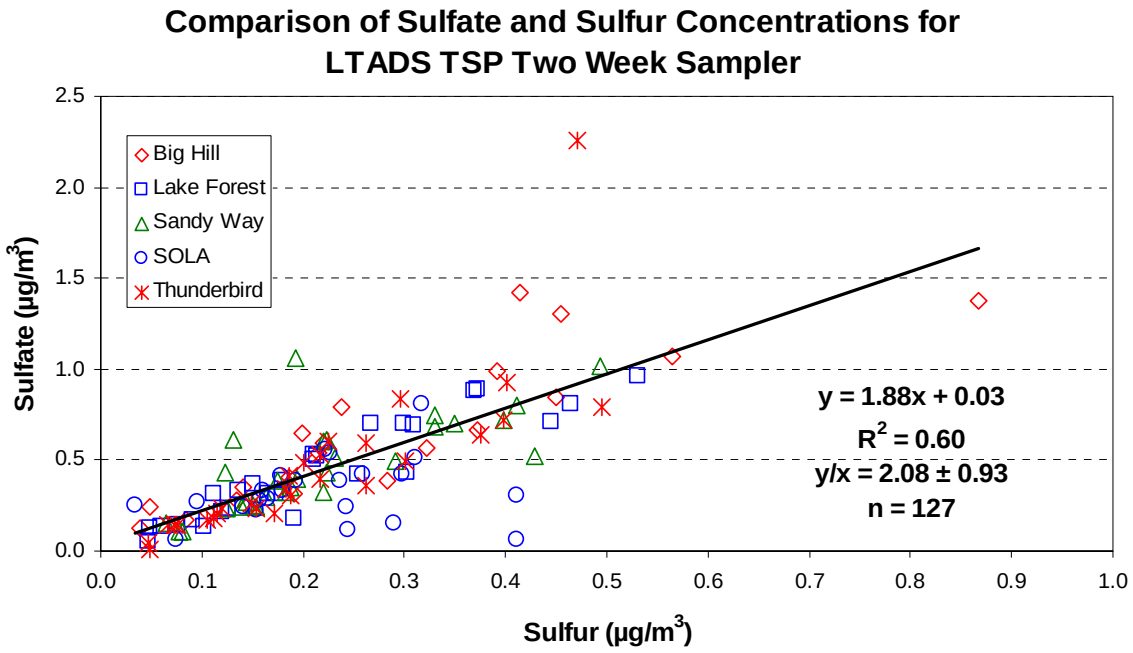

(a)

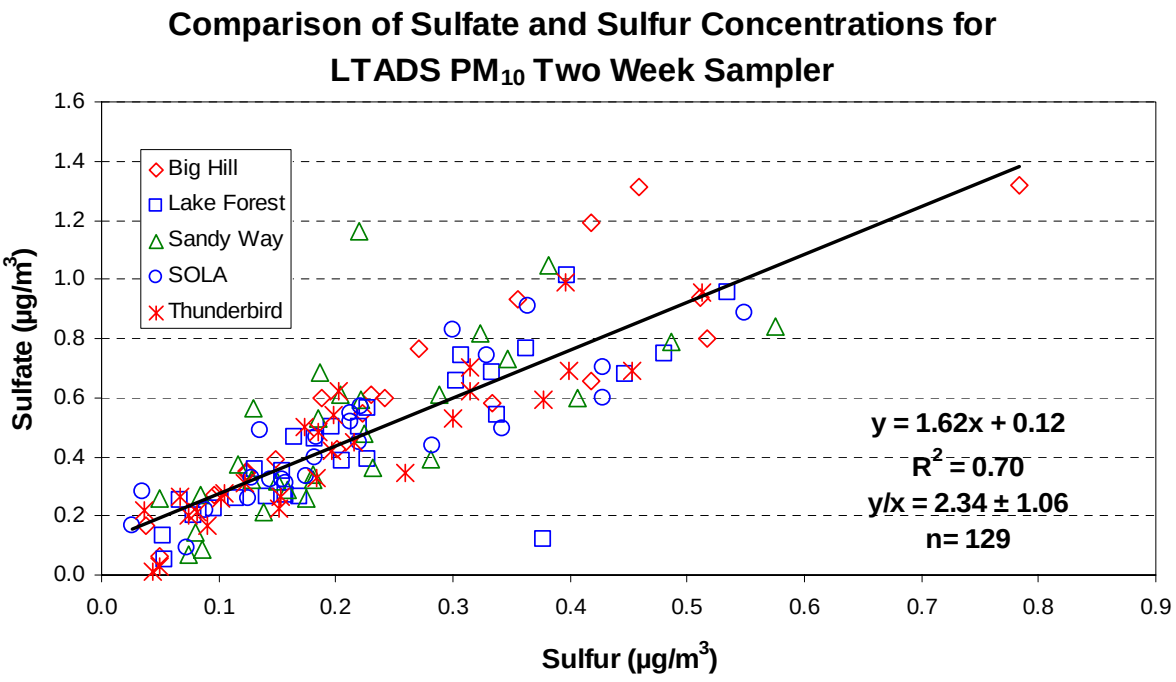

(b)

Figure 3-3. Scatter plot of sulfate versus sulfur concentrations at the five sites for: a) TSP, b) PM_{10}, c) $PM_{2.5}$, d) Bouy MiniVol TSP, and e) non-Bouy MiniVol TSP.

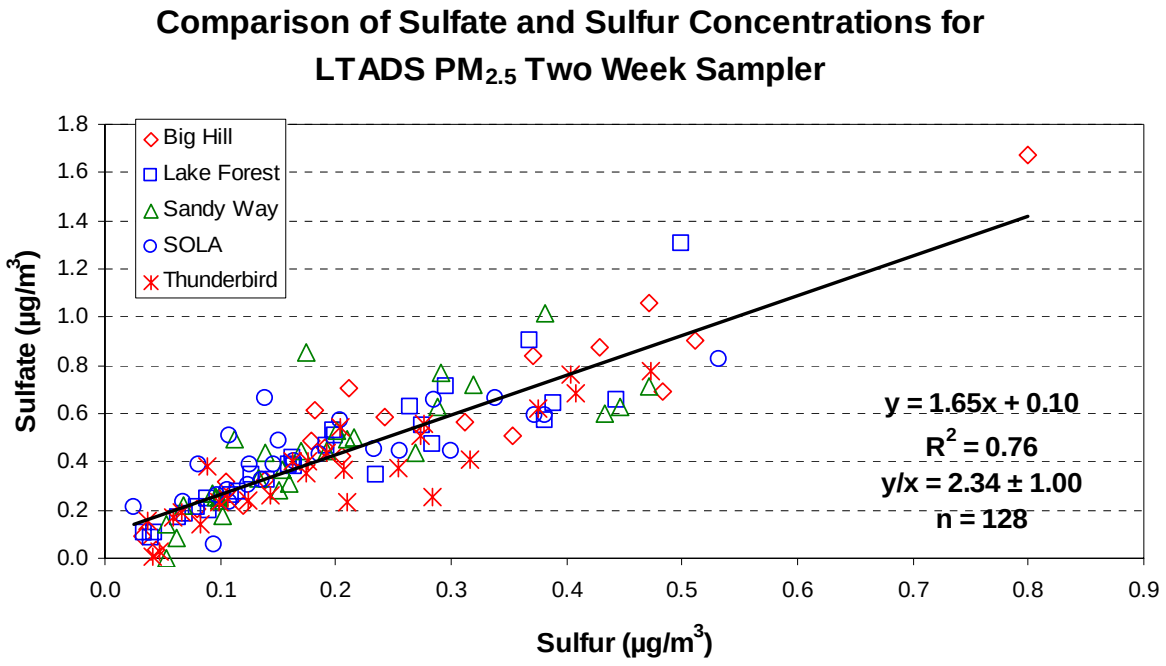

(c)

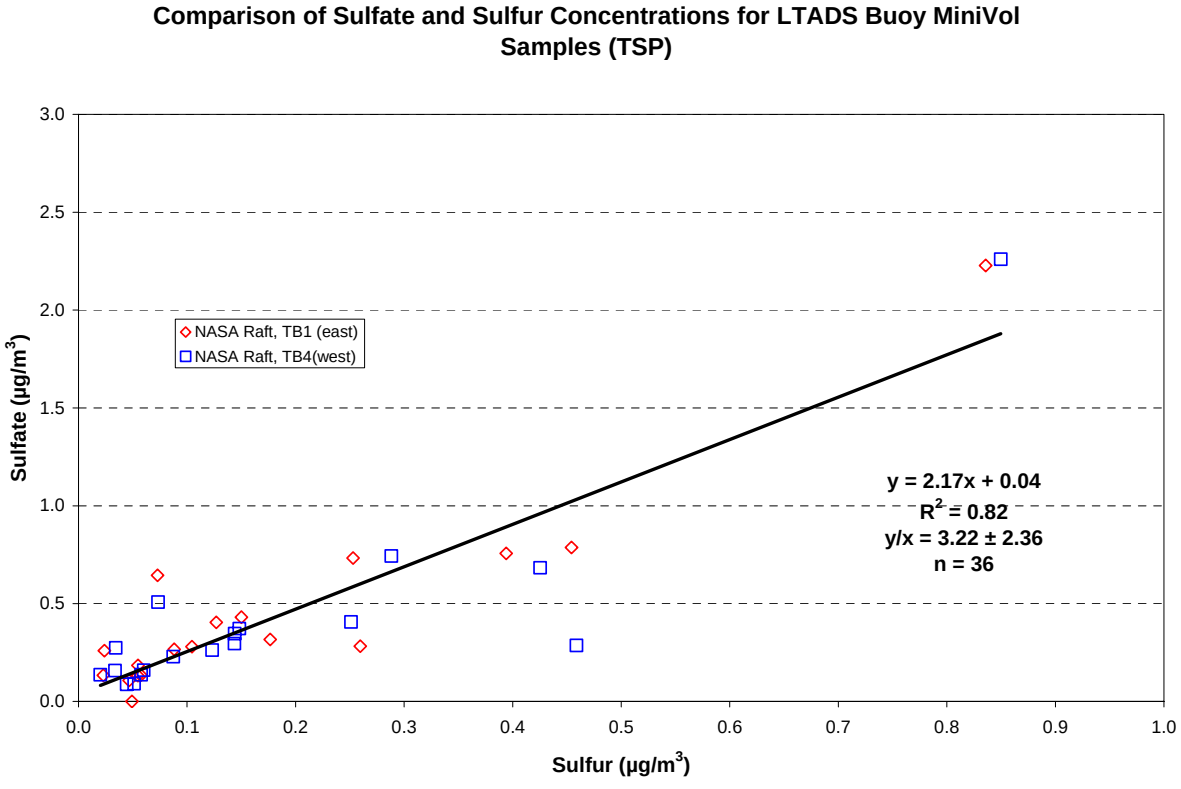

(d)

Figure 3-3, cont'd

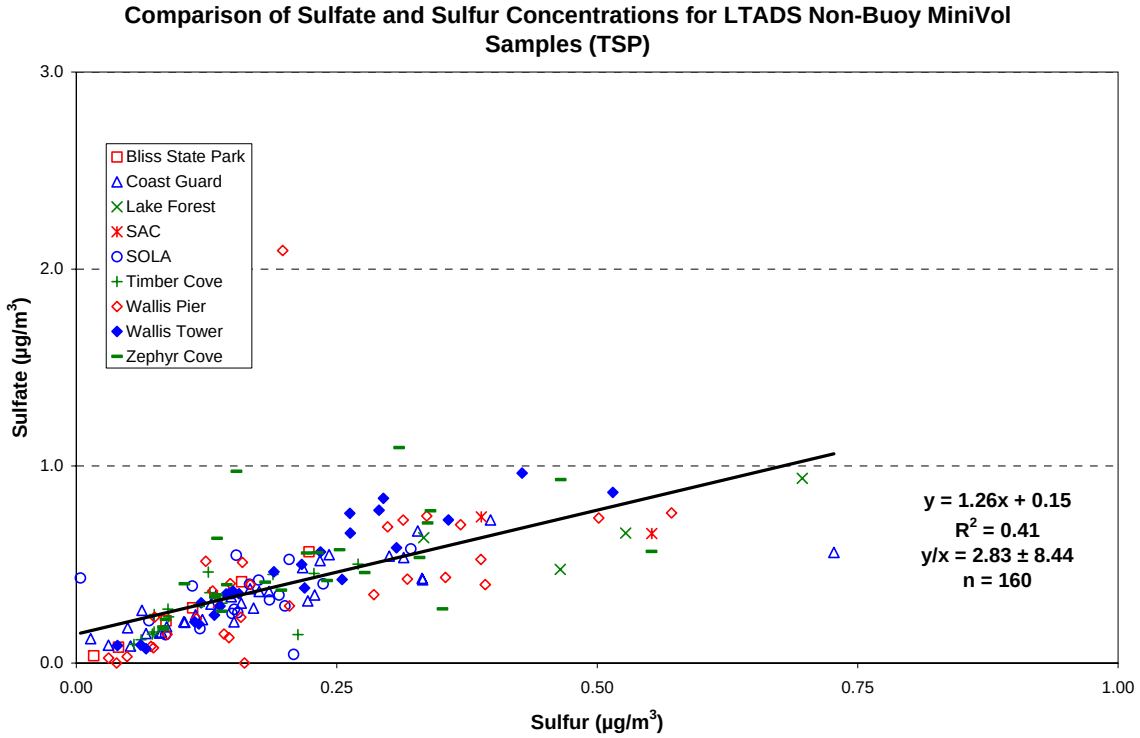

(e)

Figure 3-3, cont'd.

3.4.1.3 Chloride (Cl^-) versus chlorine (Cl)

Cl^- was measured by IC on quartz-fiber filters and Cl was measured by XRF on Teflon-membrane filters. Because Cl^- is the water-soluble portion of Cl, the ratio of Cl^-:Cl was expected to be less than unity. The number of samples above the analytical uncertainty for Cl^- was less than 35 for TWS TSP and PM_{10} and was only two for $PM_{2.5}$; it was less than 70 for TWS TSP and PM_{10} and nine for $PM_{2.5}$. Less than half of the samples collected by buoy and non-buoy MiniVol samples show Cl concentration above analytical uncertainty. Figure 3-4a shows that the Cl^- concentrations for TSP are less than 0.7 µg/m^3 with moderate correlations (r^2 = 0.70) between Cl^- and Cl measurements. Cl and/or Cl^- concentrations were slightly higher at BH than at the other four sites in the Lake Tahoe region. Figure 3-4(b,c) shows Cl^- concentrations for PM_{10} and $PM_{2.5}$ below 0.5 µg/m^3 with low correlations (r^2 = 0.29 and 0.05 for PM_{10} and $PM_{2.5}$, respectively) between Cl^- and Cl measurements. No correlation was found between Cl^- and Cl measurements for buoy MiniVol TSP samples. Although the slope for non-buoy MiniVol TSP samples was close to unity with moderate to high r^2 of 0.80, the standard deviation of the ratio between Cl^- and Cl measurements was 97.26. The uncertainty of Cl^- measurements was higher at low concentrations because its elution peak in gas chromatographic analysis is close to the distilled water dip which, in turn, shifts the baseline of the chromatogram (Chow and Watson, 1999). In addition, Cl collected on the Teflon-membrane filter may be lost through volatilization because XRF analysis is conducted in a vacuum chamber. Such losses are especially apparent when Cl concentrations are low; however, the Cl^-:Cl ratio greatly depends on the chemical forms of Cl in PM.

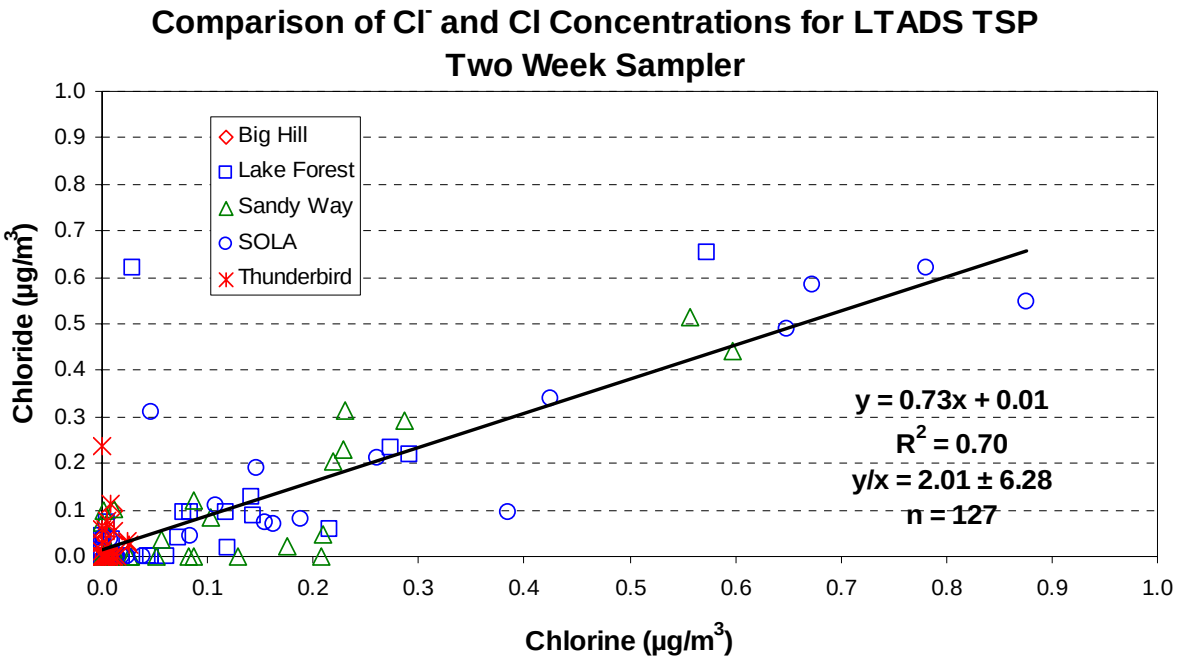

(a)

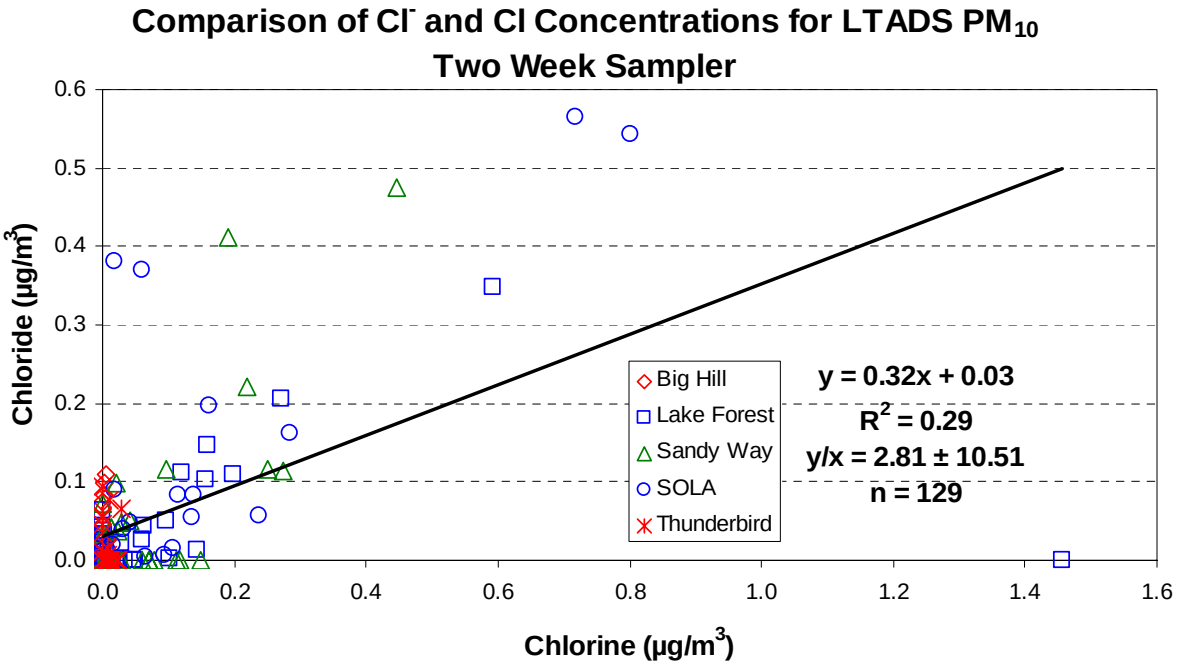

(b)

Figure 3-4. Chloride versus chlorine concentrations at five sites for: a) TSP, b) PM_{10}, c) $PM_{2.5}$, d) Bouy MiniVol TSP, and e) non-Bouy MiniVol TSP.

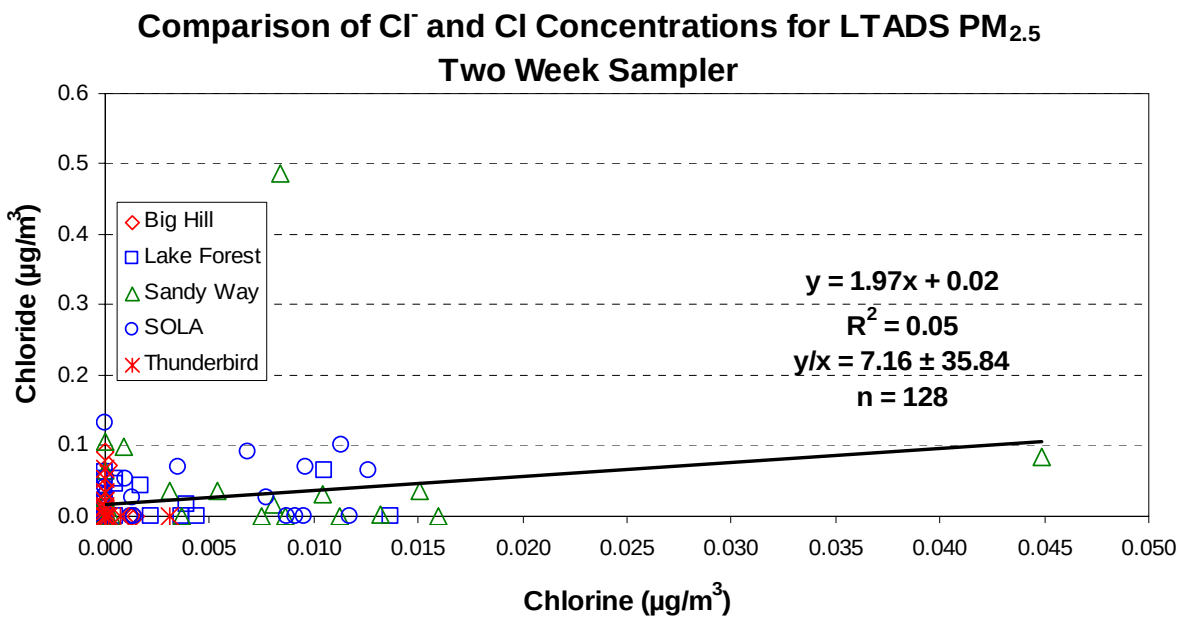

(c)

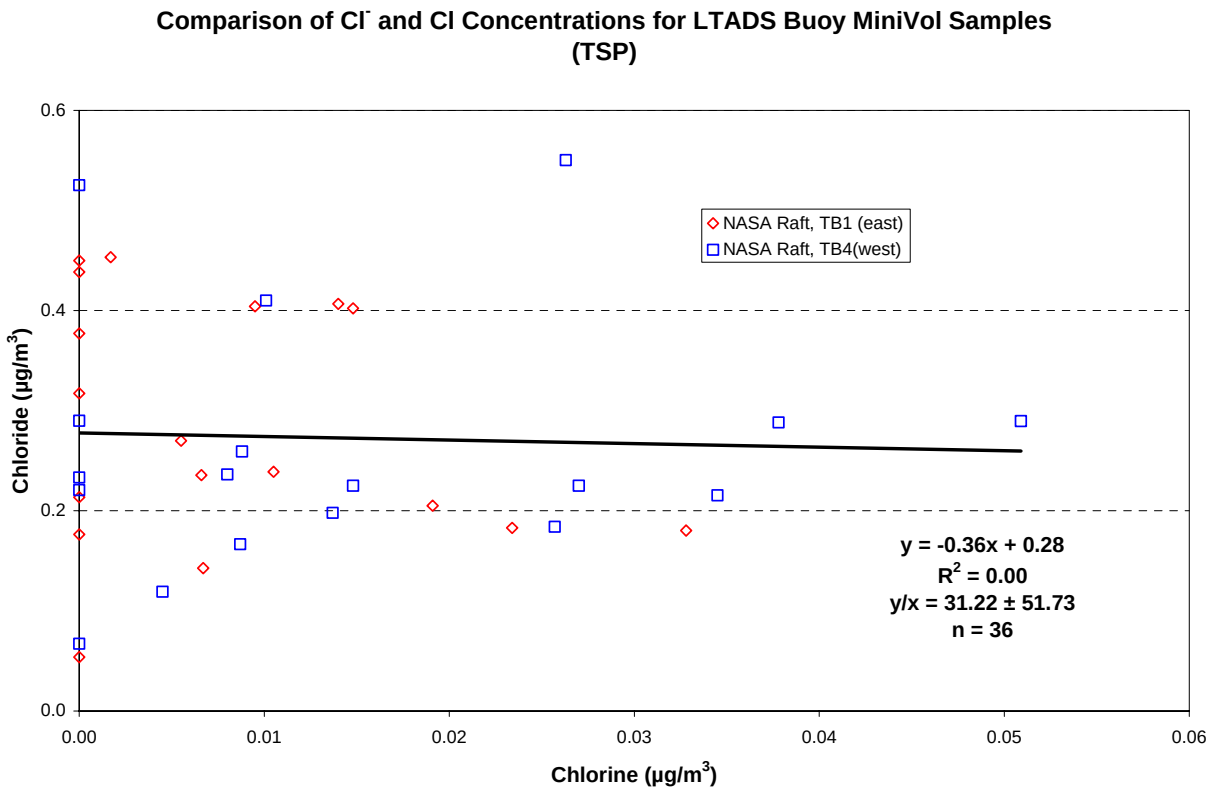

(d)

Figure 3-4, cont'd.

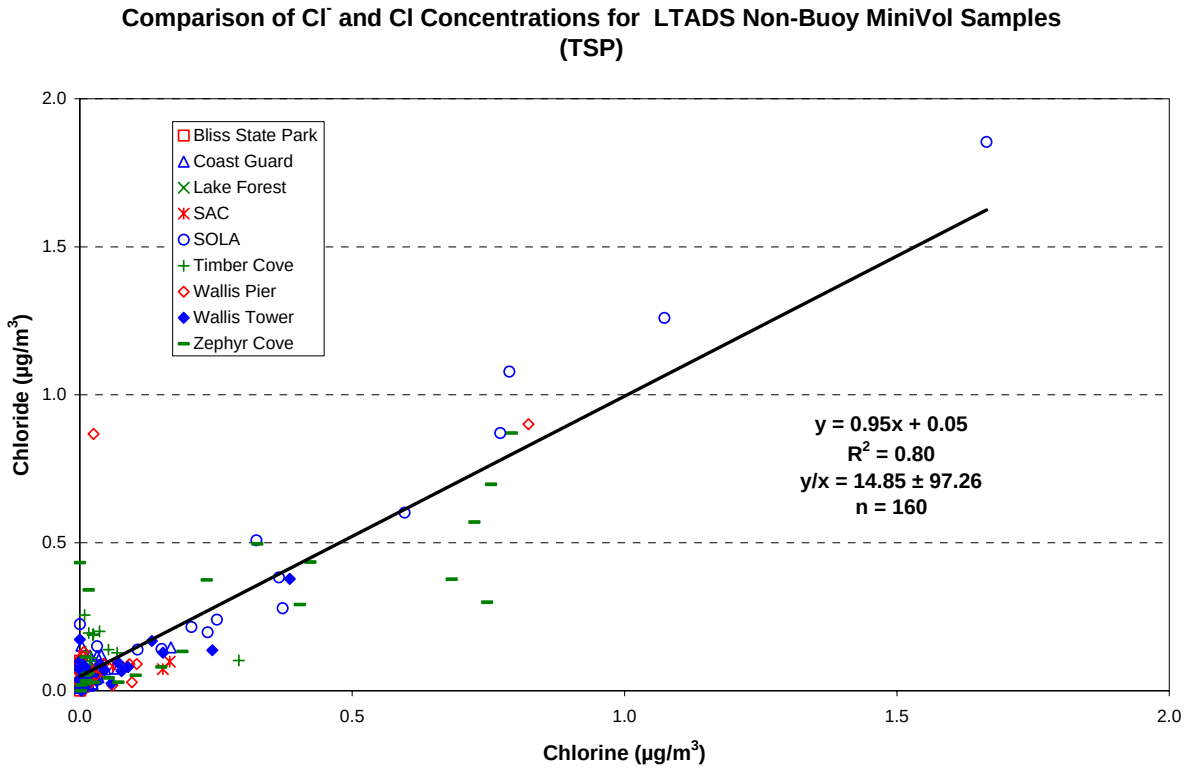

(e)

Figure 3-4, cont'd

3.4.1.4 Water-soluble potassium (K^+) versus potassium (K)

K^+ was measured by atomic adsorption spectrophotometry (AAS) analysis on quartz-fiber filter and K was measured by XRF on Teflon-membrane filters. Figure 3-5 (a-c) shows scatter plots of K^+ versus K concentrations for TWS TSP, PM_{10}, and $PM_{2.5}$; and Figure 3-5 (d, e) show those for bouy and non-bouy MiniVol TSP samples. Very weak correlations between K^+ and K were observed in TWS TSP and PM_{10}, bouy MiniVol TSP, and non-bouy MiniVol TSP. A high K concentration (1.544 µg/m^3) in PM_{10} and much lower K^+ concentrations (0.061 µg/m^3 and 0.043 µg/m^3 in TSP and $PM_{2.5}$, respectively) were observed on 11/15/03. It is suspected that the sample was contaminated. The regression statistics show moderate correlations (r^2 = 0.62) between K^+ and K measured in $PM_{2.5}$. This suggests the major sources of K^+ in $PM_{2.5}$ in the Lake Tahoe area are wood smoke or biomass burning from cooking and heating processes.

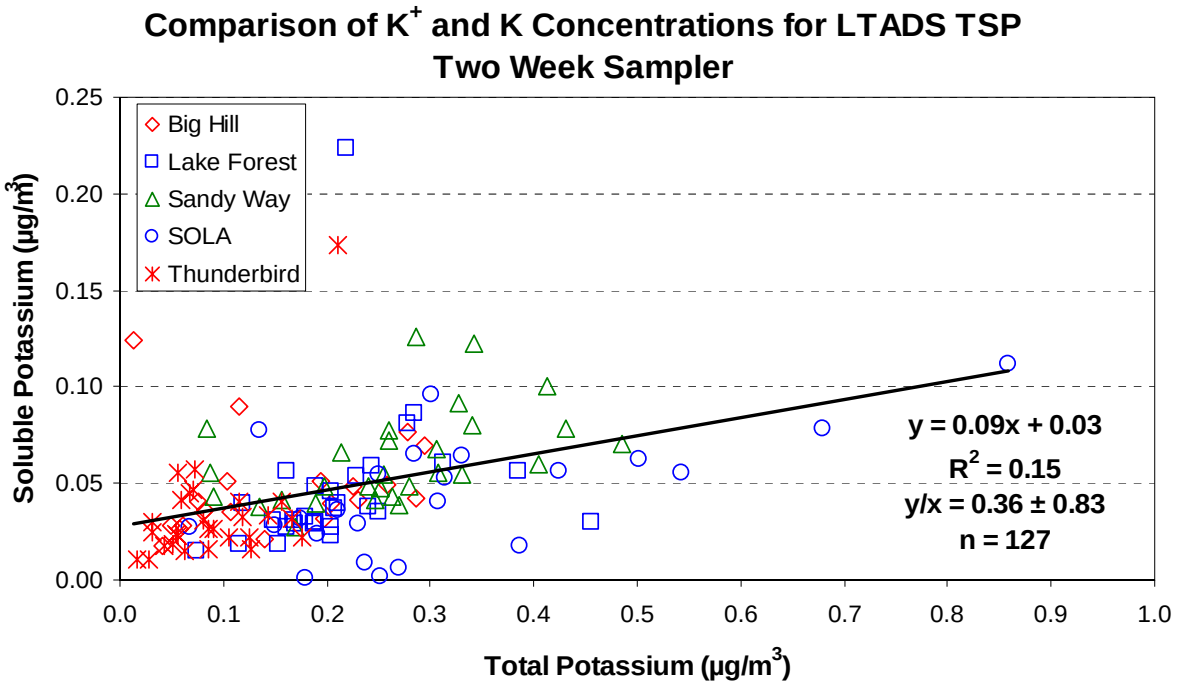

(a)

Figure 3-5. Scatter plot of water-soluble potassium versus potassium concentrations for: a) TSP, b) PM_{10}, c) $PM_{2.5}$, d) Bouy MiniVol TSP, and e) non-Bouy MiniVol TSP.

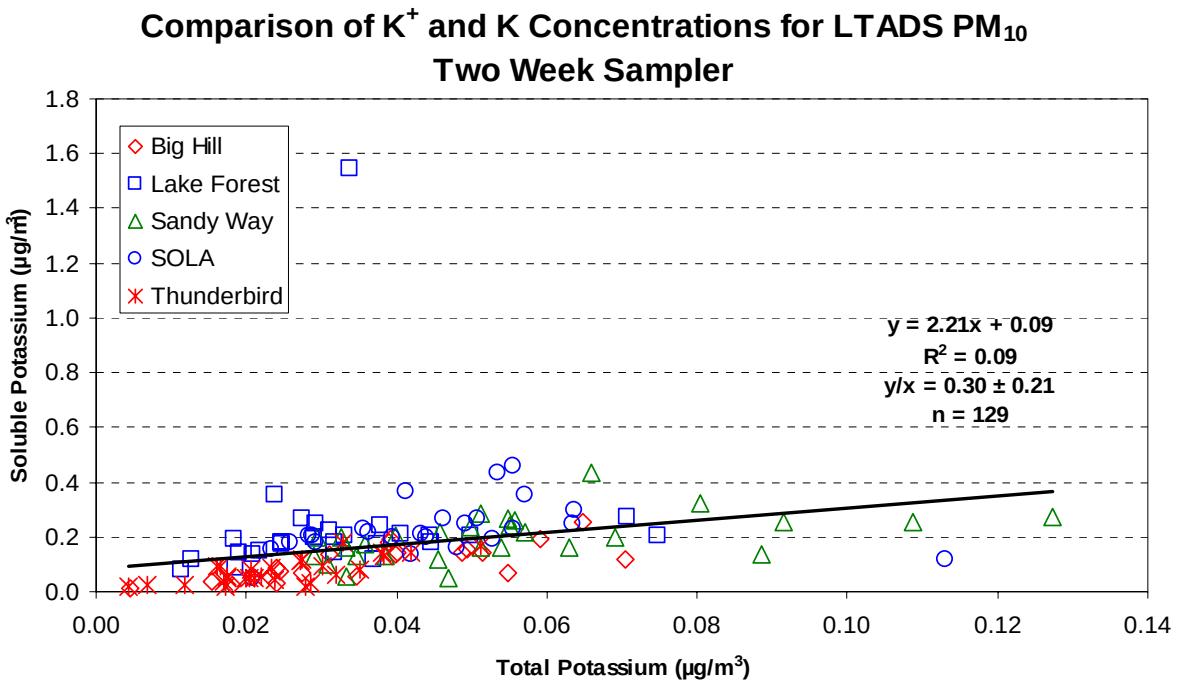

(b)

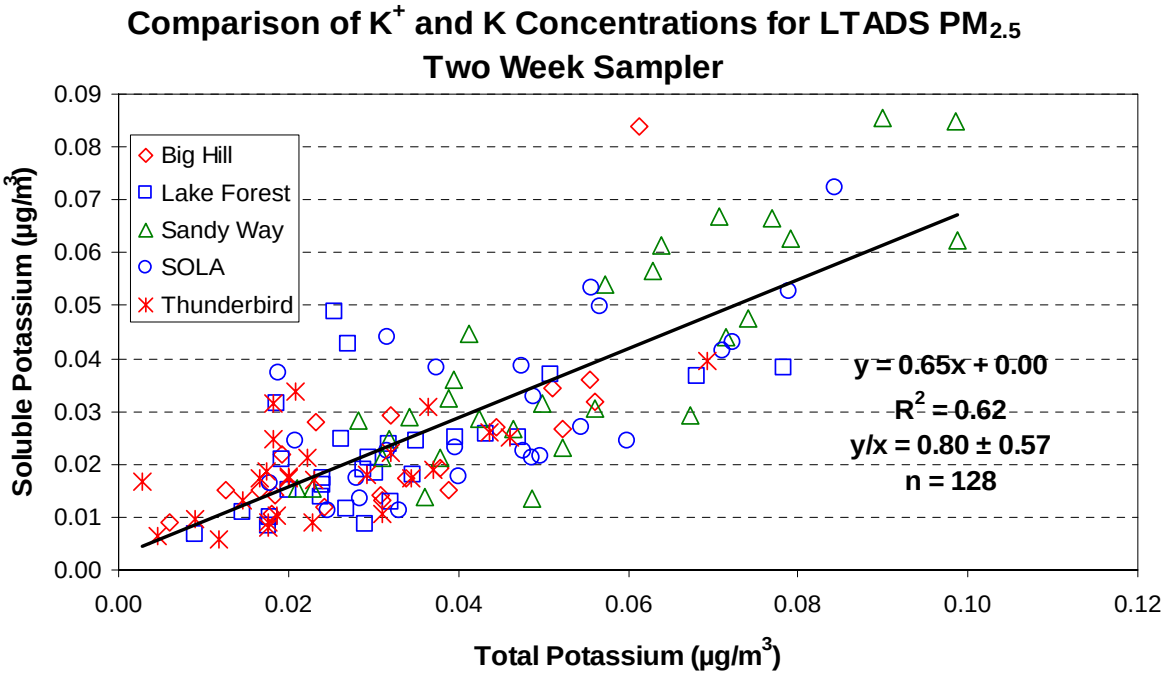

(c)

Figure 3-5, cont'd

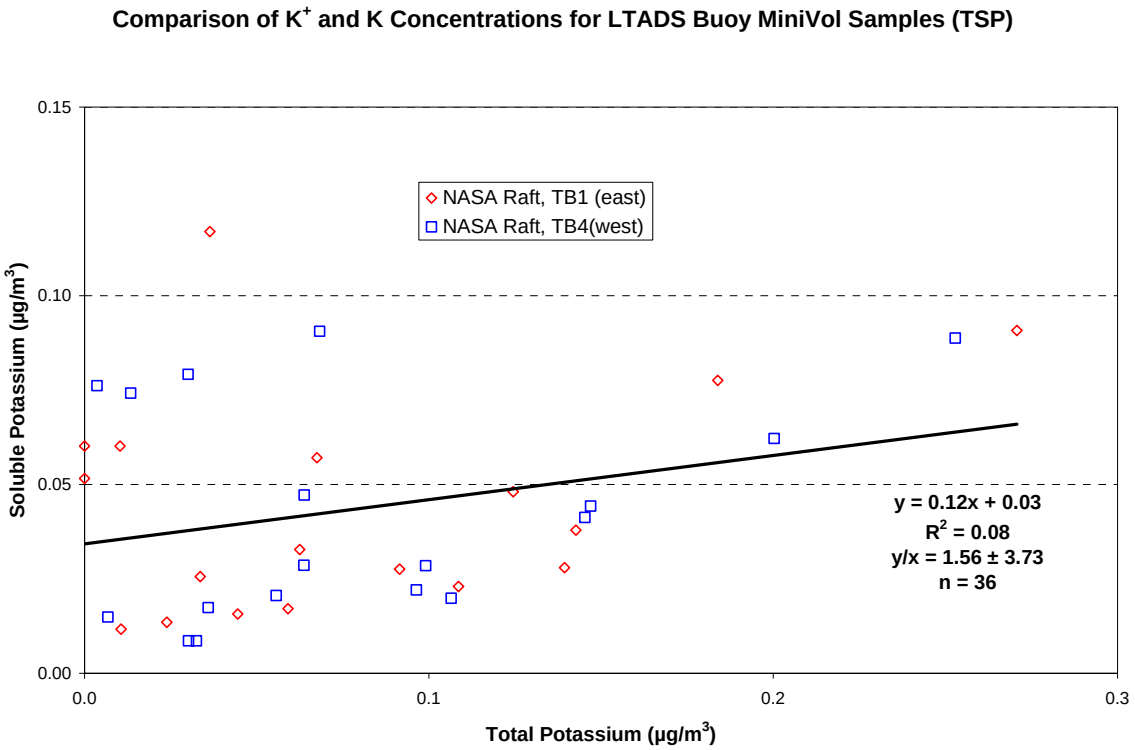

(d)

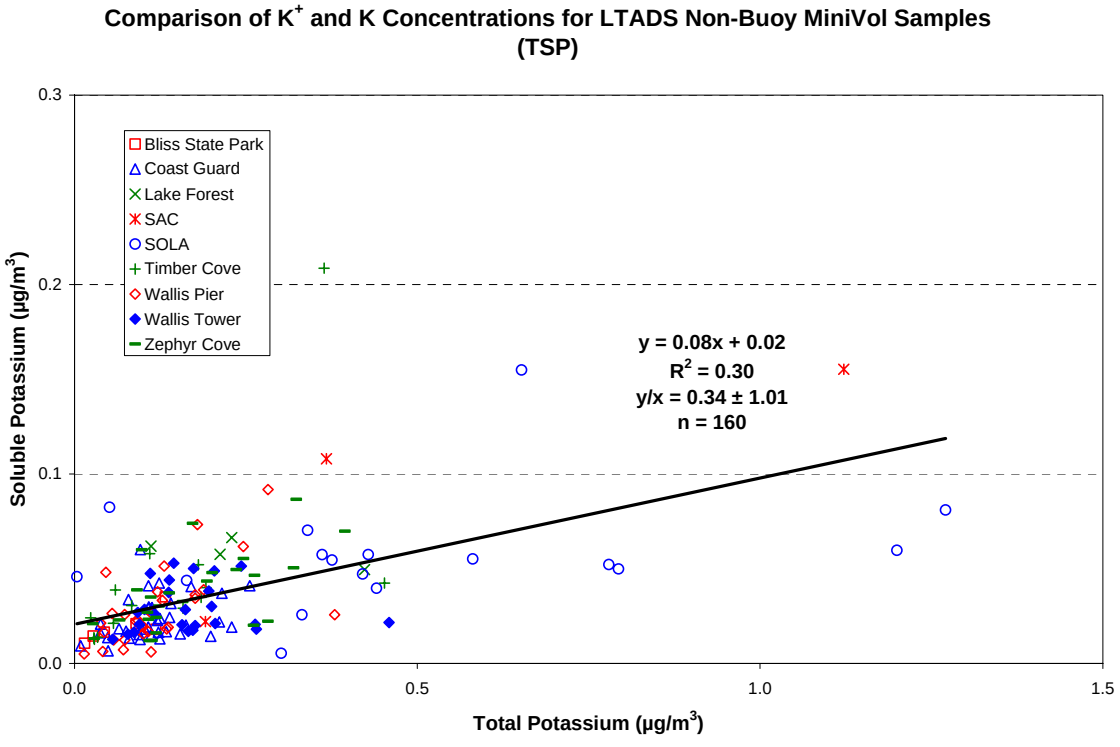

(e)

Figure 3-5, cont'd

3.4.1.5 Ammonium balance

Major ammonium in particles are found in the chemical forms of ammonium nitrate (NH_4NO_3), ammonium sulfate [$(NH_4)_2SO_4$], ammonium bisulfate [$(NH_4)HSO_4$], and ammonium chloride (NH_4Cl). The balance of ammonium can be compared with ammonium to calculated ammonium, which is the sum of ammonium nitrate and ammonium sulfate ($0.29xNO_3^- + 0.192xHSO_4^-$), or the sum of ammonium nitrate and ammonium bisulfate ($0.29 \times NO_3^- + 0.3xSO_4^=$). NH_4Cl was not used for ammonium balance because Lake Tahoe is generally not influenced by sea salt.

The slopes between sulfate based ammonium and measured ammonium are shown in Figure 3-6 (a-c) and were 0.92, 0.85, and 0.71 for TWS TSP, PM_{10}, and $PM_{2.5}$, respectively. These slopes were higher than the bisulfate based ammonium slopes of 0.57, 0.49, and 0.40 for TWS TSP, PM_{10}, and $PM_{2.5}$, respectively. The regression slopes between sulfate and bisulfate based ammonium and measured ammonium (Figure 3-6d) are 1.00 and 0.52 for buoy MiniVol TSP samples with poor correlation (<0.44); those slopes for non-buoy MiniVol TSP samples showed moderate correlation (0.60). This agrees with atmospheric chemistry, where ammonium sulfate is more stable than ammonium bisulfate. The slopes of measured ammonium and sulfate based ammonium were less than unity, which suggests potential excess ammonia in the atmosphere was absorbed onto the quartz-fiber filter. The decreasing slopes between calculated ammonium and measured ammonium as particle size fraction decreases from TSP to $PM_{2.5}$ can be attributed to the sampling artifacts of volatilized ammonium nitrate, which becomes ammonia and nitric acid gas. The disassociated ammonia is absorbed onto the quartz-fiber filter media. Such sampling artifacts are more pronounced at low ammonium nitrate particulate concentrations (Chang et al., 2000; Pathak et al., 2004).

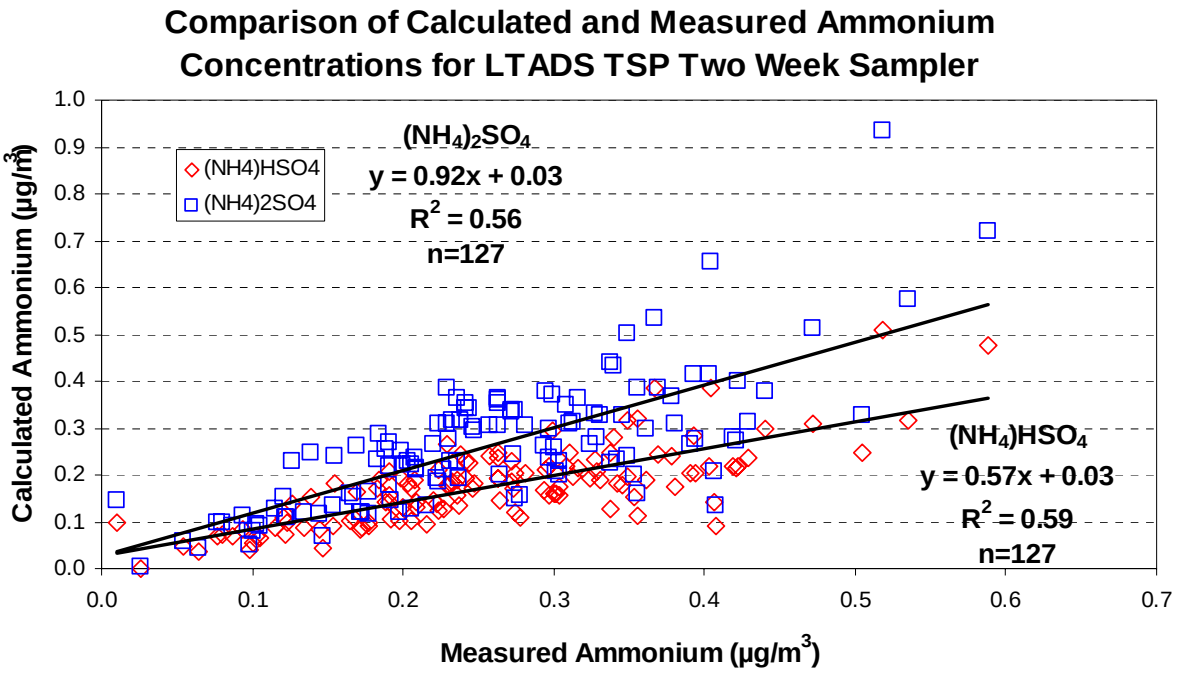

(a)

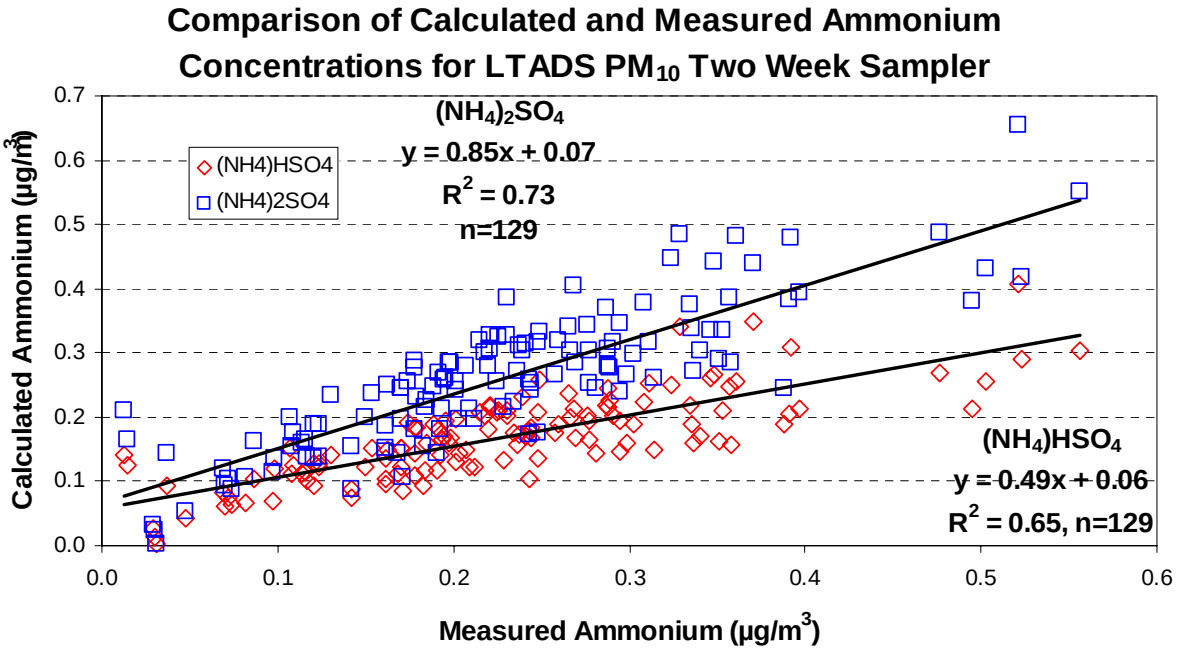

(b)

Figure 3-6. Scatter plot of calculated and measured ammonium concentrations for: a) TSP, b) PM_{10}, c) $PM_{2.5}$, d) Bouy MiniVol TSP, and e) non-Bouy MiniVol TSP.

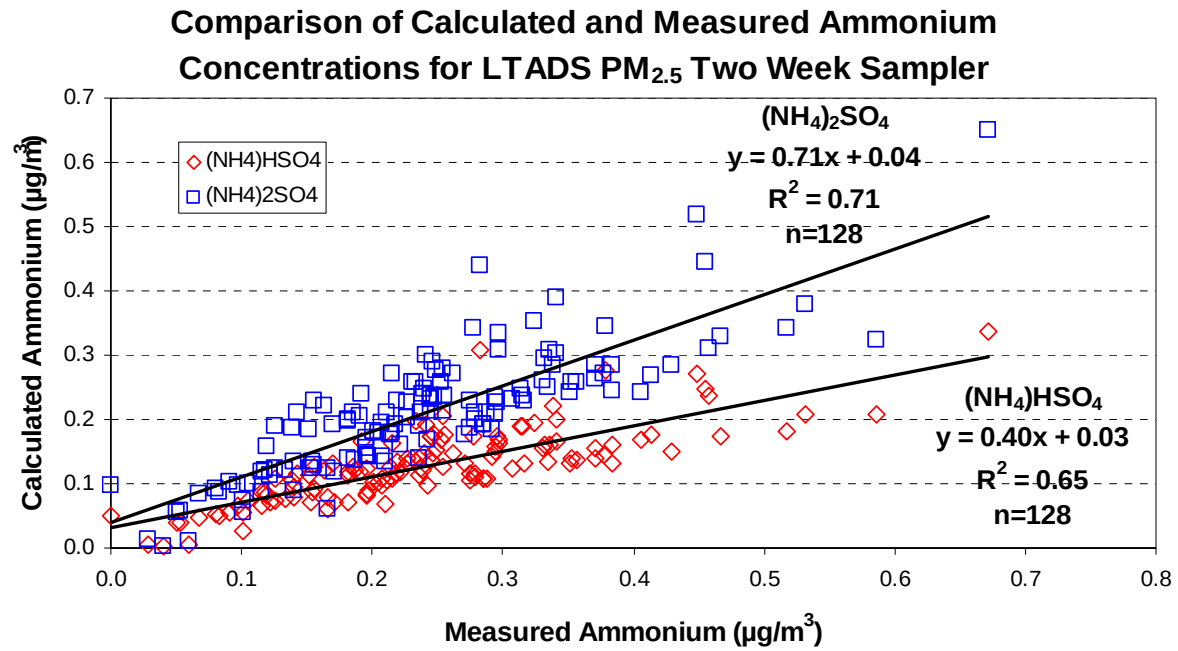

(c)

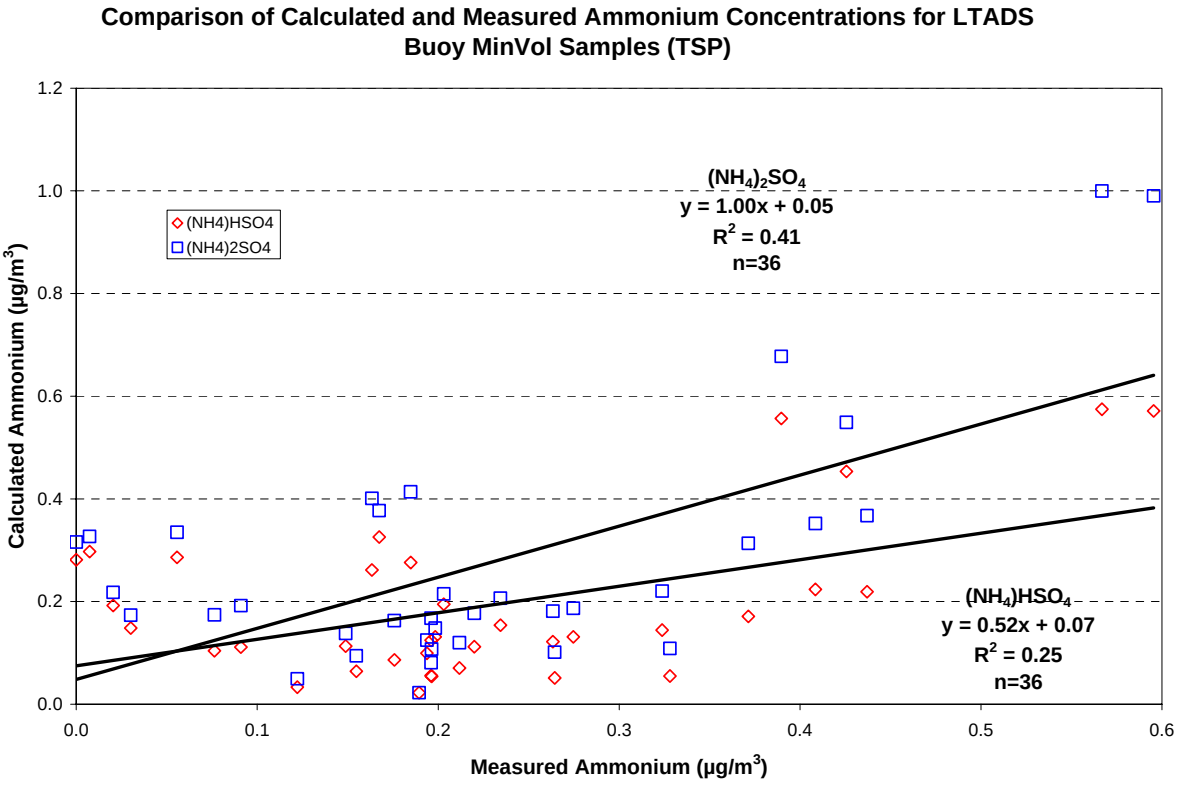

(d)

Figure 3-6, cont'd

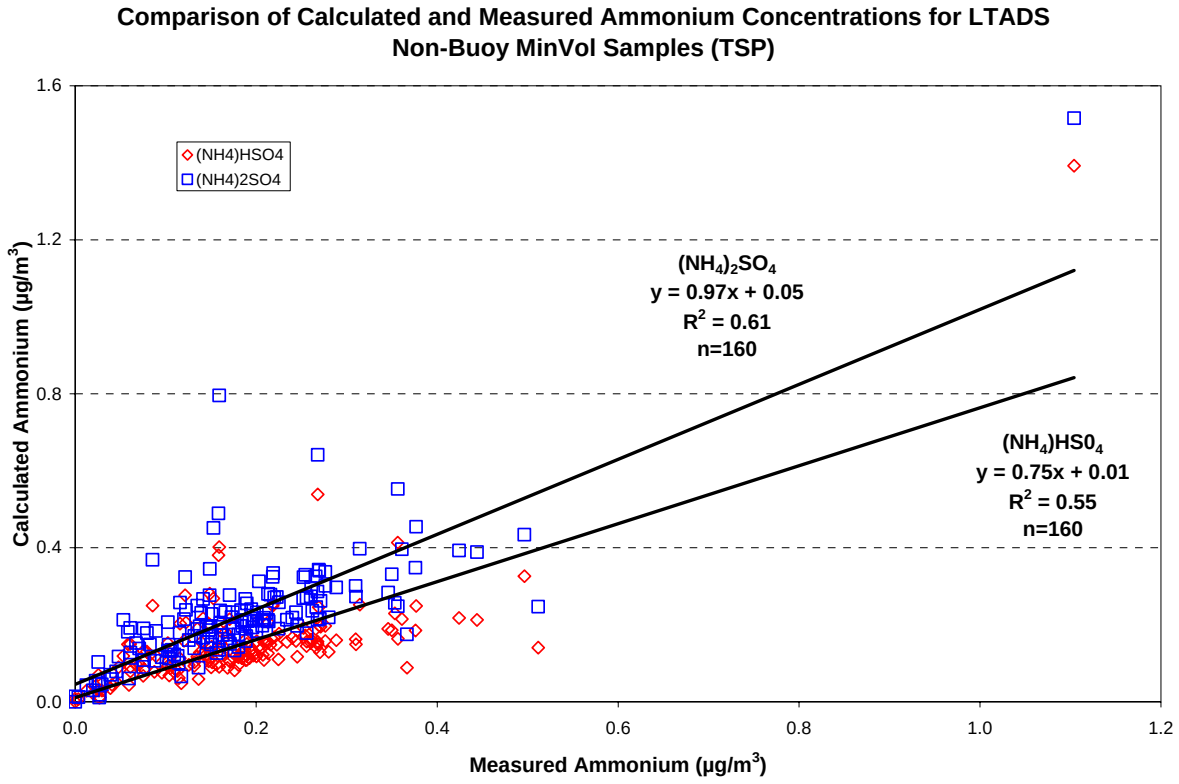

(e)

Figure 3-6, cont'd

3.4.1.6 Anion and cation balance

The balance of anions and cations was calculated by comparing the sum of Cl^-, NO_3^-, and $SO_4^=$ to the sum of NH_4^+, K^+, and Na^+ in microequivalence/m^3. Microequivalence/m^3 of each species is calculated as the product of mass concentration (in µg/m^3) divided by the atomic weight of the chemical species multiplied by the species' charge. Therefore,

$$\text{Microequivalence/m}^3 \text{ for anion} = C_{m,Cl^-}/35.453 + C_{m,NO3^-}/62 + C_{m,SO4^=}/98x2$$
$$\text{Microequivalence/m}^3 \text{ for cations} = C_{m,NH4^+}/18 + C_{m,K^+}/39.1 + C_{m,Na^+}/23$$

Figure 3-7 (a-c) shows plots of anion and cation balance in microequivalence/m^3 for TWS TSP, PM_{10}, and $PM_{2.5}$. The slopes are within the range of 0.65-0.67 for all particle sizes, and have moderate correlation (r^2=0.65-0.69). The ratios between anions and cations for TWS TSP, PM_{10}, and $PM_{2.5}$ were 0.84±0.23, 0.94±0.27, and 0.92±0.98, respectively. The slopes between anions and cations are 1.14 (r^2=0.67) and 1.08 (r^2=0.75), and average ratios are 1.14±0.66 and 1.1±0.62 for bouy and non-bouy MiniVol TSP samples, respectively. The slightly difference between the average ratio of anion and cations versus slopes for TWS samples were because the slopes are more sensitive to high and low concentrations in the data. However, each pair of anion and cation data was weighed equally in ratio. The average $PM_{2.5}$ anion and cation ratio was 11.6 measured at the TB site on 05/07/03, which is suspected to be an outlier.

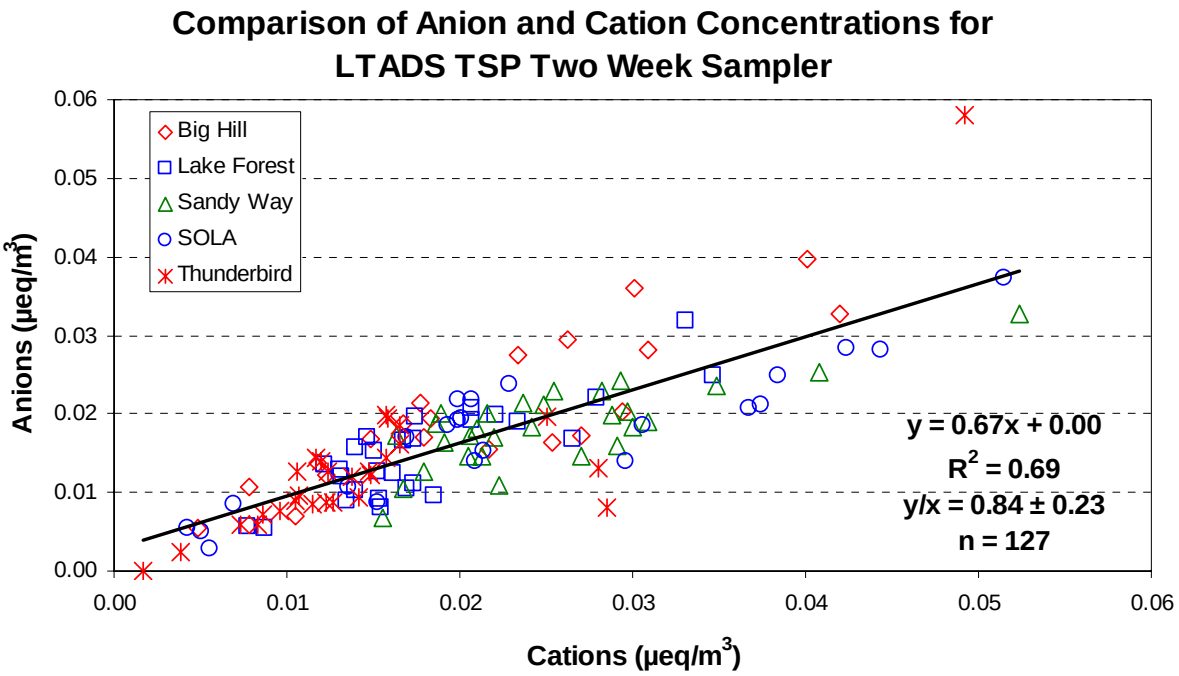

(a)

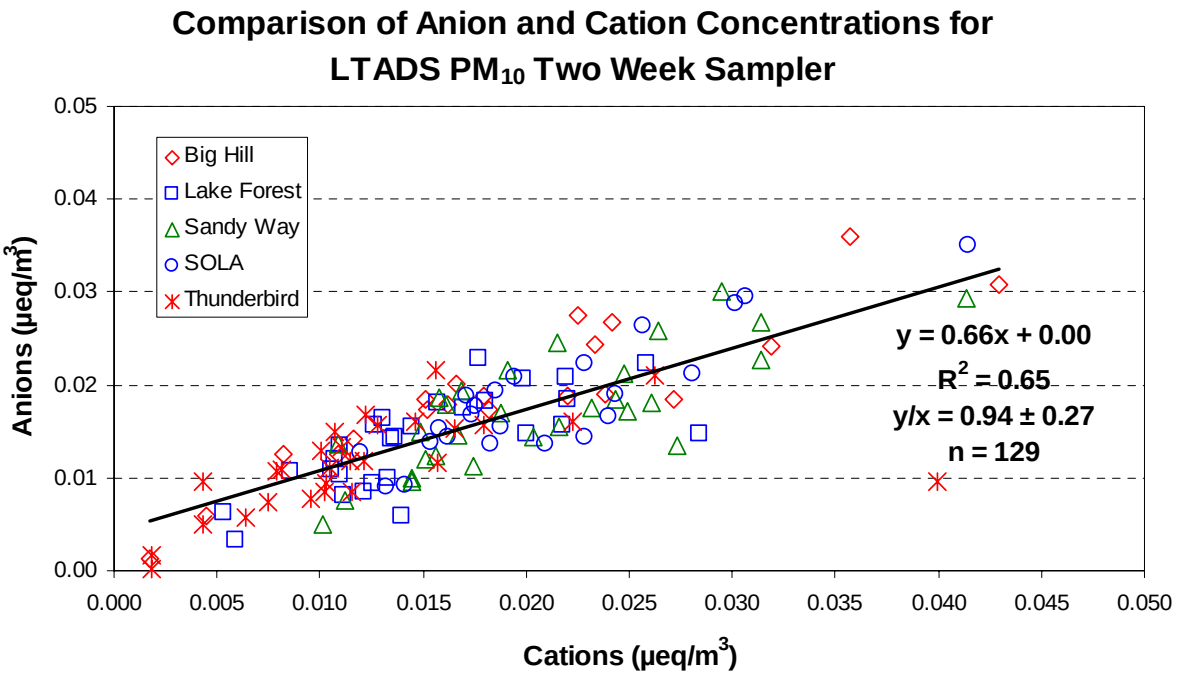

(b)

Figure 3-7. Scatter plot of anion and cation balance in microequivalence/m^3 for: a) TSP, b) PM_{10}, c) $PM_{2.5}$, d) Bouy MiniVol TSP, and e) non-Bouy MiniVol TSP.

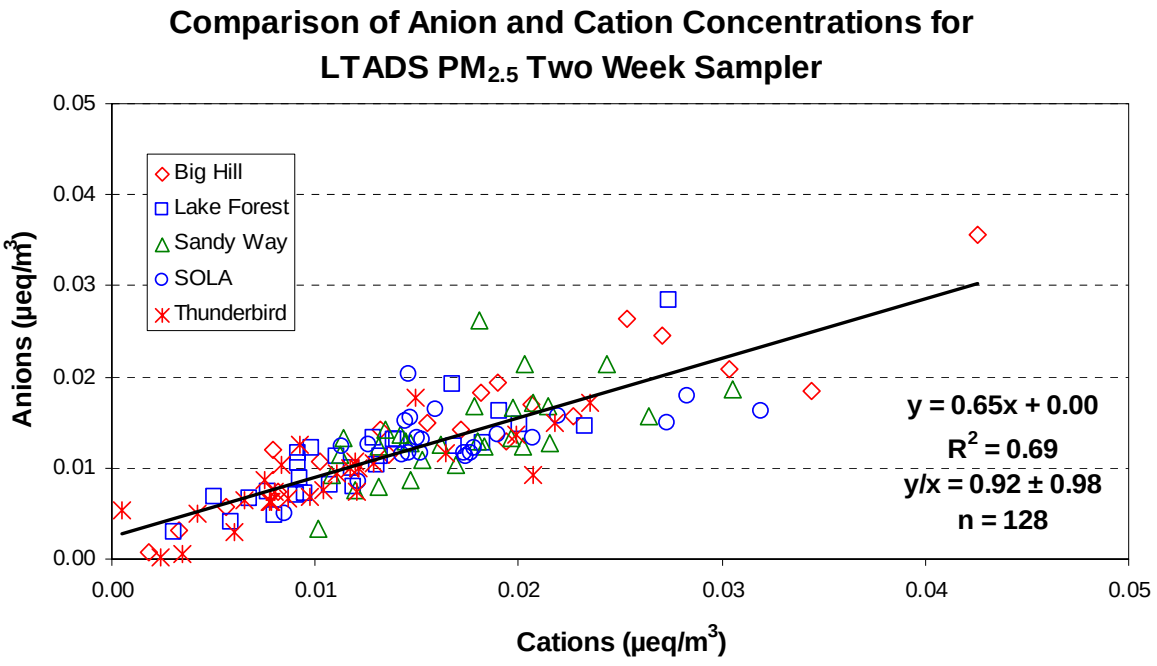

(c)

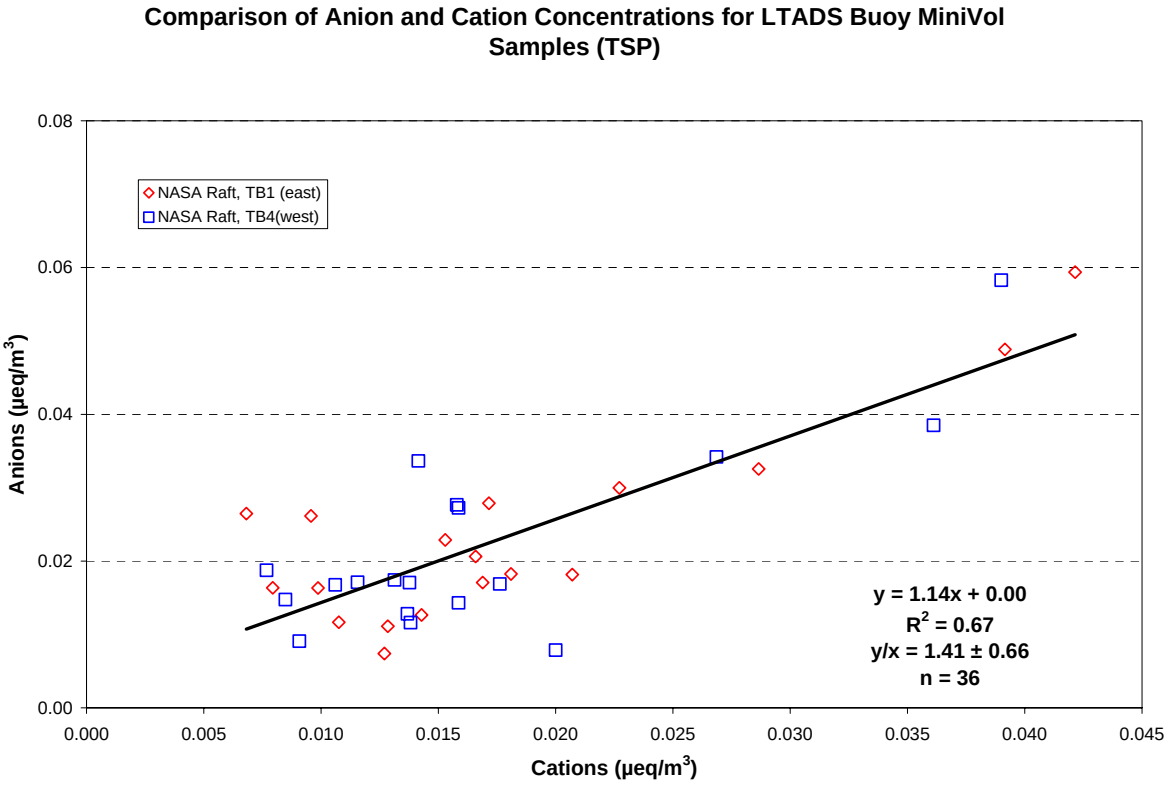

(d)

Figure 3-7, cont'd

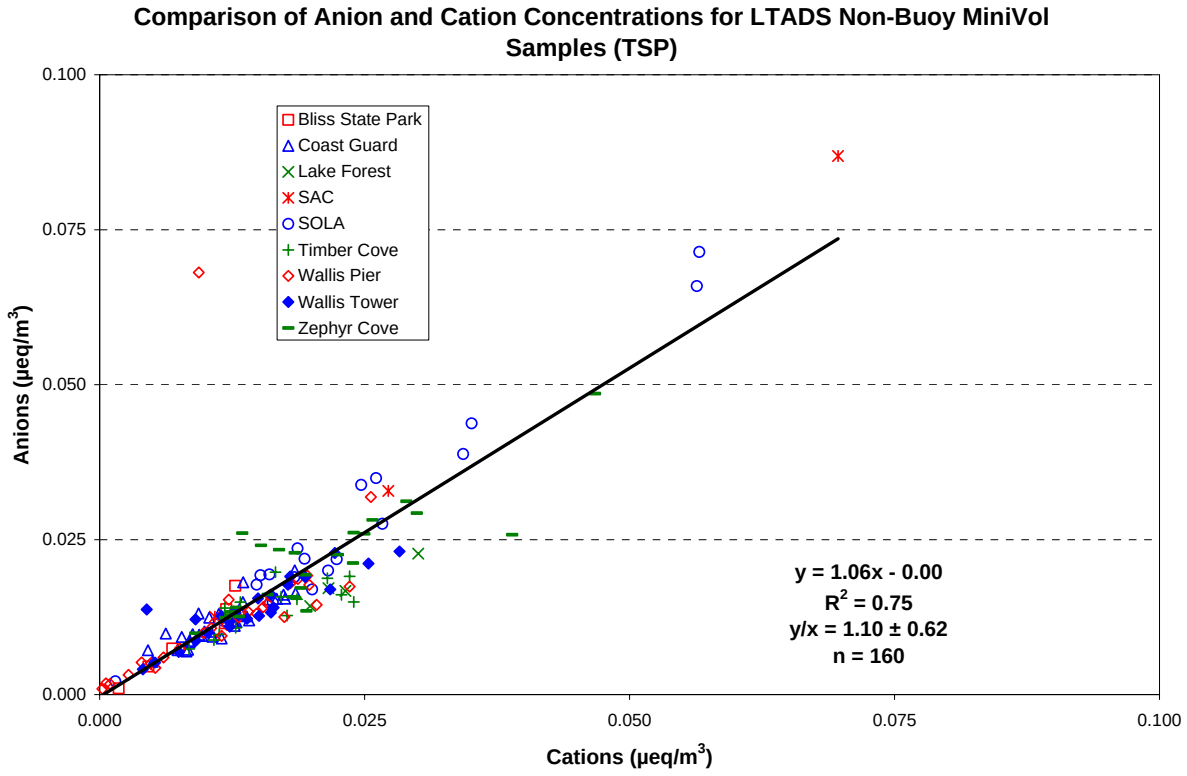

(e)

Figure 3-7, cont'd

3.4.1.7 Gas/Particle equilibrium of semi-volatile organic compounds

One significant parameter that can greatly affect aerosol sampling accuracy is the measurement of semi-volatile species such as OC and ammonium nitrate. The sampling bias is the result of positive artifacts due to the adsorption of semi-volatile species onto the quartz-fiber filter and/or negative artifacts of evaporation from the filter during sampling, due to the gas/aerosol equilibrium. The other parameters that can result in sampling bias include: 1) the types of aerosol samplers: in general, less volatilization of aerosols and adsorption of gaseous species in the impactor than the filter sampling system, 2) the disassociation constant of semi-volatile compound as the function of aerosol temperature and RH, and 3) ratio of gas to particles of the semi-volatile organic compounds (SVOCs; Chang et al 2000b; Eatough et al. 1990; McDow and Huntsiker, 1990, Turpin et al. 1994; Stelson and Seinfeld, 1982; Zhang and McMurry 1987, 1992).

Several denuding and backup filter sampling configurations for SVOCs have been applied to evaluate these artifacts. In general, a denuder is placed before the aerosol sampler to remove gaseous species prior to aerosol collection. A quartz-fiber filter collects the SVOCs in particle phase and another quartz-fiber placed in a different sampling channel, after the Teflon-membrane filter, quantifies the volatized aerosols (Watson and Chow, 2002). Nevertheless, the removal of gaseous species with denuder can affect the gas-to-particle equilibrium and the evaluation of sampling artifact.

In LATADS, the evaluation of sampling artifacts, other than SVOCs, was evaluated by the TWS, assuming all nitrate measured is in the form of NH_4NO_3 and in $PM_{2.5}$. Figure 3-8 compares the ratios of NO_3^- measured on the backup quartz-fiber filter behind the front Teflon-membrane filter to: 1) NH_4NO_3 measured on the front quartz-fiber filter, and 2) the sum of non-volatilized NH_4NO_3 measured on the front quartz-fiber filter plus the volatilized NH_4NO_3 measured on the backup quartz-fiber filter, as a function of total NH_4NO_3 in the TWS $PM_{2.5}$ samples. The plot shows that at all sites, the NH_4NO_3 concentrations on the backup filter (i.e., volatilization of NH_4NO_3) is at least 20% and as much as 100% of the non-volatilized NH_4NO_3 from the front filter. No correlation was observed between the volatilization of NH_4NO_3 particles with total particulate NH_4NO_3. This can be explained by the disassociation constant of particulate NH_4NO_3 as a function of temperature and RH of sampling air. Such parameters will vary throughout the two-week sampling period.

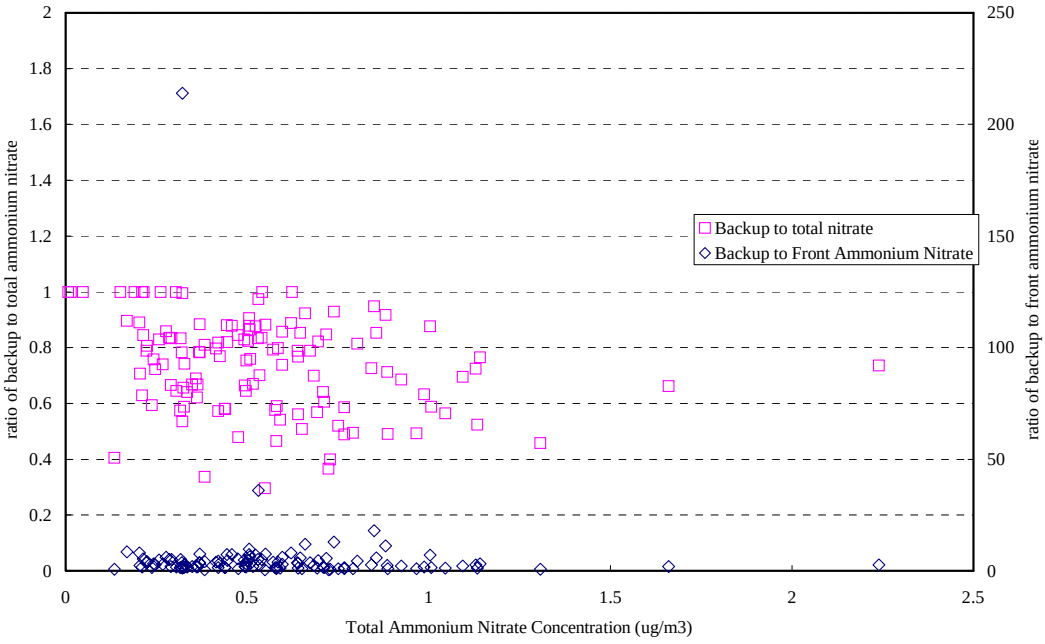

Figure 3-8. Relationship between the ratio of the backup to total and front ammonium nitrate as a function of total ammonium nitrate in TWS $PM_{2.5}$ during the Lake Tahoe Ambient Deposition Study (LTADS).

3.4.1.8 Reconstructed mass versus measured mass

Major PM components were used to reconstruct PM mass, including: 1) soil material, which is estimated as 1.63xAl+2.49xSi+2.2xCa+1.94xTi+2.42xFe (to account for unmeasured oxides; IMPROVE); 2) organic matter (1.4xOC; IMPROVE) to account for unmeasured hydrogen and oxygen; 3) soot (EC); 4) sulfate (3xsulfur); 5) total nitrate (front filter nitrate + volatilized nitrate

measured on the backup filter [for TWS only]); 6) ammonium (front filter ammonium + calculated backup filter ammonium [14/62xbackup filter nitrate]); 7) noncrustal trace elements (sum of elements measured by XRF other than Al, Si, Ca, Ti, and Fe); and 8) salt (1.65xCl). Scatter plots of reconstructed mass and measured mass are shown in Figure 3-9(a-c) for TWS TSP, PM_{10}, and $PM_{2.5}$ respectively; Figure 3-8(d, e) for bouy and non-bouy MiniVol TSP samples, respectively.

The slope between the reconstructed and measured TWS TSP mass concentrations was 0.69 with a moderate correlation of 0.63. If the sample collected at the Lake Forest site on 12/04/02 is excluded, the slope would increases to 0.99 (with an intercept of 1.55) and a high correlation of 0.93, which would show excellent mass balance. TWS PM_{10} samples collected on 01/02/03 and 01/15/03 at the LF site and on 01/03/03 and 01/14/03 at the SOLA site were suspected as outliers, which resulted in a slope of 0.89 with a moderate correlation of 0.59 (as shown in Figure 3-8b). If these observations are removed, the slope would be 1.02 (with an intercept of 1.24) and a high correlation of 0.90. Nevertheless, the ratios between reconstructed and measured mass concentrations are 1.12±0.27, 1.14±0.31, and 1.21±0.41 for TWS TSP, PM_{10} and $PM_{2.5}$, respectively, which are very close to unity. The slopes of reconstructed and measured mass for buoy and non-buoy MiniVol TSP samples are less than unity with moderate to high r^2; the average ratios of those are close to unity, but with high standard variation.

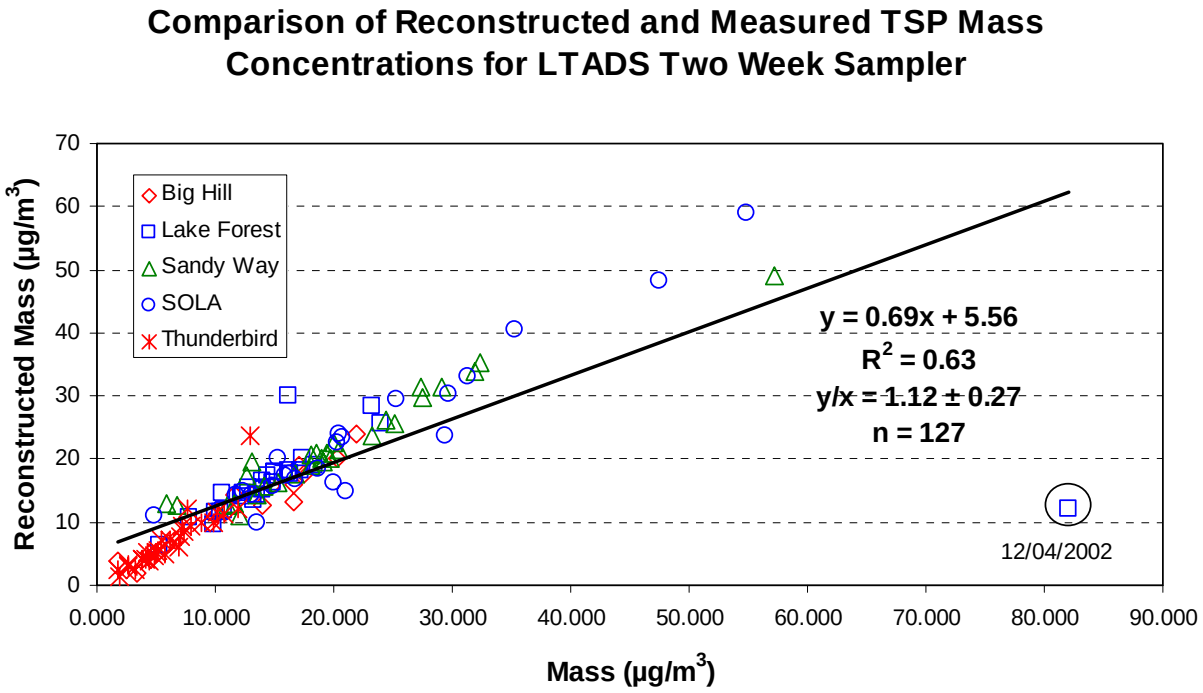

(a)

Figure 3-9. Scatter plots of comparing reconstructed and measured mass at all five sites for: a) TSP, b) PM_{10}, c) $PM_{2.5}$, d) Bouy MiniVol TSP, and e) non-Bouy MiniVol TSP.

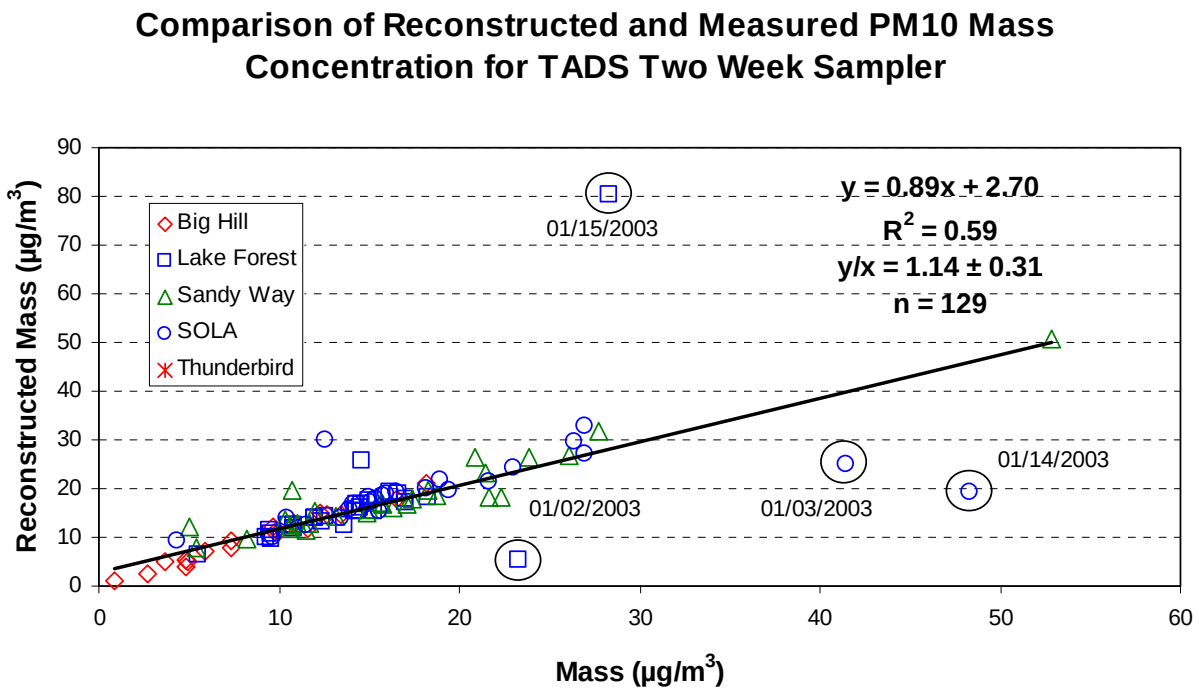

(b)

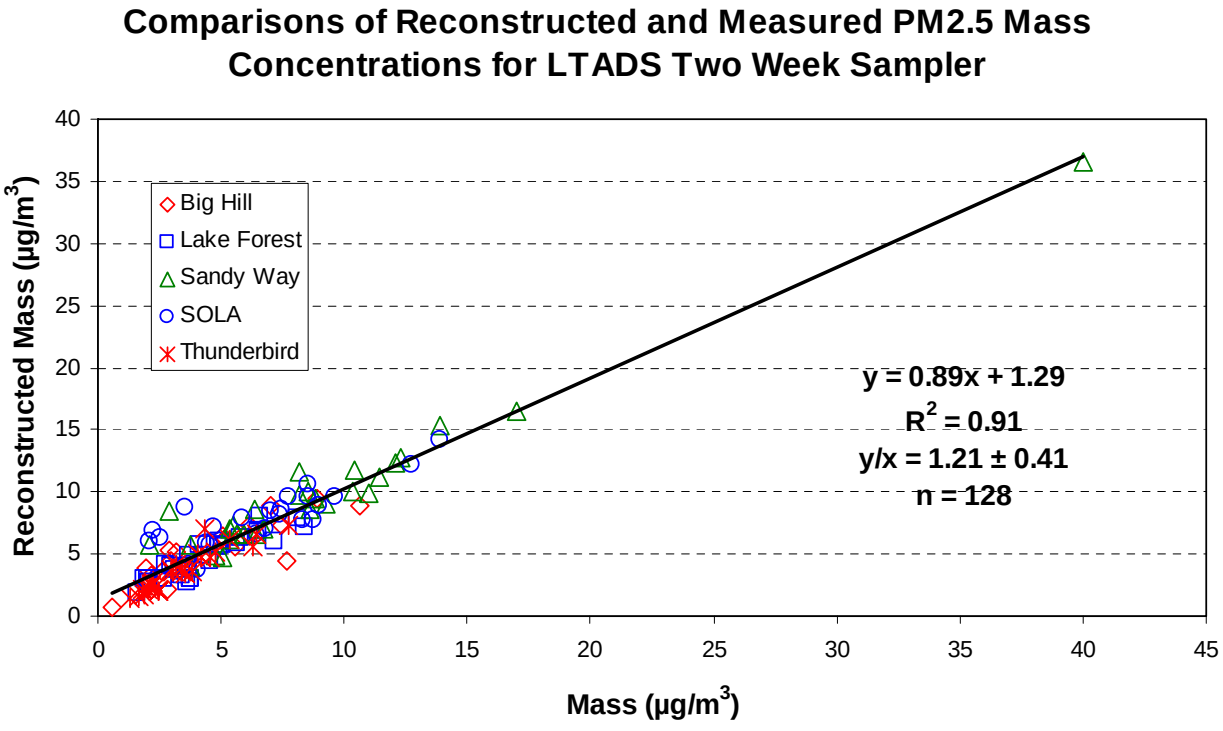

(c)

Figure 3-9, cont'd

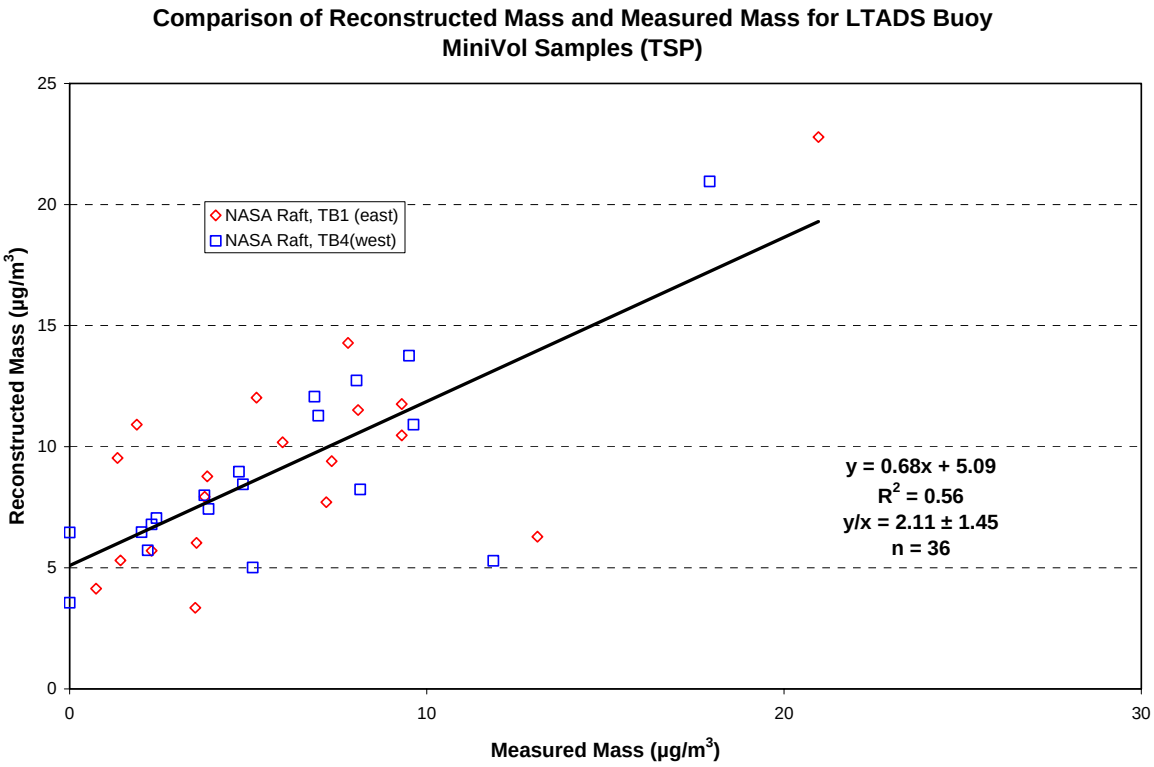

(d)

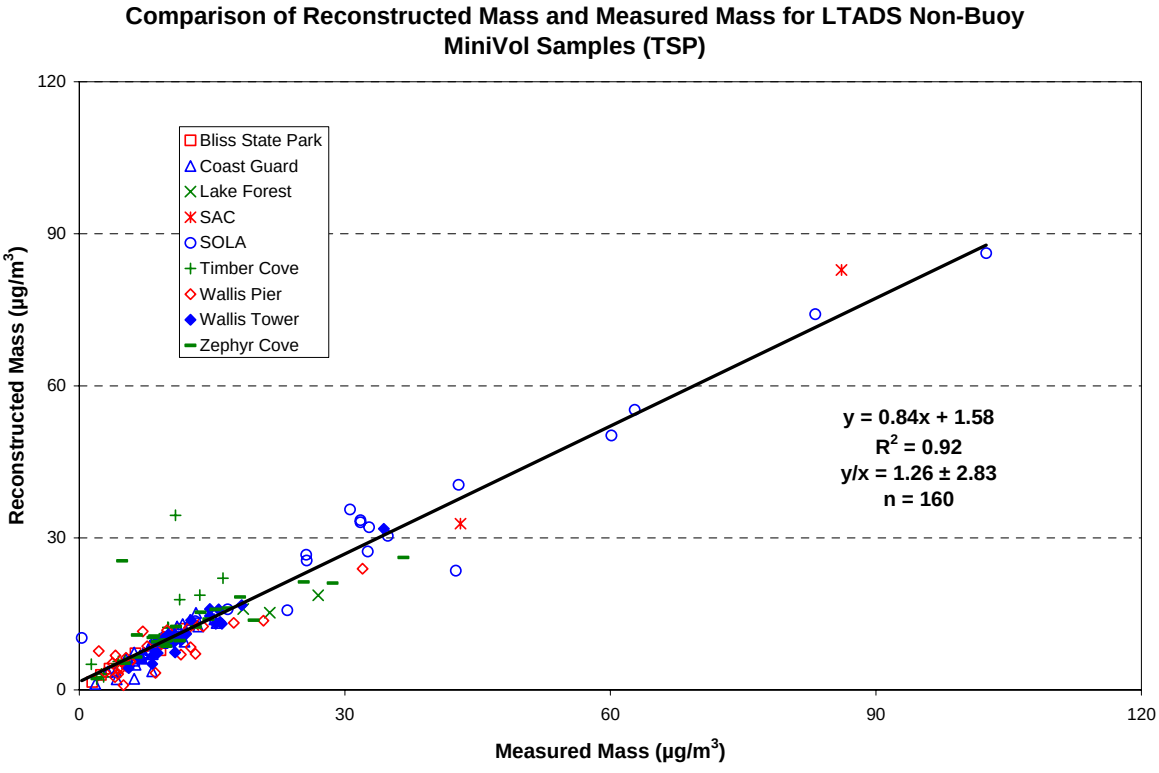

(e)

Figure 3-9, cont'd

4. CHEMICAL SPECIATION AND SPATIAL DISTRIBUTION OF PARTICULATE MEASUREMENTS IN LTADS

Due to the complex sampling matrix, scatter plots of TWS sampling durations at the BH, LF, TB, SW, and SOLA sites are shown in Figure 4-1(a-c). In general, good contemporaneous TWS sampling durations were found at these sites, with the exception of sampling at the BH site that began approximately three months later in late February 2003 due to storm damage.

MiniVol sampler sampling location (buoy and non-buoy), duration, and number of samples collected are summarized in Table 4-1, which shows that the average sampling duration (which exceeded 140 hours) and the number of samples collected (more than 20) were the most comparable to the following five sites: Coast Guard, Wallis Pier, Zephyr Cove, Wallis Tower, and SOLA. The sampling durations at these sites are plotted in Figure 4-1(d) but a clear pattern for contemporaneous sampling did not emerge; therefore, the spatial and temporal variations of the MiniVol samples are difficult to characterize and will not be discussed here.

Table 4-1. Number of samples and sampling duration for MiniVol samplers

Site Name	Number of Samples Collected	Average Sampling Duration (hours)*	Minimum Sampling Duration (hours)*	Maximum Sampling Duration (hours)*
Bliss State Park	6	165.08	65.60	283.50
Coast Guard	44	178.88	38.60	338.50
Lake Forest	8	182.55	117.10	298.60
SAC	5	138.64	90.30	240.30
SOLA	20	245.54	55.00	368.00
Timber Cove	14	43.21	11.50	60.30
Wallis Pier	39	148.93	14.30	341.90
Wallis Tower	30	168.08	59.50	338.70
Zephyr Cove	37	160.18	4.10	394.00
NASA Raft, TB1 (east)	21	29.96	24.00	47.10
NASA Raft, TB4(west)	21	29.28	14.80	48.20

* Data shown for only when both Quarz and Teflon filters were collected for the same time period

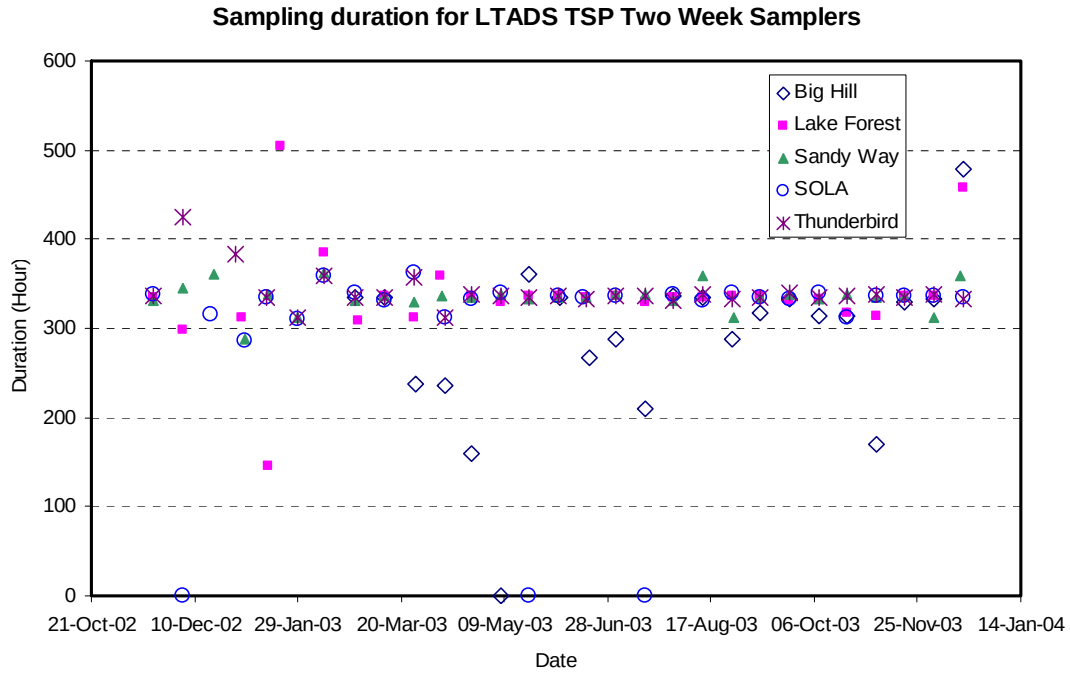

(a)

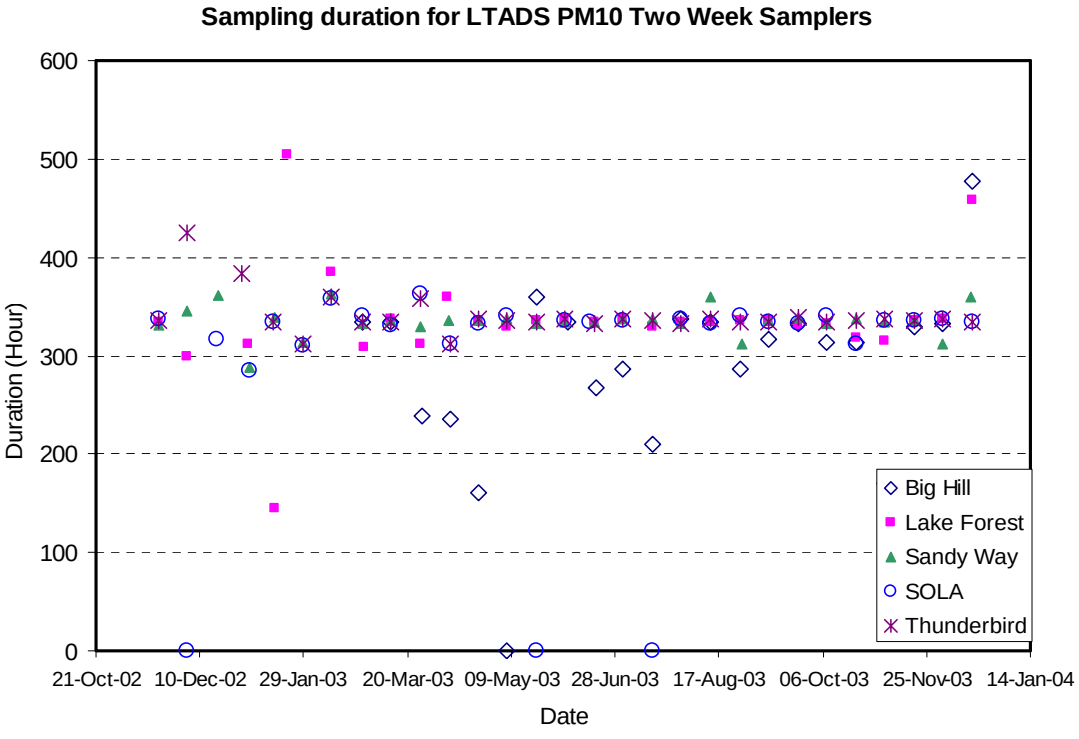

(b)

Figure 4-1 Scatter plots of sampling duration at different sites for: a) TSP two week samplers, b) PM_{10} two week samplers, c) $PM_{2.5}$ two week samplers, and d) buoy and non-buoy MiniVol (TSP) sampler (only sites with total sample number >20 based on Table 4-1).

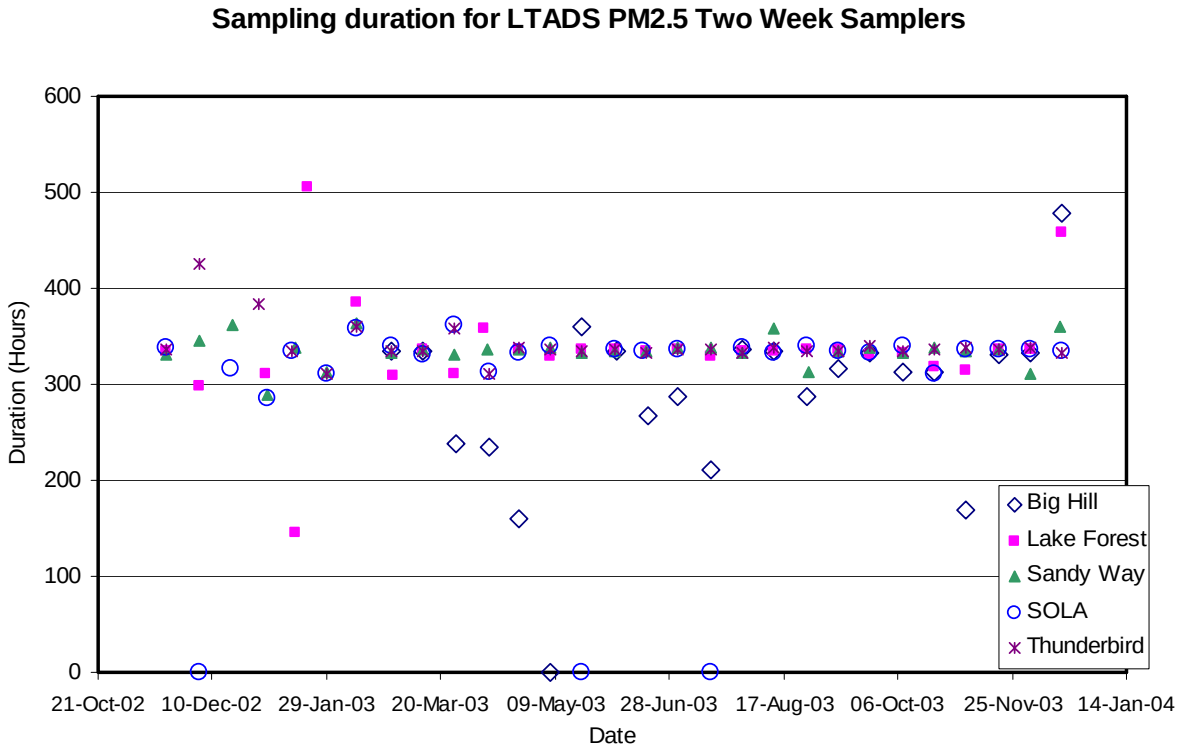

(c)

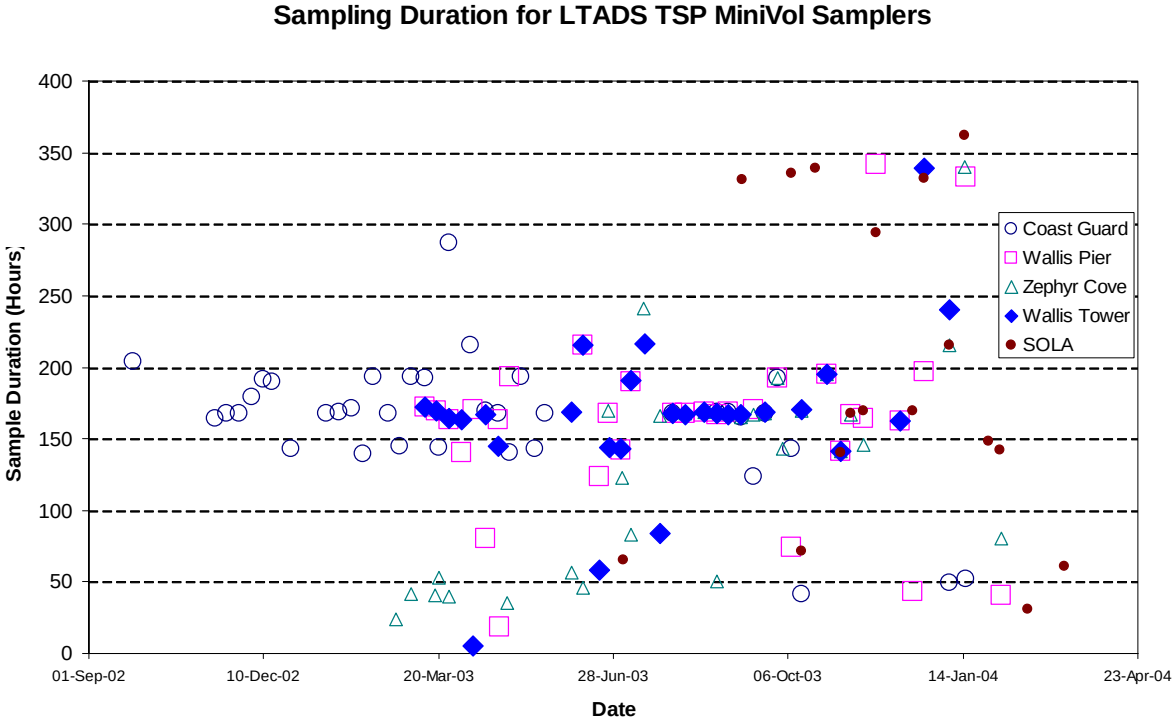

(d)

Figure 4-1, cont'd

4.1 Statistical Summary of TWS TSP, PM_{10}, and $PM_{2.5}$ Mass and Chemical Concentrations

Table 4-2(a-c) presents the annual averages for TWS TSP, PM_{10}, and $PM_{2.5}$ mass and chemical fractions concentrations from November 2002 to December 2003 at the BH, LF, TB, SW, and SOLA sites. The highest annual average TSP mass concentration was found at the SOLA site (21.9 $\mu g/m^3$), followed by the SW (20.1 $\mu g/m^3$), LF (14.5 $\mu g/m^3$), BH (11.4 $\mu g/m^3$), and TB (6.2 $\mu g/m^3$) sites. The most abundant chemical species (>1%) in TSP were OC (16.5-29.8%), silicon (10.8-16.0%), aluminum (3.9-4.7%), EC (2.5-6.2%), calcium (1.7-2.4%), iron (2.1-2.7%), potassium (1.3-1.4%), nitrate (1.2-3.5%), ammonium (1.2-3.3%), and sulfur (1.1-3.4%).

Annual average PM_{10} mass concentration was highest at the SOLA site (18.8 $\mu g/m^3$), followed by the SW (16.8 $\mu g/m^3$), LF (14.0 $\mu g/m^3$), BH (8.8 $\mu g/m^3$), and TB (6.0 $\mu g/m^3$) sites. The most abundant chemical species in PM_{10} were OC (16.2-27.8%), silicon (10.0-21.1%), aluminum (3.5-6.7%), EC (3.0-7.0%), iron (1.8-3.3%), calcium (1.6-2.9%), nitrate (1.3- 3.6%), ammonium (1.3-3.2%), potassium (1.2-1.7%), and sulfur (1.2%-3.5%).

The highest annual average $PM_{2.5}$ mass concentration was found at the SW site (9.0 $\mu g/m^3$), followed by the SOLA (6.5 $\mu g/m^3$), BH (5.0 $\mu g/m^3$), LF (4.3 $\mu g/m^3$), and TB (3.6 $\mu g/m^3$) sites. The most abundant chemical species in $PM_{2.5}$ were OC (42- 51%), EC (4.9- 16.4%), ammonium (3.1-5.8%), sulfur (2.2-5.7%), nitrate (1.6-3.4%), and silicon (1.3- 2.6%).

The lowest annual average PM_{10} and $PM_{2.5}$ mass concentrations were observed at the TB site and the highest PM_{10} and $PM_{2.5}$ mass concentrations were observed at the SOLA and SW sites. Mass concentrations of TSP, PM_{10} and $PM_{2.5}$ at the BH site were higher than those at the TB site. Similar trends were found for OC, EC, nitrate, ammonium, and sulfate concentrations in PM_{10} and $PM_{2.5}$. PM_{10} and $PM_{2.5}$ OC and EC concentrations at the SW and SOLA sites were two to three times greater than those at the LF and TB sites, which could be explained by the influence of greater traffic volumes and population density at the South Lake Tahoe sites (i.e., SOLA and SW).

These results agree with the assumed characteristics of the sites identified for the LTADS: the TB site represents a local background site and the SOLA and SW sites represent urban sites. $PM_{2.5}$ mass and chemical concentrations were lower at the TB site than those at the BH site, which suggests that PM losses due to deposition and settling during transportation from the BH site to the Lake Tahoe region. Silicon and aluminum concentrations at these in-basin sites were high in PM_{10} but low in $PM_{2.5}$, which suggests a significant contribution of resuspended dust to coarse particles.

Table 4-2a. Annual average TSP mass and chemical fractions for Two Week Samplers

	Big Hill		Thunderbird		Lake Forest		Sandy Way		SOLA	
	Average Concentration (ug/m3)	% Mass	Average Concentration (ug/m3)	% Mass	Average Concentration (ug/m3)	% Mass	Average Concentration (ug/m3)	% Mass	Average Concentration (ug/m3)	% Mass
Number in Average	19		28		28		29		25	
Mass	11.355	100.000	6.206	100.000	16.466	100.000	20.118	100.000	21.895	100.000
Volatalized Nitrate	0.833	7.340	0.429	6.907	0.345	2.093	0.671	3.335	0.446	2.037
Chloride	0.009	0.079	0.026	0.415	0.090	0.549	0.089	0.444	0.167	0.761
Nitrite	0.000	0.000	0.000	0.000	0.000	0.000	0.000	0.000	0.000	0.000
Nitrate	0.394	3.470	0.171	2.753	0.205	1.246	0.382	1.899	0.373	1.705
Phosphate	0.000	0.000	0.000	0.000	0.000	0.000	0.000	0.000	0.000	0.000
Sulfate	0.655	5.768	0.452	7.285	0.435	2.643	0.470	2.335	0.331	1.512
Ammonium	0.305	2.689	0.206	3.314	0.214	1.302	0.318	1.579	0.258	1.178
Soluble Sodium	0.075	0.663	0.056	0.905	0.111	0.671	0.137	0.683	0.187	0.856
Soluble Magnesium	0.012	0.107	0.010	0.161	0.012	0.074	0.015	0.072	0.012	0.057
Soluble Potassium	0.047	0.417	0.034	0.549	0.046	0.282	0.063	0.311	0.045	0.204
Soluble Calcium	0.109	0.958	0.080	1.296	0.117	0.708	0.144	0.717	0.165	0.752
O1TC	0.106	0.934	0.063	1.010	0.097	0.586	0.420	2.087	0.280	1.277
O2TC	0.304	2.677	0.213	3.432	0.321	1.951	0.920	4.572	0.661	3.021
O3TC	1.170	10.304	0.846	13.628	1.437	8.728	3.269	16.247	2.468	11.274
O4TC	0.487	4.289	0.350	5.644	0.588	3.572	1.157	5.749	0.869	3.967
OPTC	0.241	2.125	0.185	2.987	0.277	1.682	0.240	1.194	0.205	0.935
OCTC	2.308	20.329	1.657	26.701	2.720	16.518	6.005	29.849	4.483	20.473
E1TC	0.342	3.012	0.265	4.268	0.481	2.919	1.129	5.610	0.986	4.503
E2TC	0.171	1.505	0.156	2.521	0.270	1.642	0.340	1.690	0.321	1.464
E3TC	0.016	0.138	0.009	0.150	0.018	0.108	0.028	0.138	0.016	0.074
ECTC	0.287	2.531	0.245	3.953	0.492	2.988	1.256	6.243	1.118	5.106
TCTC	2.596	22.860	1.902	30.654	3.212	19.506	7.261	36.093	5.601	25.580
Sodium	0.029	0.258	0.019	0.303	0.053	0.323	0.042	0.211	0.050	0.227
Magnesium	0.012	0.106	0.017	0.270	0.024	0.144	0.011	0.054	0.016	0.071
Aluminum	0.529	4.658	0.255	4.102	0.839	5.096	0.779	3.873	1.006	4.595
Silicon	1.230	10.830	0.767	12.356	2.643	16.049	2.556	12.703	3.472	15.859
Phosphorus	0.000	0.001	0.000	0.005	0.001	0.008	0.001	0.003	0.001	0.003
Sulfur	0.291	2.561	0.211	3.403	0.215	1.305	0.222	1.103	0.236	1.079
Chlorine	0.004	0.037	0.006	0.099	0.084	0.512	0.119	0.591	0.203	0.928
Potassium	0.151	1.328	0.089	1.432	0.212	1.289	0.263	1.307	0.307	1.403
Calcium	0.180	1.586	0.121	1.943	0.388	2.359	0.334	1.661	0.460	2.101
Titanium	0.024	0.210	0.011	0.181	0.047	0.288	0.043	0.214	0.050	0.227
Vanadium	0.001	0.005	0.000	0.007	0.001	0.006	0.001	0.006	0.001	0.004
Chromium	0.001	0.005	0.000	0.004	0.001	0.004	0.001	0.004	0.001	0.004
Manganese	0.008	0.067	0.003	0.050	0.009	0.053	0.009	0.044	0.011	0.049
Iron	0.263	2.315	0.130	2.100	0.446	2.708	0.458	2.276	0.596	2.724
Cobalt	0.002	0.017	0.001	0.015	0.004	0.023	0.004	0.018	0.005	0.022
Nickel	0.000	0.003	0.000	0.003	0.000	0.002	0.000	0.002	0.000	0.002
Cupper	0.009	0.077	0.002	0.028	0.003	0.019	0.007	0.033	0.006	0.027
Zinc	0.008	0.067	0.004	0.063	0.008	0.046	0.017	0.083	0.019	0.085
Gallium	0.000	0.001	0.000	0.002	0.000	0.000	0.000	0.000	0.000	0.000
Arsenic	0.000	0.001	0.000	0.002	0.000	0.001	0.000	0.002	0.000	0.001
Selenium	0.000	0.001	0.000	0.001	0.000	0.000	0.000	0.000	0.000	0.000
Bromine	0.001	0.013	0.001	0.021	0.001	0.009	0.002	0.008	0.002	0.008
Rubidium	0.001	0.006	0.000	0.005	0.001	0.004	0.001	0.005	0.001	0.005
Strontium	0.001	0.010	0.001	0.015	0.006	0.039	0.004	0.021	0.006	0.028
Yttrium	0.000	0.003	0.000	0.005	0.000	0.002	0.000	0.002	0.000	0.002
Zirconium	0.000	0.004	0.000	0.004	0.002	0.010	0.001	0.006	0.002	0.007
Molybdenum	0.000	0.003	0.000	0.002	0.000	0.002	0.000	0.001	0.000	0.001
Palladium	0.000	0.002	0.000	0.003	0.000	0.001	0.000	0.001	0.000	0.001
Silver	0.000	0.002	0.000	0.003	0.000	0.002	0.000	0.001	0.000	0.002
Cadmium	0.000	0.001	0.000	0.003	0.000	0.002	0.000	0.002	0.000	0.001
Indium	0.001	0.007	0.000	0.006	0.000	0.002	0.001	0.003	0.001	0.003
Tin	0.001	0.013	0.001	0.023	0.001	0.009	0.001	0.007	0.002	0.007
Antimony	0.001	0.011	0.001	0.019	0.001	0.007	0.001	0.006	0.001	0.005
Barium	0.005	0.046	0.006	0.097	0.013	0.080	0.013	0.063	0.021	0.095
Lanthanum	0.008	0.071	0.007	0.118	0.006	0.038	0.005	0.023	0.006	0.028
Gold	0.000	0.001	0.000	0.002	0.000	0.001	0.000	0.001	0.000	0.001
Mercury	0.000	0.001	0.000	0.002	0.000	0.001	0.000	0.000	0.000	0.001
Thallium	0.000	0.001	0.000	0.001	0.000	0.001	0.000	0.000	0.000	0.001
Lead	0.001	0.010	0.001	0.015	0.001	0.008	0.002	0.008	0.001	0.006
Uranium	0.000	0.001	0.000	0.003	0.000	0.001	0.000	0.001	0.000	0.001

Table 4-2b. Annual average PM_{10} mass and chemical fractions for Two Week Samplers

	Big Hill		Thunderbird		Lake Forest		Sandy Way		SOLA	
	Average Concentration (ug/m3)	% Mass	Average Concentration (ug/m3)	% Mass	Average Concentration (ug/m3)	% Mass	Average Concentration (ug/m3)	% Mass	Average Concentration (ug/m3)	% Mass
Number in Average	19		28		28		29		25	
Mass	8.814	100.000	5.957	100.000	13.981	100.000	16.762	100.000	18.822	100.000
Volatalized Nitrate	0.519	5.885	0.243	4.082	0.270	1.933	0.559	3.332	0.482	2.560
Chloride	0.022	0.254	0.016	0.275	0.050	0.360	0.065	0.387	0.111	0.591
Nitrite	0.007	0.076	0.000	0.000	0.000	0.000	0.000	0.000	0.000	0.000
Nitrate	0.313	3.556	0.131	2.205	0.182	1.304	0.329	1.963	0.346	1.838
Phosphate	0.004	0.041	0.000	0.000	0.004	0.027	0.000	0.000	0.000	0.000
Sulfate	0.644	7.301	0.425	7.142	0.458	3.274	0.486	2.897	0.467	2.479
Ammonium	0.282	3.197	0.157	2.636	0.182	1.300	0.272	1.621	0.261	1.388
Soluble Sodium	0.066	0.747	0.067	1.126	0.095	0.679	0.097	0.582	0.135	0.718
Soluble Magnesium	0.010	0.117	0.006	0.107	0.010	0.070	0.012	0.070	0.011	0.057
Soluble Potassium	0.038	0.431	0.025	0.412	0.032	0.231	0.055	0.329	0.046	0.244
Soluble Calcium	0.074	0.842	0.054	0.906	0.093	0.668	0.117	0.700	0.146	0.778
O1TC	0.352	3.998	0.255	4.284	0.267	1.910	0.673	4.013	0.388	2.062
O2TC	0.296	3.362	0.194	3.259	0.281	2.010	0.844	5.034	0.604	3.211
O3TC	1.067	12.104	0.723	12.137	1.167	8.346	2.869	17.114	2.414	12.826
O4TC	0.484	5.490	0.310	5.202	0.470	3.359	1.037	6.186	0.905	4.807
OPTC	0.225	2.552	0.172	2.895	0.221	1.583	0.216	1.290	0.194	1.030
OCTC	2.424	27.506	1.655	27.777	2.406	17.209	5.638	33.636	4.505	23.936
E1TC	0.298	3.386	0.237	3.974	0.381	2.725	1.009	6.017	1.018	5.408
E2TC	0.178	2.018	0.152	2.557	0.267	1.907	0.357	2.128	0.382	2.028
E3TC	0.015	0.168	0.016	0.269	0.016	0.111	0.032	0.190	0.021	0.112
ECTC	0.266	3.020	0.233	3.906	0.442	3.161	1.181	7.046	1.227	6.518
TCTC	2.691	30.527	1.887	31.682	2.848	20.369	6.819	40.682	5.732	30.454
Sodium	0.045	0.506	0.017	0.287	0.052	0.371	0.032	0.190	0.038	0.201
Magnesium	0.018	0.206	0.017	0.280	0.019	0.135	0.010	0.061	0.023	0.123
Aluminum	0.371	4.206	0.208	3.496	0.928	6.636	0.590	3.519	0.799	4.244
Silicon	0.881	9.992	0.623	10.456	2.955	21.137	1.837	10.962	2.594	13.781
Phosphorus	0.000	0.002	0.001	0.017	0.001	0.007	0.000	0.002	0.001	0.005
Sulfur	0.287	3.251	0.206	3.451	0.233	1.666	0.217	1.294	0.220	1.169
Chlorine	0.002	0.025	0.006	0.096	0.130	0.928	0.080	0.480	0.123	0.656
Potassium	0.112	1.276	0.075	1.258	0.236	1.691	0.198	1.179	0.232	1.235
Calcium	0.137	1.551	0.098	1.649	0.402	2.876	0.237	1.413	0.340	1.805
Titanium	0.015	0.175	0.008	0.142	0.045	0.325	0.028	0.165	0.038	0.201
Vanadium	0.001	0.008	0.000	0.006	0.001	0.005	0.001	0.005	0.001	0.006
Chromium	0.000	0.005	0.001	0.019	0.001	0.005	0.001	0.003	0.001	0.003
Manganese	0.005	0.061	0.003	0.046	0.009	0.062	0.006	0.038	0.008	0.041
Iron	0.218	2.476	0.108	1.808	0.462	3.303	0.324	1.934	0.443	2.354
Cobalt	0.002	0.019	0.001	0.014	0.004	0.028	0.003	0.016	0.003	0.019
Nickel	0.000	0.004	0.000	0.007	0.000	0.002	0.000	0.002	0.000	0.002
Cupper	0.002	0.022	0.001	0.021	0.003	0.024	0.007	0.041	0.004	0.023
Zinc	0.003	0.033	0.002	0.032	0.009	0.065	0.013	0.076	0.014	0.072
Gallium	0.000	0.001	0.000	0.001	0.000	0.001	0.000	0.001	0.000	0.000
Arsenic	0.000	0.001	0.000	0.003	0.000	0.002	0.000	0.001	0.000	0.001
Selenium	0.000	0.001	0.000	0.002	0.000	0.001	0.000	0.001	0.000	0.000
Bromine	0.002	0.018	0.001	0.022	0.002	0.011	0.002	0.009	0.002	0.008
Rubidium	0.000	0.003	0.000	0.004	0.001	0.006	0.001	0.004	0.001	0.004
Strontium	0.001	0.010	0.001	0.013	0.006	0.045	0.003	0.016	0.004	0.023
Yttrium	0.000	0.002	0.000	0.004	0.000	0.003	0.000	0.001	0.000	0.002
Zirconium	0.000	0.005	0.000	0.004	0.002	0.012	0.001	0.005	0.001	0.007
Molybdenum	0.000	0.001	0.000	0.003	0.000	0.003	0.000	0.002	0.000	0.001
Palladium	0.000	0.001	0.000	0.002	0.000	0.001	0.000	0.001	0.000	0.001
Silver	0.000	0.003	0.000	0.004	0.000	0.002	0.000	0.001	0.000	0.001
Cadmium	0.000	0.003	0.000	0.004	0.000	0.001	0.000	0.002	0.000	0.002
Indium	0.001	0.007	0.000	0.006	0.001	0.004	0.000	0.003	0.000	0.002
Tin	0.002	0.025	0.001	0.016	0.001	0.010	0.002	0.011	0.002	0.011
Antimony	0.001	0.008	0.001	0.011	0.001	0.008	0.001	0.007	0.001	0.006
Barium	0.004	0.045	0.006	0.105	0.015	0.110	0.011	0.064	0.013	0.067
Lanthanum	0.007	0.082	0.006	0.103	0.006	0.046	0.004	0.024	0.006	0.032
Gold	0.000	0.000	0.000	0.003	0.000	0.002	0.000	0.000	0.000	0.001
Mercury	0.000	0.002	0.000	0.001	0.000	0.001	0.000	0.001	0.000	0.001
Thallium	0.000	0.000	0.000	0.000	0.000	0.000	0.000	0.000	0.000	0.000
Lead	0.001	0.014	0.001	0.017	0.002	0.013	0.002	0.011	0.002	0.008
Uranium	0.000	0.002	0.000	0.001	0.000	0.002	0.000	0.001	0.000	0.001

Table 4-2c. Annual average $PM_{2.5}$ mass and chemical fractions for Two Week Samplers

	Big Hill		Thunderbird		Lake Forest		Sandy Way		SOLA	
	Average Concentration (ug/m3)	% Mass	Average Concentration (ug/m3)	% Mass	Average Concentration (ug/m3)	% Mass	Average Concentration (ug/m3)	% Mass	Average Concentration (ug/m3)	% Mass
Number in Average	19		28		28		29		25	
Mass	4.950	100.000	3.629	100.000	4.307	100.000	8.952	100.000	6.530	100.000
Volatalized Nitrate	0.470	9.505	0.231	6.375	0.253	5.868	0.527	5.883	0.471	7.214
Chloride	0.015	0.299	0.009	0.252	0.015	0.348	0.036	0.404	0.031	0.469
Nitrite	0.004	0.090	0.000	0.000	0.000	0.000	0.000	0.000	0.005	0.080
Nitrate	0.167	3.381	0.059	1.630	0.099	2.288	0.218	2.438	0.222	3.405
Phosphate	0.004	0.082	0.000	0.000	0.000	0.000	0.000	0.000	0.004	0.055
Sulfate	0.579	11.696	0.360	9.926	0.428	9.944	0.436	4.872	0.433	6.625
Ammonium	0.285	5.762	0.172	4.743	0.204	4.732	0.277	3.093	0.288	4.405
Soluble Sodium	0.031	0.632	0.016	0.440	0.011	0.265	0.018	0.204	0.026	0.391
Soluble Magnesium	0.002	0.035	0.001	0.038	0.001	0.033	0.001	0.015	0.001	0.020
Soluble Potassium	0.024	0.478	0.018	0.506	0.022	0.508	0.040	0.446	0.031	0.477
Soluble Calcium	0.006	0.126	0.005	0.150	0.009	0.200	0.009	0.101	0.012	0.191
O1TC	0.589	11.893	0.386	10.644	0.384	8.906	0.603	6.741	0.455	6.968
O2TC	0.330	6.669	0.186	5.124	0.236	5.478	0.746	8.338	0.462	7.073
O3TC	0.873	17.638	0.574	15.814	0.755	17.529	2.171	24.254	1.486	22.760
O4TC	0.334	6.745	0.231	6.378	0.299	6.938	0.788	8.803	0.568	8.697
OPTC	0.179	3.625	0.163	4.495	0.174	4.036	0.265	2.957	0.232	3.559
OCTC	2.305	46.570	1.541	42.454	1.847	42.887	4.574	51.092	3.203	49.058
E1TC	0.260	5.250	0.195	5.367	0.271	6.289	0.976	10.905	0.819	12.550
E2TC	0.151	3.060	0.156	4.298	0.247	5.739	0.379	4.237	0.444	6.804
E3TC	0.008	0.170	0.017	0.469	0.026	0.605	0.039	0.441	0.042	0.639
ECTC	0.240	4.855	0.205	5.639	0.370	8.596	1.130	12.626	1.073	16.433
TCTC	2.545	51.425	1.746	48.093	2.217	51.483	5.704	63.718	4.276	65.491
Sodium	0.009	0.188	0.034	0.937	0.015	0.339	0.025	0.281	0.034	0.516
Magnesium	0.007	0.147	0.007	0.194	0.010	0.222	0.007	0.081	0.008	0.121
Aluminum	0.024	0.489	0.017	0.456	0.030	0.705	0.032	0.356	0.035	0.529
Silicon	0.066	1.333	0.060	1.650	0.113	2.619	0.117	1.305	0.121	1.853
Phosphorus	0.000	0.004	0.000	0.005	0.000	0.001	0.000	0.000	0.000	0.000
Sulfur	0.273	5.517	0.208	5.732	0.197	4.572	0.194	2.172	0.190	2.916
Chlorine	0.000	0.004	0.000	0.004	0.001	0.034	0.005	0.060	0.004	0.058
Potassium	0.033	0.670	0.025	0.696	0.031	0.724	0.054	0.605	0.045	0.691
Calcium	0.016	0.326	0.015	0.402	0.026	0.613	0.025	0.282	0.028	0.431
Titanium	0.002	0.032	0.001	0.041	0.002	0.054	0.001	0.014	0.003	0.053
Vanadium	0.000	0.006	0.000	0.008	0.000	0.006	0.000	0.002	0.000	0.006
Chromium	0.000	0.004	0.000	0.003	0.000	0.003	0.000	0.001	0.000	0.002
Manganese	0.001	0.013	0.001	0.015	0.001	0.020	0.001	0.009	0.001	0.014
Iron	0.024	0.491	0.023	0.629	0.043	1.005	0.043	0.477	0.054	0.831
Cobalt	0.000	0.008	0.000	0.008	0.001	0.012	0.001	0.006	0.000	0.007
Nickel	0.000	0.004	0.000	0.002	0.000	0.002	0.000	0.001	0.000	0.002
Cupper	0.001	0.011	0.002	0.041	0.001	0.029	0.007	0.079	0.002	0.036
Zinc	0.002	0.033	0.002	0.059	0.003	0.062	0.009	0.097	0.005	0.080
Gallium	0.000	0.001	0.000	0.001	0.000	0.002	0.000	0.000	0.000	0.002
Arsenic	0.000	0.002	0.000	0.004	0.000	0.001	0.000	0.003	0.000	0.002
Selenium	0.000	0.003	0.000	0.002	0.000	0.003	0.000	0.001	0.000	0.001
Bromine	0.001	0.029	0.002	0.043	0.001	0.028	0.001	0.015	0.001	0.021
Rubidium	0.000	0.003	0.000	0.003	0.000	0.002	0.000	0.003	0.000	0.003
Strontium	0.000	0.003	0.000	0.005	0.000	0.010	0.000	0.004	0.000	0.007
Yttrium	0.000	0.005	0.000	0.005	0.000	0.003	0.000	0.002	0.000	0.004
Zirconium	0.000	0.002	0.000	0.003	0.000	0.003	0.000	0.001	0.000	0.001
Molybdenum	0.000	0.003	0.000	0.006	0.000	0.007	0.000	0.002	0.000	0.002
Palladium	0.000	0.002	0.000	0.001	0.000	0.003	0.000	0.002	0.000	0.002
Silver	0.000	0.003	0.000	0.007	0.000	0.005	0.000	0.002	0.000	0.004
Cadmium	0.000	0.009	0.000	0.004	0.000	0.007	0.000	0.004	0.000	0.004
Indium	0.000	0.006	0.000	0.009	0.001	0.014	0.000	0.003	0.000	0.003
Tin	0.001	0.025	0.001	0.022	0.001	0.034	0.001	0.013	0.001	0.018
Antimony	0.001	0.025	0.001	0.022	0.001	0.022	0.001	0.009	0.001	0.012
Barium	0.008	0.161	0.005	0.125	0.006	0.131	0.007	0.083	0.006	0.087
Lanthanum	0.005	0.111	0.005	0.146	0.006	0.139	0.008	0.088	0.005	0.074
Gold	0.000	0.002	0.000	0.003	0.000	0.003	0.000	0.001	0.000	0.003
Mercury	0.000	0.002	0.000	0.002	0.000	0.003	0.000	0.001	0.000	0.002
Thallium	0.000	0.001	0.000	0.000	0.000	0.001	0.000	0.000	0.000	0.001
Lead	0.001	0.012	0.001	0.022	0.001	0.021	0.002	0.018	0.001	0.013
Uranium	0.000	0.001	0.000	0.004	0.000	0.003	0.000	0.002	0.000	0.003

4.2 Temporal and Spatial Variation of TWS TSP, PM_{10}, and $PM_{2.5}$ Mass and Chemical Compositions

Temporal and spatial variation of TWS TSP, PM_{10}, and $PM_{2.5}$ mass and chemical compositions will be discussed in this section. Figures 4-2 to 4-4 show the variation of contributions of each major component to TSP, PM_{10}, and $PM_{2.5}$ at each site. Figures 4-5 to 4-7 show the variation of fractional contributions of each major component to TSP, PM_{10}, and $PM_{2.5}$ at each site. The dates in these figures indicate the start of TWS sampling. The negative mass concentrations of unidentified species suggests that reconstructed mass concentration was higher than measured mass concentration in that TWS sample. The unidentified mass was not considered in the fractional contribution, shown in Figures 4-5 to 4-7.

The BH site was selected as the background site to evaluate the transport of atmospheric pollutants from urbanized areas west (typically upwind) of the Lake Tahoe region. The TWS TSP mass concentrations measured at the BH site during summer and fall (from 05/21/03 to 10/22/03) ranged from 10-22 $\mu g/m^3$ and were more than twice the TSP mass concentrations (1.8-6.7 $\mu g/m^3$) measured at this site during spring and winter (from 02/26/03 to 04/23/03 and 12/03/03 to 12/17/03). Geological material and unidentified mass contributed more than 60% of TSP mass during summer/fall and less than 50% during spring and winter (when snow frequently covers the ground) (Figure 4-5a).

TSP mass concentrations at the TB site (Figure 4-2e), considered to be the local background site, were generally less than 5 $\mu g/m^3$ during winter and spring (11/20/02 to 04/10/03 and 11/05/03 to 12/17/03) but increased during the period from 05/07/03 to 10/22/03. The temporal variation of TSP mass concentrations observed at the TB site was similar to that observed at the BH site; however, a temporal pattern of geological and unidentified material contributions to TSP did not emerge at the TB location.

Figure 4-2b shows that if the highest TSP mass concentration (82 $\mu g/m^3$) observed on 12/04/02 (Lake Forrest) is excluded, TSP mass concentration would decrease from > 25 $\mu g/m^3$ in January to 10 $\mu g/m^3$ in March and April, with a slight increase to 15 $\mu g/m^3$ in summer and fall (05/07/03 to 11/19/03). Figure 4-2(c,d) shows that similar temporal trends and comparable TSP mass concentrations were observed at the SOLA and SW sites. TSP mass concentrations observed at the LF, SOLA, and SW sites were approximately two to three times greater than those observed at the BH and TB sites.

In addition to geological and unidentified material, organic matter (OC x 1.2) and soot (EC) were the second and the third largest chemical species that contributed to the temporal variation of TSP mass concentrations observed at the sites. Contributions of organic matter and soot to TSP mass concentration increased at the SOLA and SW sites during the period from 11/20/02 to 03/12/03, which was likely the result of increased traffic volumes and wood-burning associated with winter sport activities in the vicinity of the SOLA and SW sites.

PM_{10} composed > 80% of TSP at the five sites in LTADS. The temporal and spatial variations of PM_{10} mass concentrations, geological material, organic matter and soot are similar to those of TSP.

No clear temporal variation of $PM_{2.5}$ mass concentration (Figure 4-4a) was observed at the BH site. The $PM_{2.5}$ mass concentrations at the TB site were generally < 3 $\mu g/m^3$ for measurements prior to 04/10/03, and increased by 50% or more from 05/07/03 to 10/08/03. Significant increases in $PM_{2.5}$ mass concentrations (8-15 $\mu g/m^3$) were observed at the SOLA and SW sites from 11/20/02 to 02/26/03. This increase was due to the increased organic matter and EC concentrations, which were twice as high as those measured at the TB site. Concentrations of geological material in $PM_{2.5}$ were similar at all five sites and temporal variation was not observed. Organic matter and EC contributed approximately 80% of $PM_{2.5}$ mass at the SOLA and SW sites from 11/20/02 to 02/26/03.

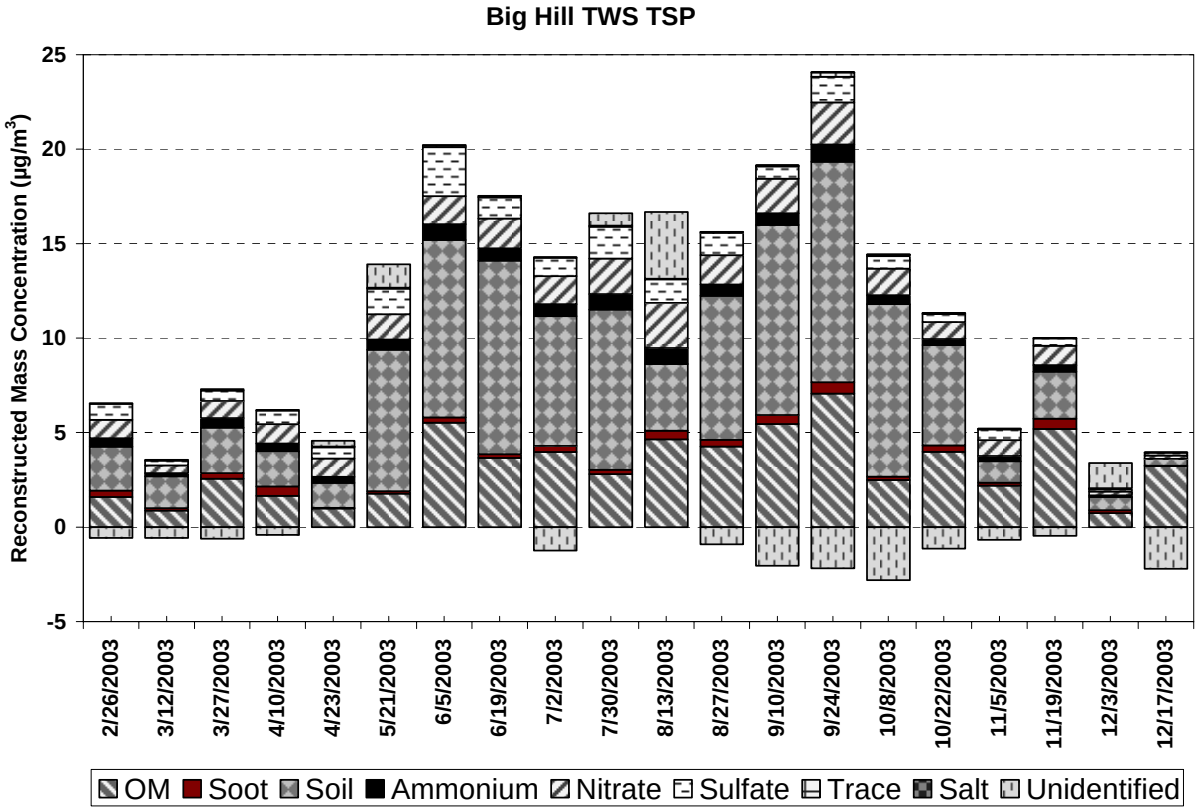

(a)

Figure 4-2. Time series plots of contribution of each major chemical components to reconstructed TSP mass at: a) Big Hill, b) Lake Forest, c) Sandy Way, d) SOLA, and e) Thunderbird.

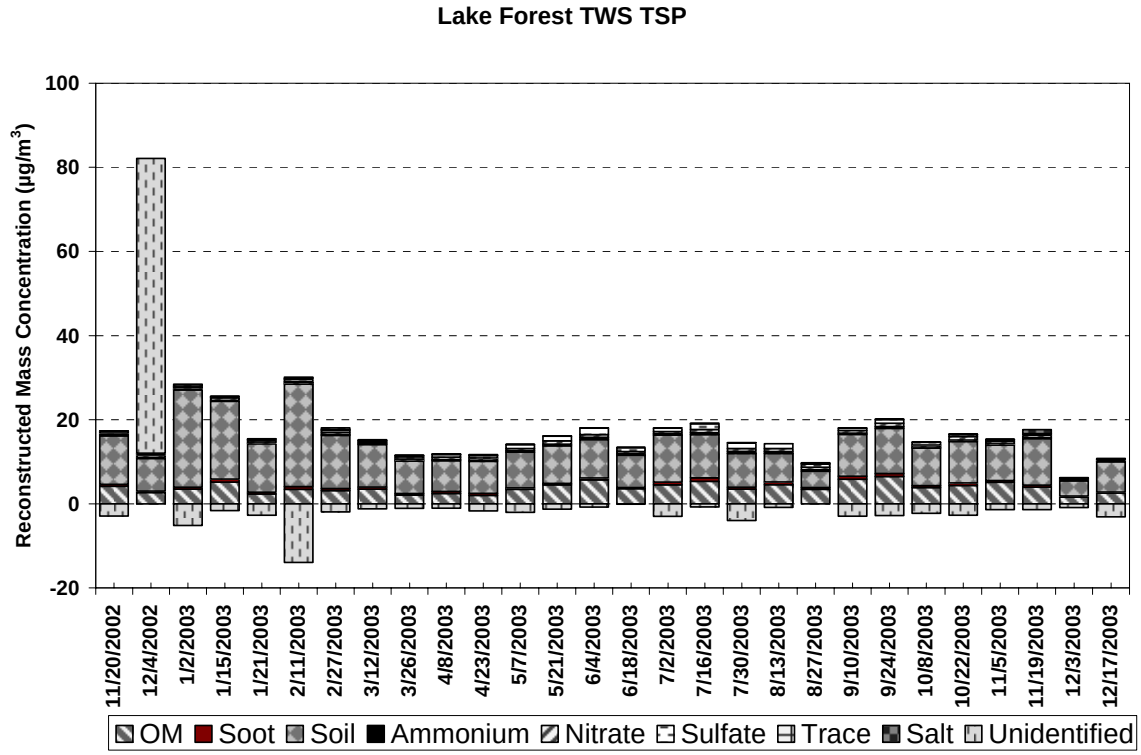
Lake Forest TWS TSP
Reconstructed Mass Concentration (µg/m3)
100
80
60
40
20
0
-20
11/20/2002
12/4/2002
1/2/2003
1/15/2003
1/21/2003
2/11/2003
2/27/2003
3/12/2003
3/26/2003
4/8/2003
4/23/2003
5/7/2003
5/21/2003
6/4/2003
6/18/2003
7/2/2003
7/16/2003
7/30/2003
8/13/2003
8/27/2003
9/10/2003
9/24/2003
10/8/2003
10/22/2003
11/5/2003
11/19/2003
12/3/2003
12/17/2003
OM
Soot
Soil
Ammonium
Nitrate
Sulfate
Trace
Salt
Unidentified

(b)

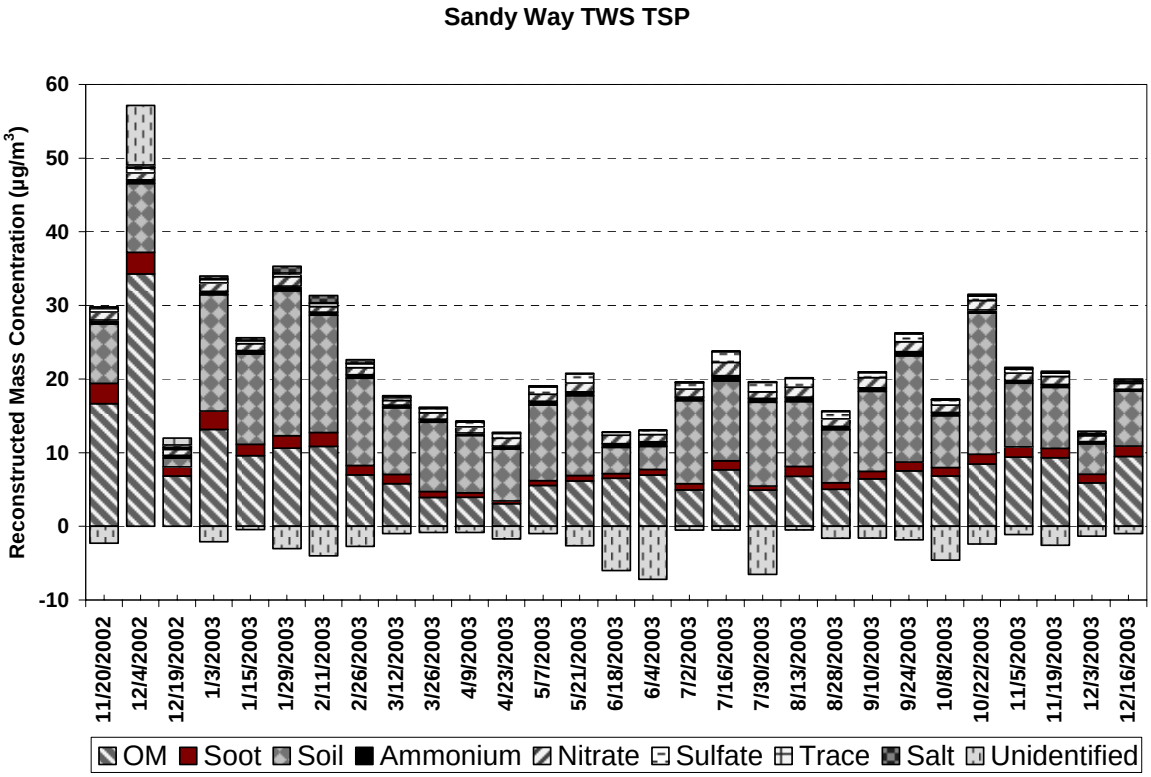
Sandy Way TWS TSP
Reconstructed Mass Concentration (µg/m3)
60
50
40
30
20
10
0
-10
11/20/2002
12/4/2002
12/19/2002
1/3/2003
1/15/2003
1/29/2003
2/11/2003
2/26/2003
3/12/2003
3/26/2003
4/9/2003
4/23/2003
5/7/2003
5/21/2003
6/18/2003
6/4/2003
7/2/2003
7/16/2003
7/30/2003
8/13/2003
8/28/2003
9/10/2003
9/24/2003
10/8/2003
10/22/2003
11/5/2003
11/19/2003
12/3/2003
12/16/2003
OM
Soot
Soil
Ammonium
Nitrate
Sulfate
Trace
Salt
Unidentified

(c)

Figure 4-2, cont'd.

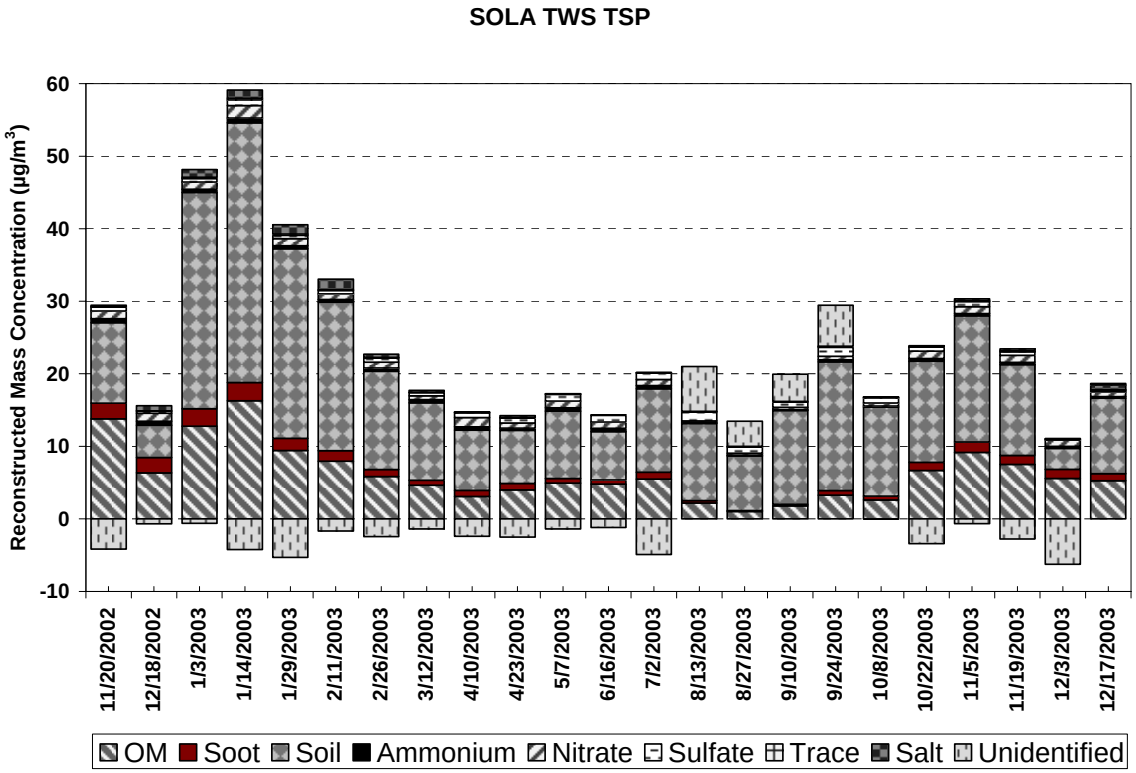

(d)

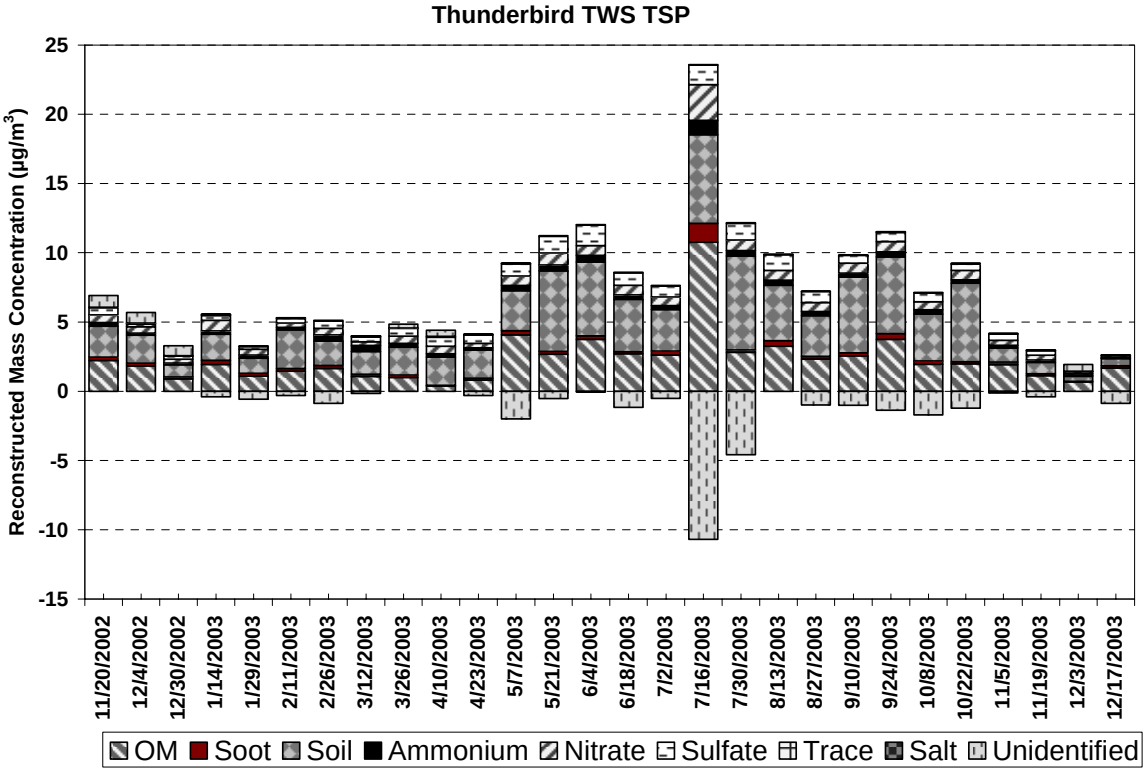

(e)

Figure 4-2, cont'd.

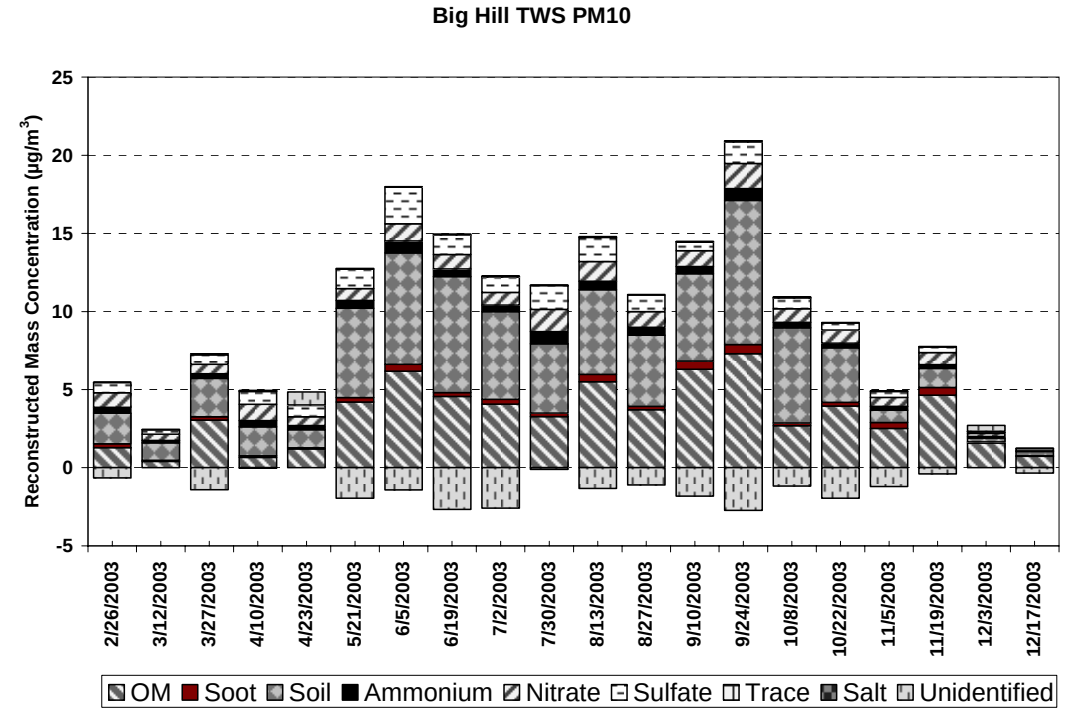

(a)

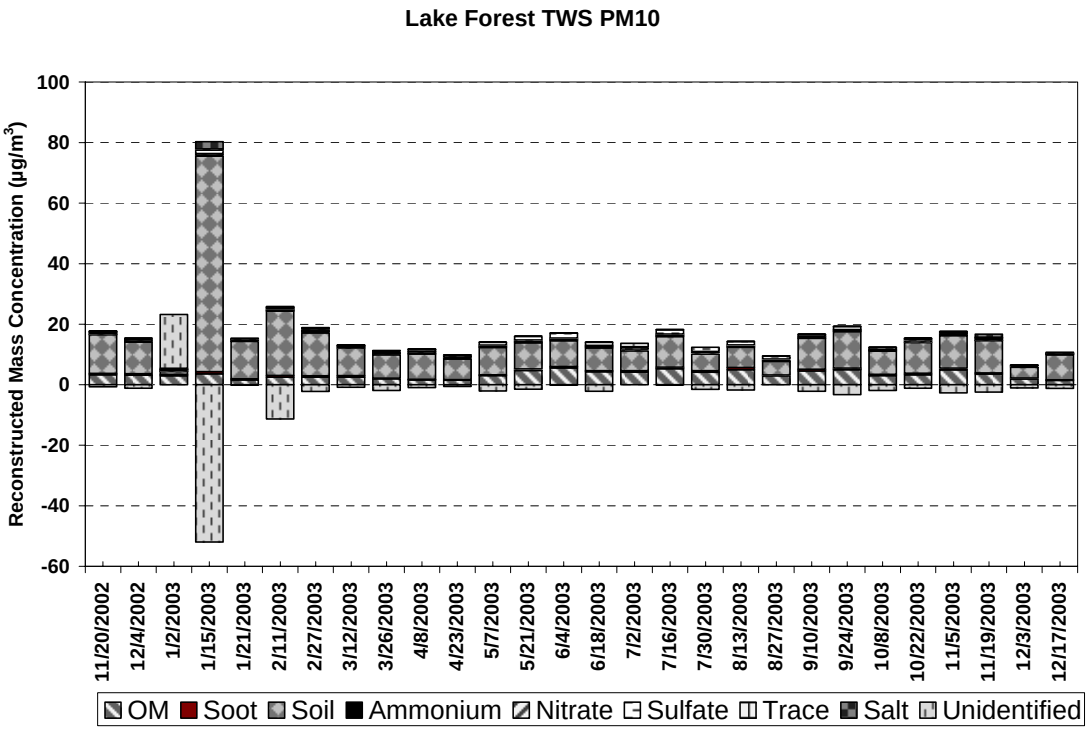

(b)

Figure 4-3. Time series plots of contribution of each major chemical components to reconstructed PM_{10} mass at: a) Big Hill, b) Lake Forest, c) Sandy Way, d) SOLA, and e) Thunderbird.

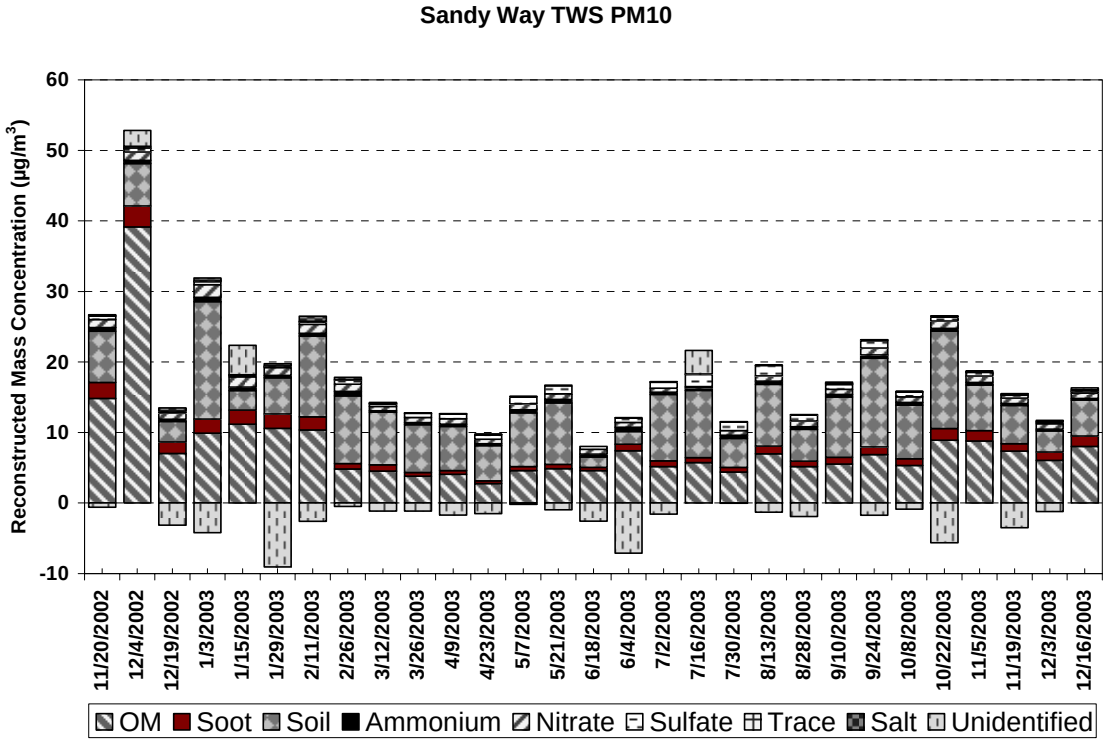

(c)

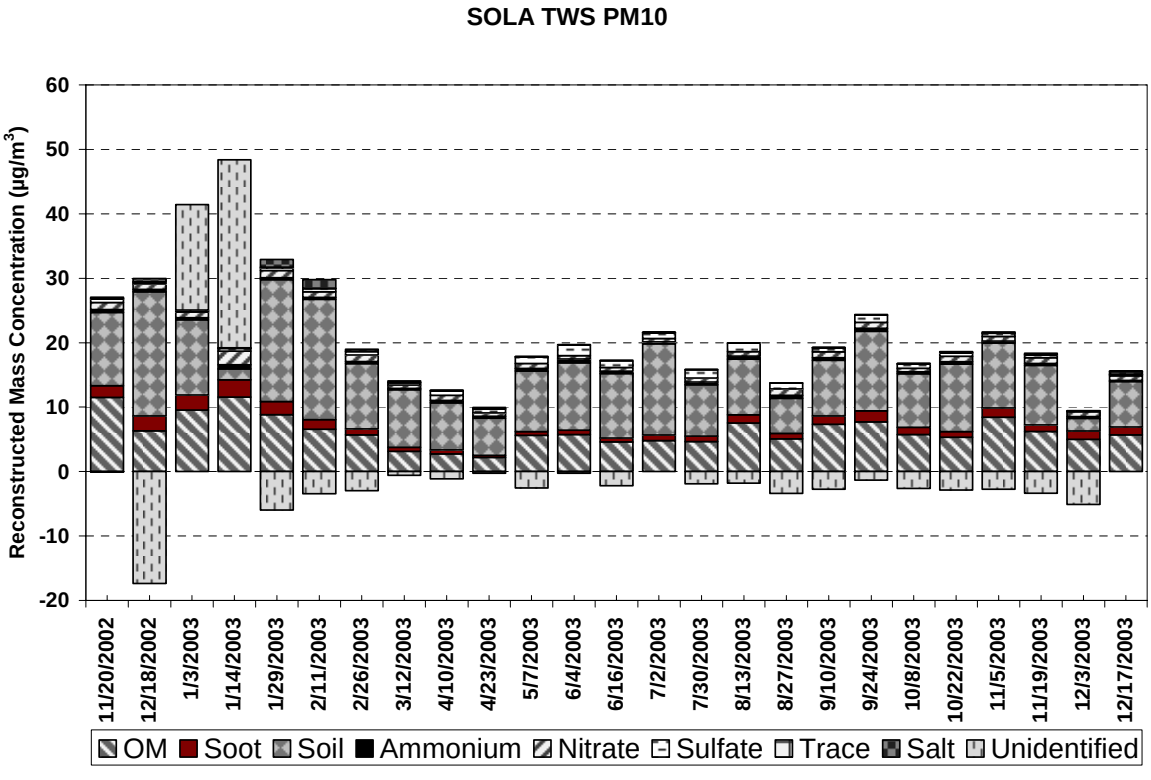

(d)

Figure 4-3, cont'd

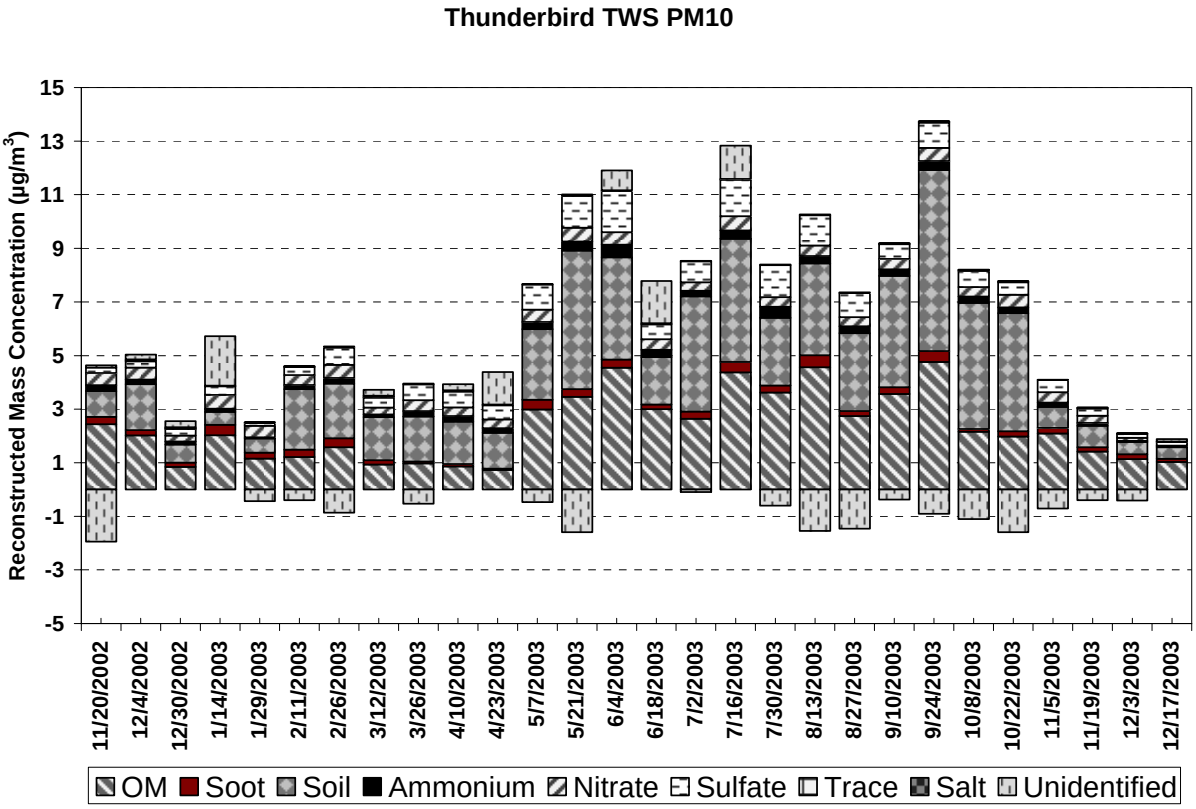

(e)

Figure 4-3, cont'd

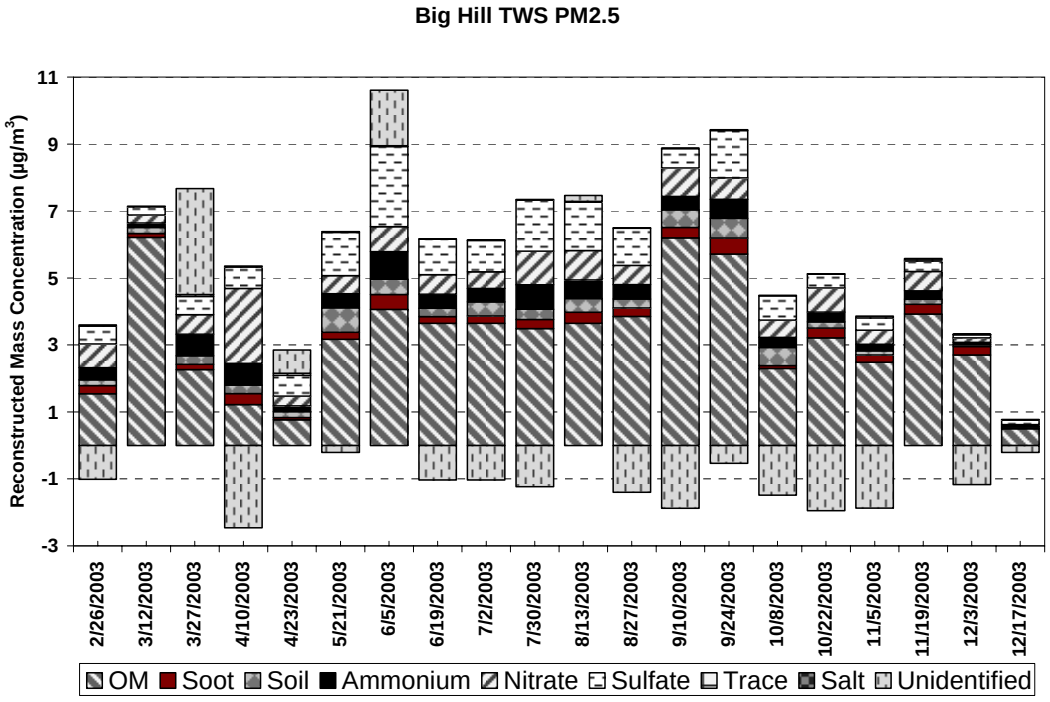

(a)

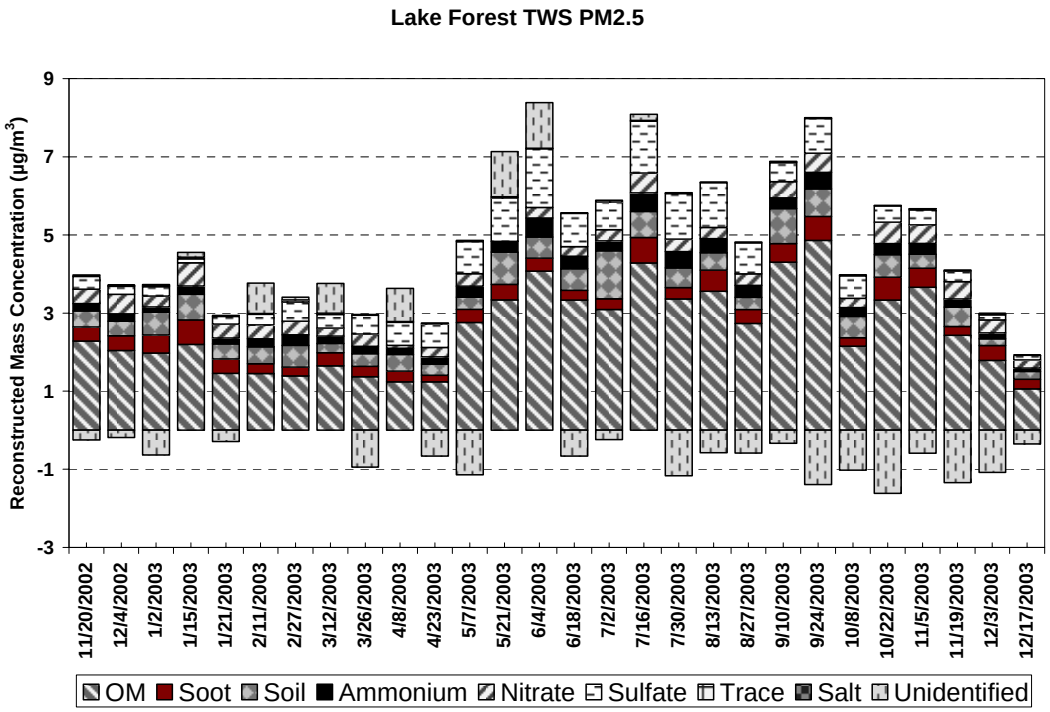

(b)

Figure 4-4. Time series plots of contribution of each major chemical components to reconstructed $PM_{2.5}$ mass at: a) Big Hill, b) Lake Forest, c) Sandy Way, d) SOLA, and e) Thunderbird.

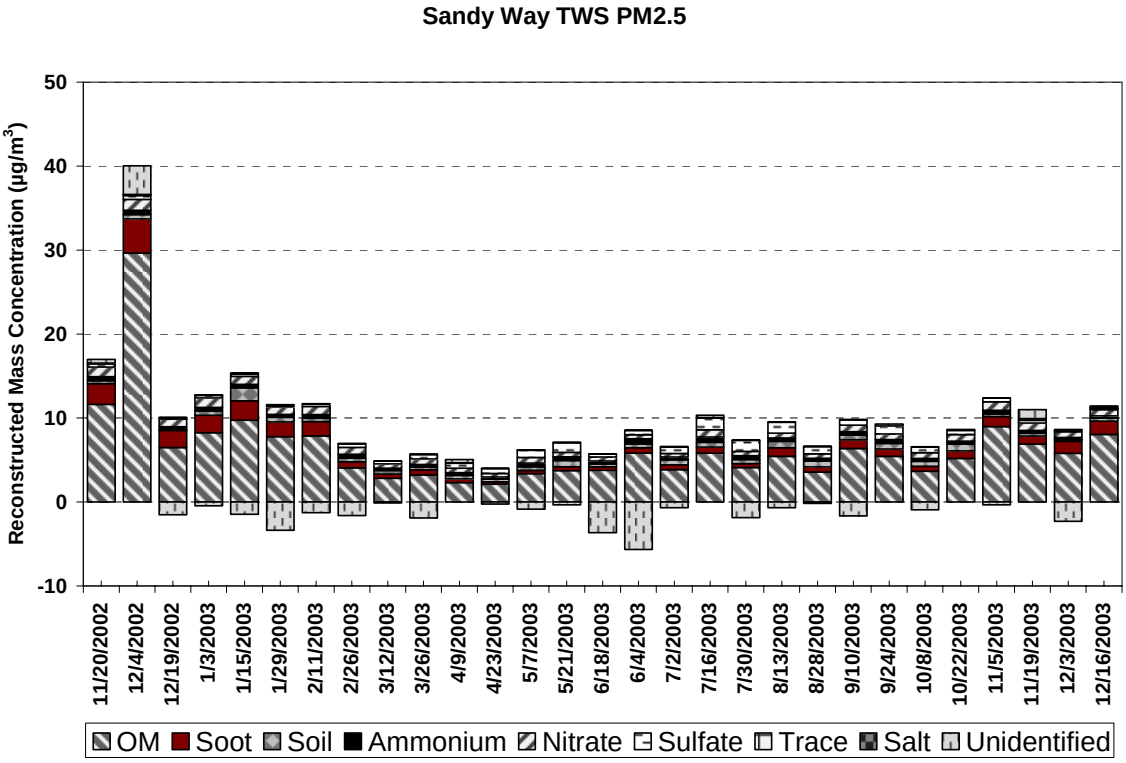

(c)

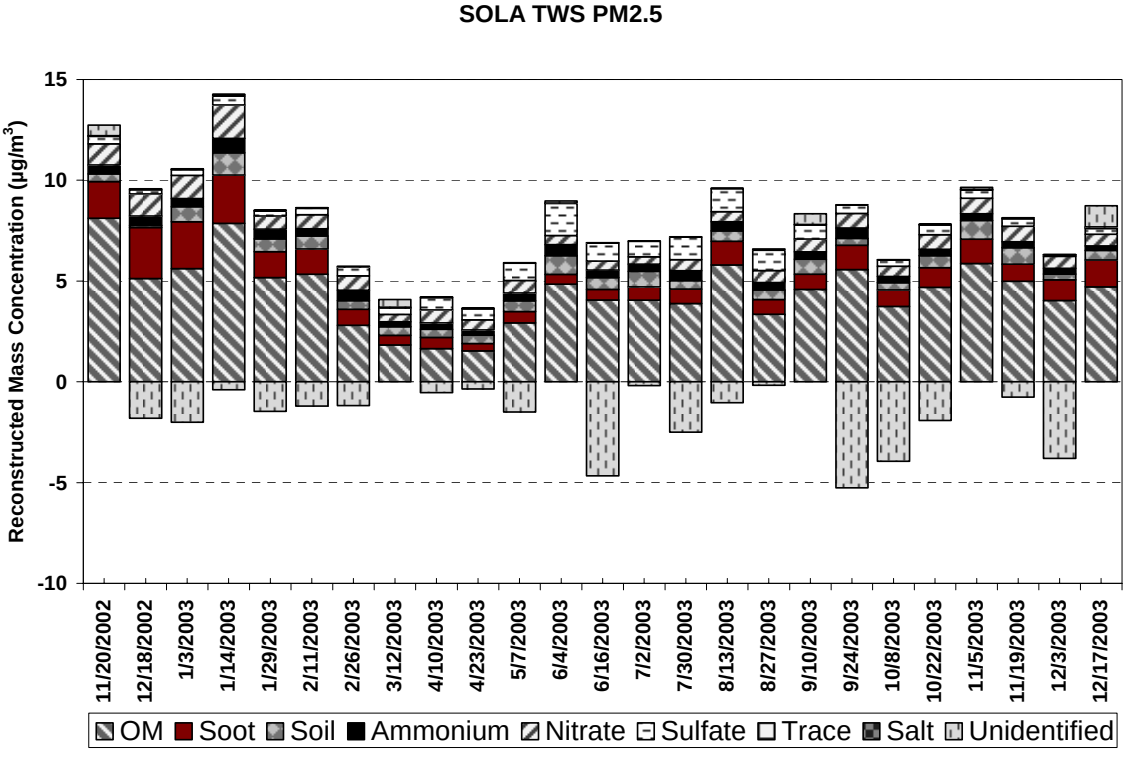

(d)

Figure 4-4, cont'd.

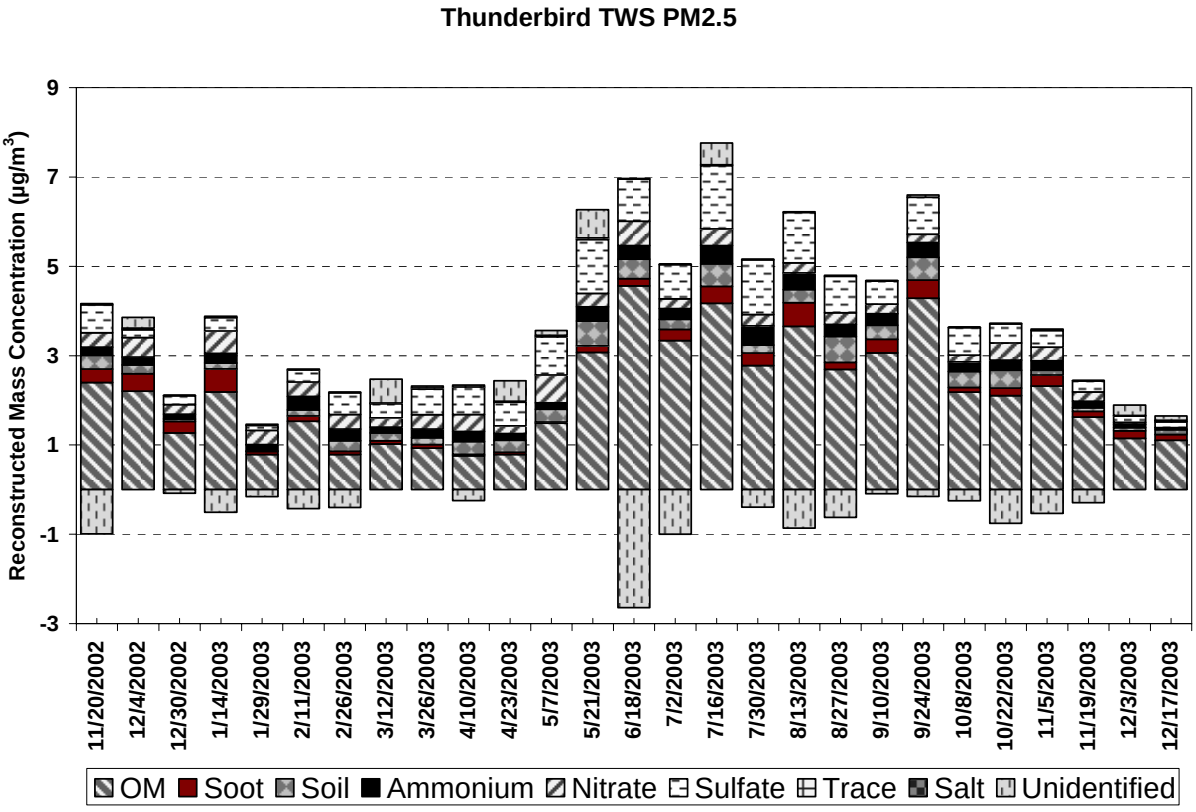

(e)

Figure 4-4, cont'd

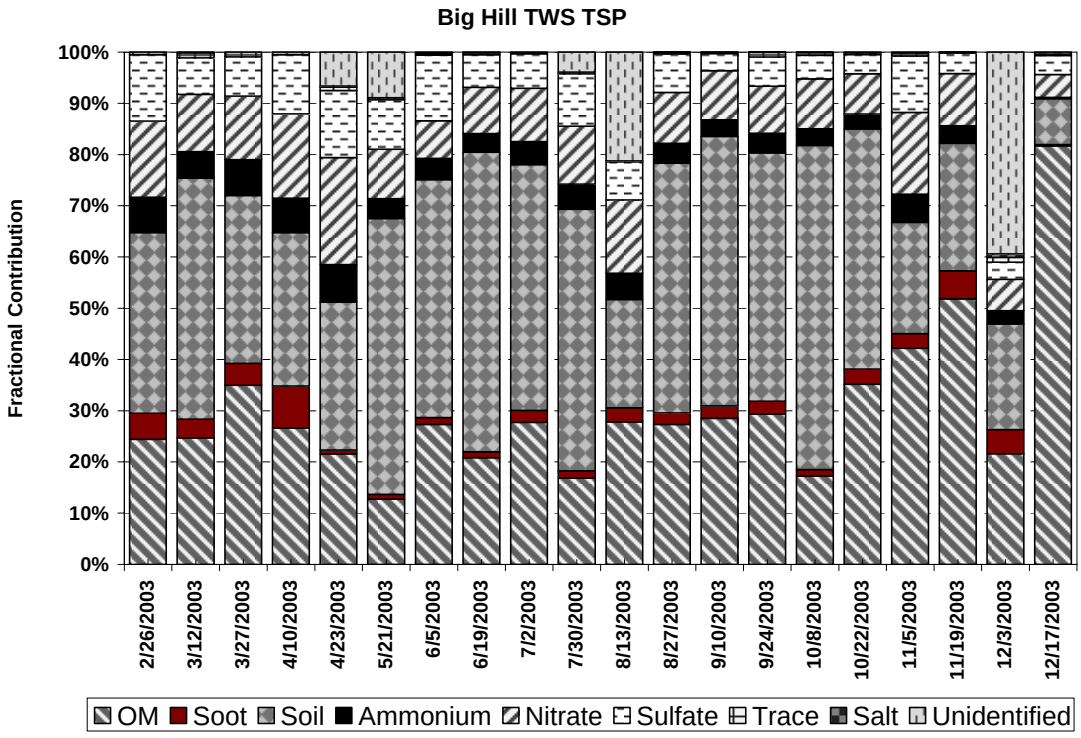
Big Hill TWS TSP
Fractional Contribution
100%
90%
80%
70%
60%
50%
40%
30%
20%
10%
0%
2/26/2003
3/12/2003
3/27/2003
4/10/2003
4/23/2003
5/21/2003
6/5/2003
6/19/2003
7/2/2003
7/30/2003
8/13/2003
8/27/2003
9/10/2003
9/24/2003
10/8/2003
10/22/2003
11/5/2003
11/19/2003
12/3/2003
12/17/2003
OM
Soot
Soil
Ammonium
Nitrate
Sulfate
Trace
Salt
Unidentified

(a)

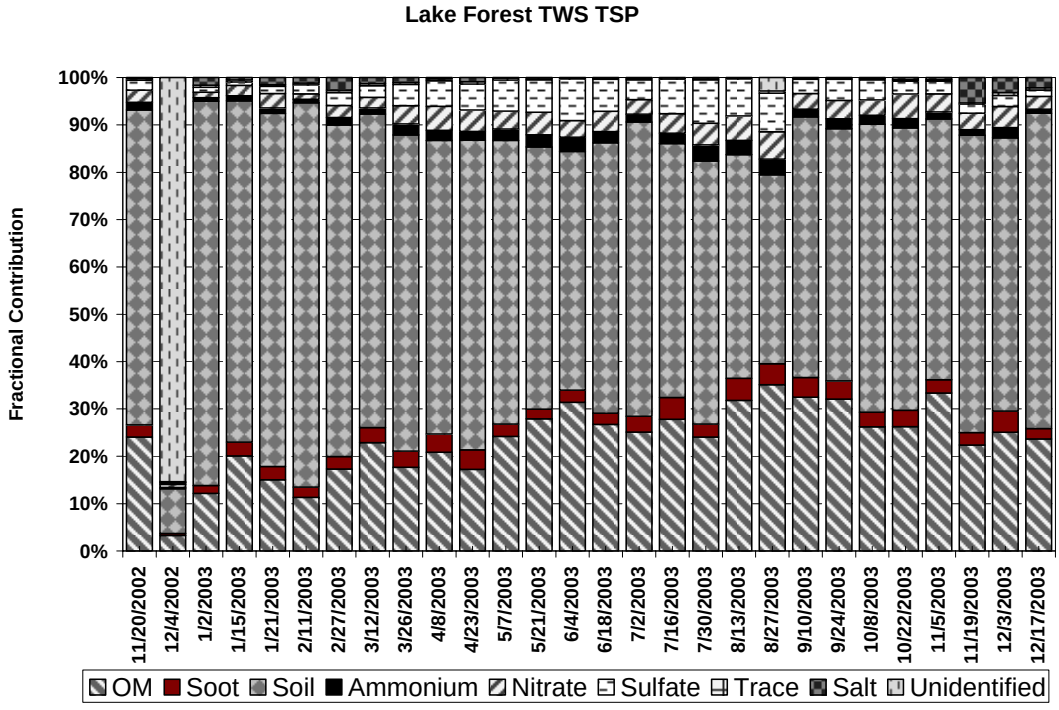
Lake Forest TWS TSP
Fractional Contribution
100%
90%
80%
70%
60%
50%
40%
30%
20%
10%
0%
11/20/2002
12/4/2002
1/2/2003
1/15/2003
1/21/2003
2/11/2003
2/27/2003
3/12/2003
3/26/2003
4/8/2003
4/23/2003
5/7/2003
5/21/2003
6/4/2003
6/18/2003
7/2/2003
7/16/2003
7/30/2003
8/13/2003
8/27/2003
9/10/2003
9/24/2003
10/8/2003
10/22/2003
11/5/2003
11/19/2003
12/3/2003
12/17/2003
OM
Soot
Soil
Ammonium
Nitrate
Sulfate
Trace
Salt
Unidentified

(b)

Figure 4-5. Time series plots of contribution of each major chemical components to fractional TSP mass at: a) Big Hill, b) Lake Forest, c) Sandy Way, d) SOLA, and e) Thunderbird.

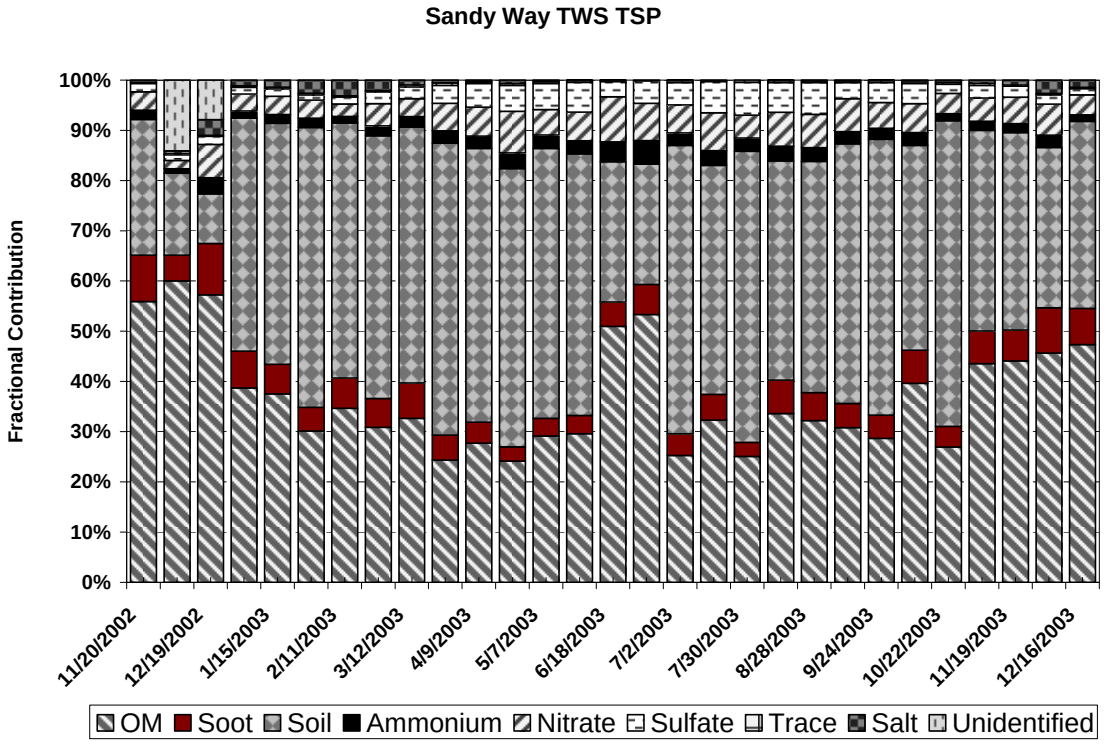

(c)

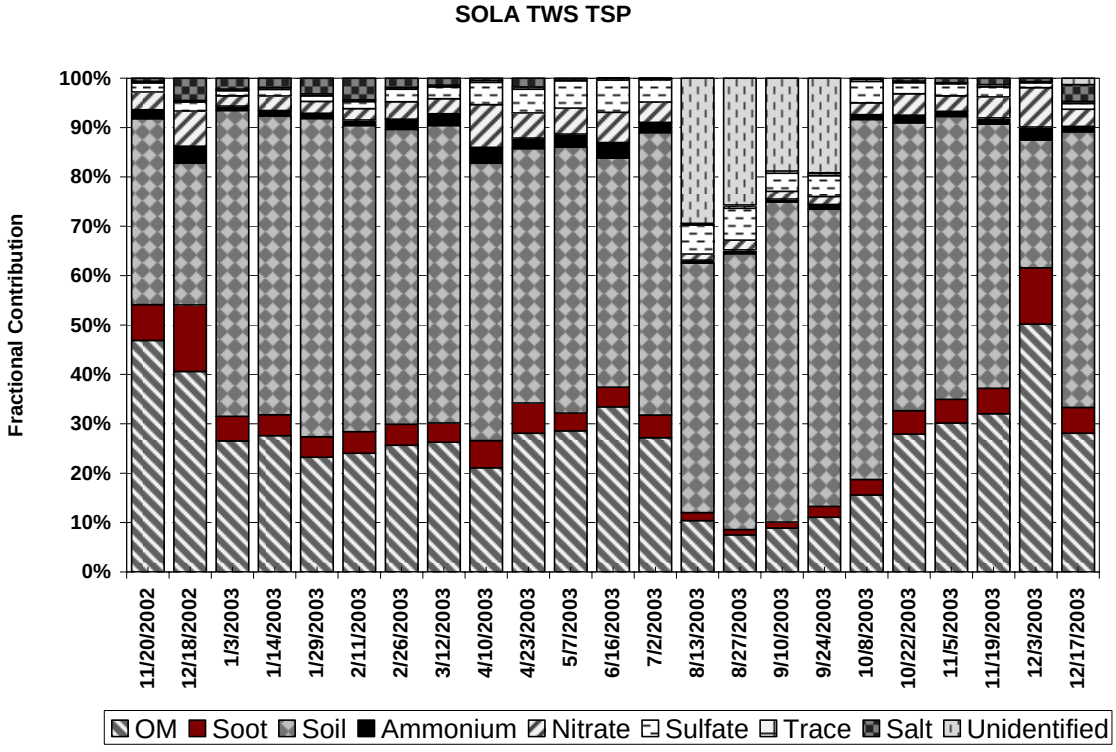

(d)

Figure 4-5, cont'd

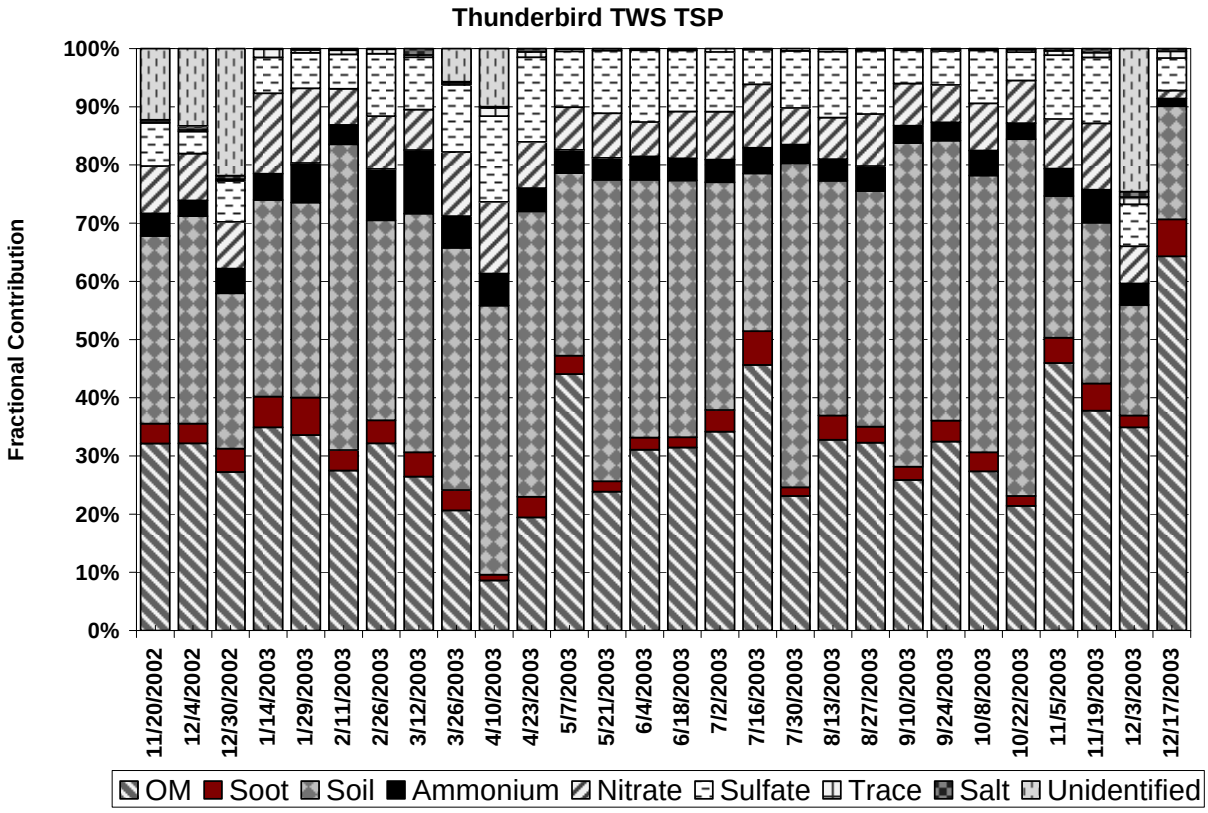

(e)

Figure 4-5, cont'd

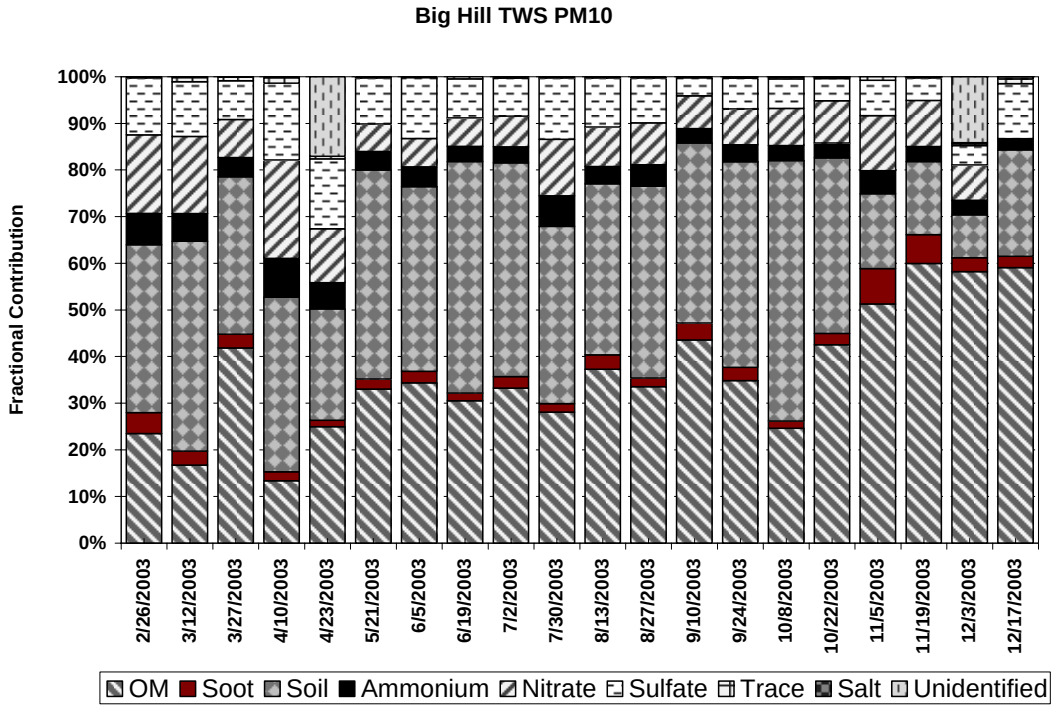

(a)

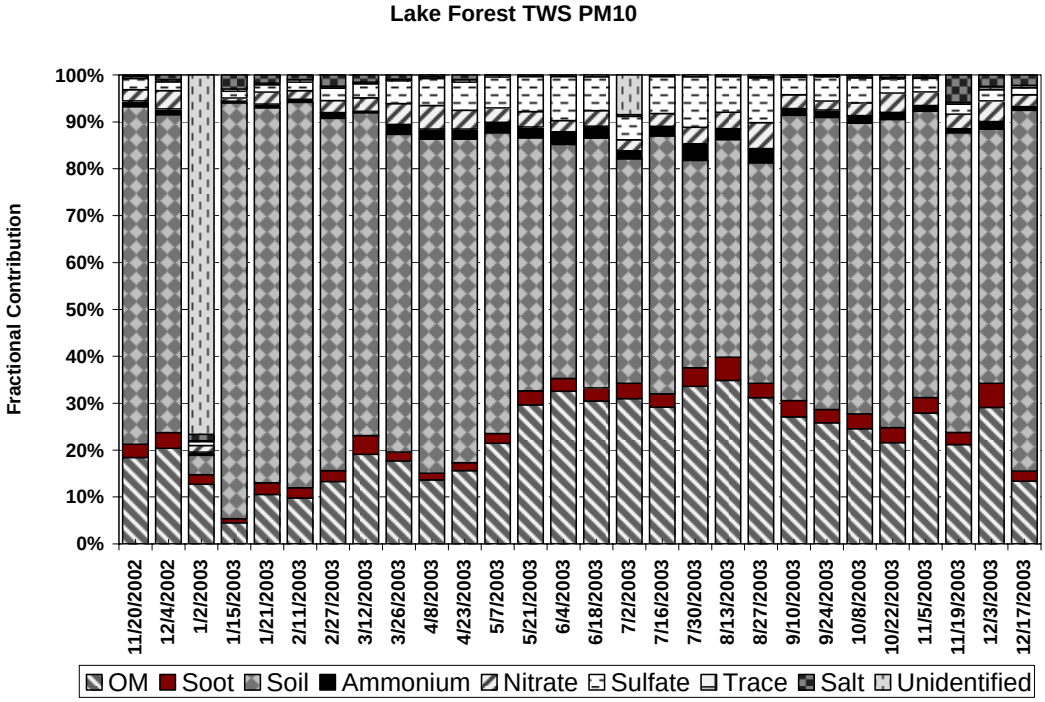

(b)

Figure 4-6. Time series plots of contribution of each major chemical components to fractional PM_{10} mass at: a) Big Hill, b) Lake Forest, c) Sandy Way, d) SOLA, and e) Thunderbird.

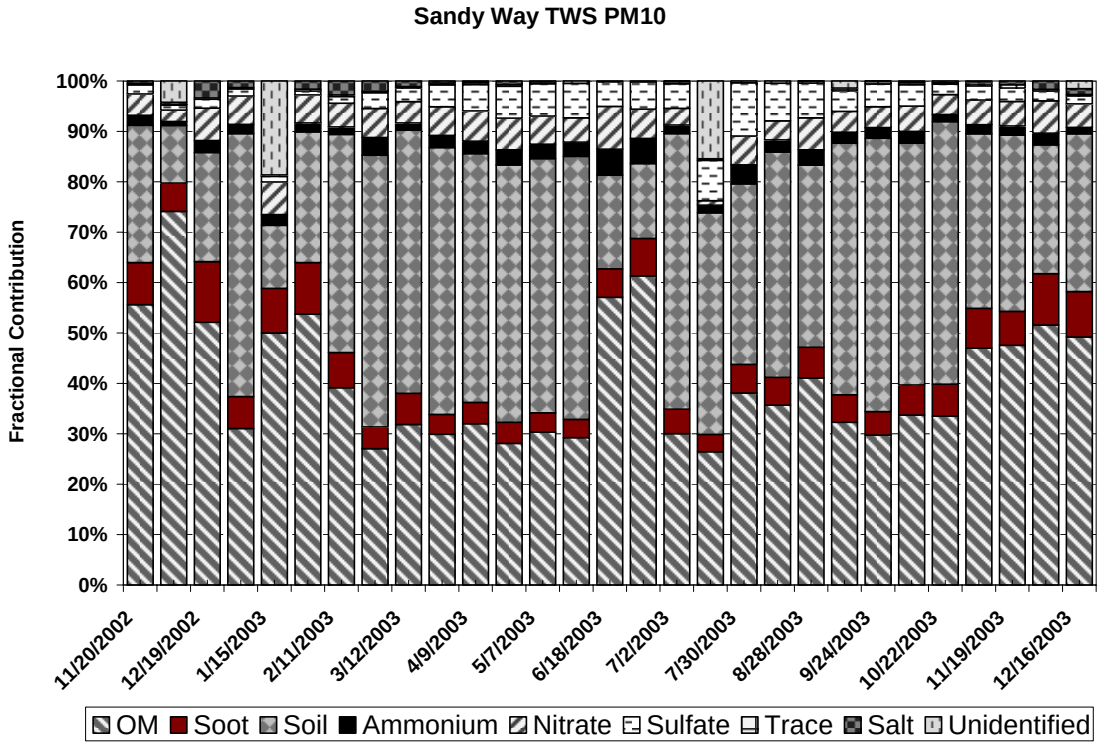

(c)

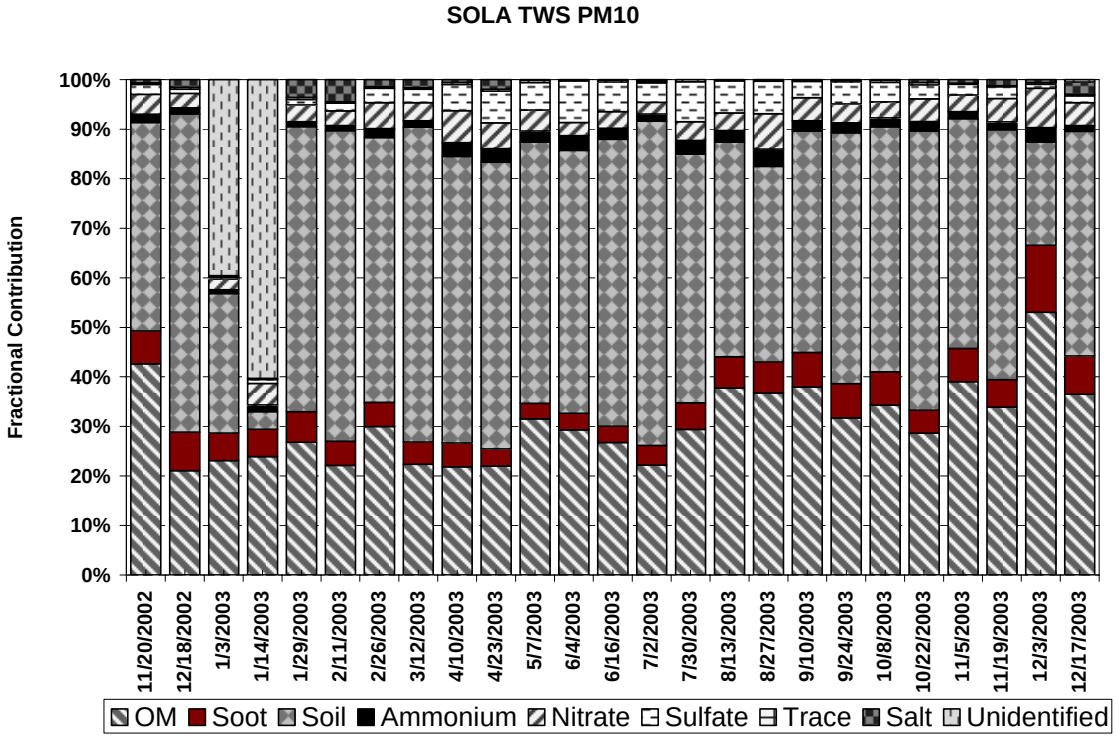

(d)

Figure 4-6, cont'd

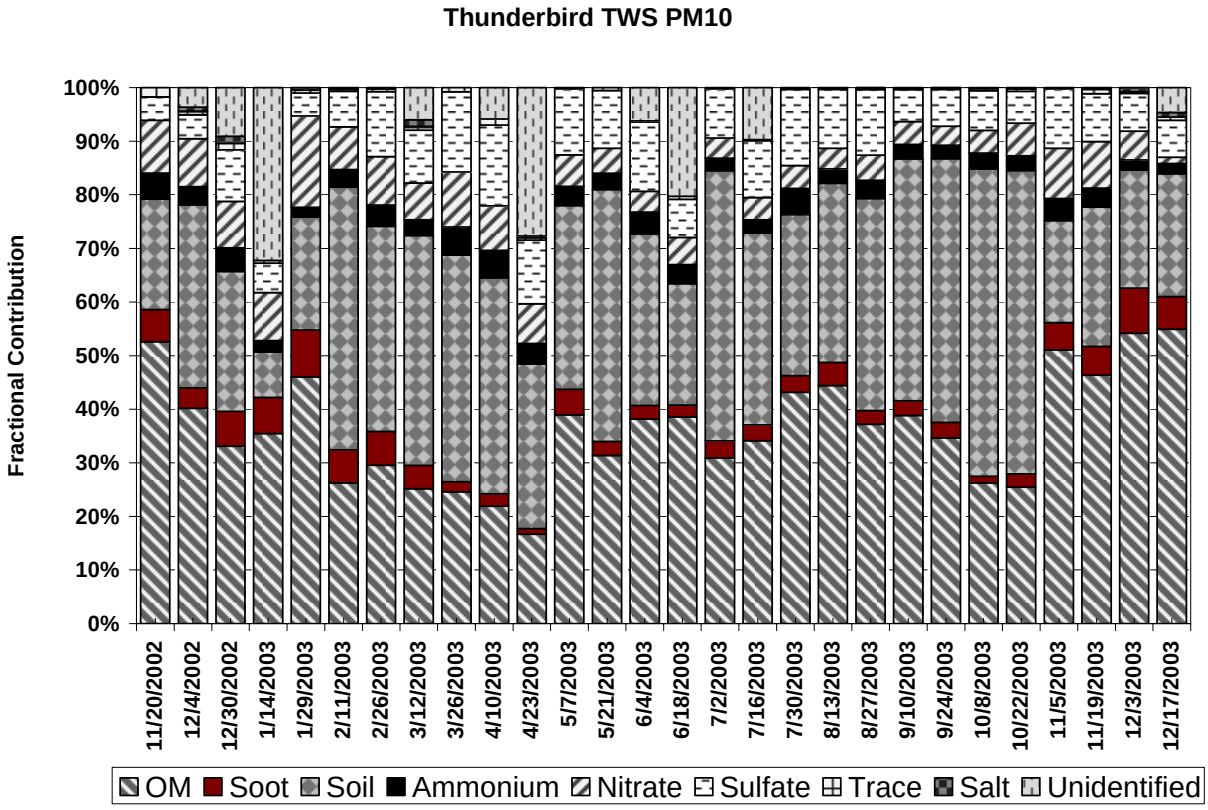

(e)

Figure 4-6, cont'd

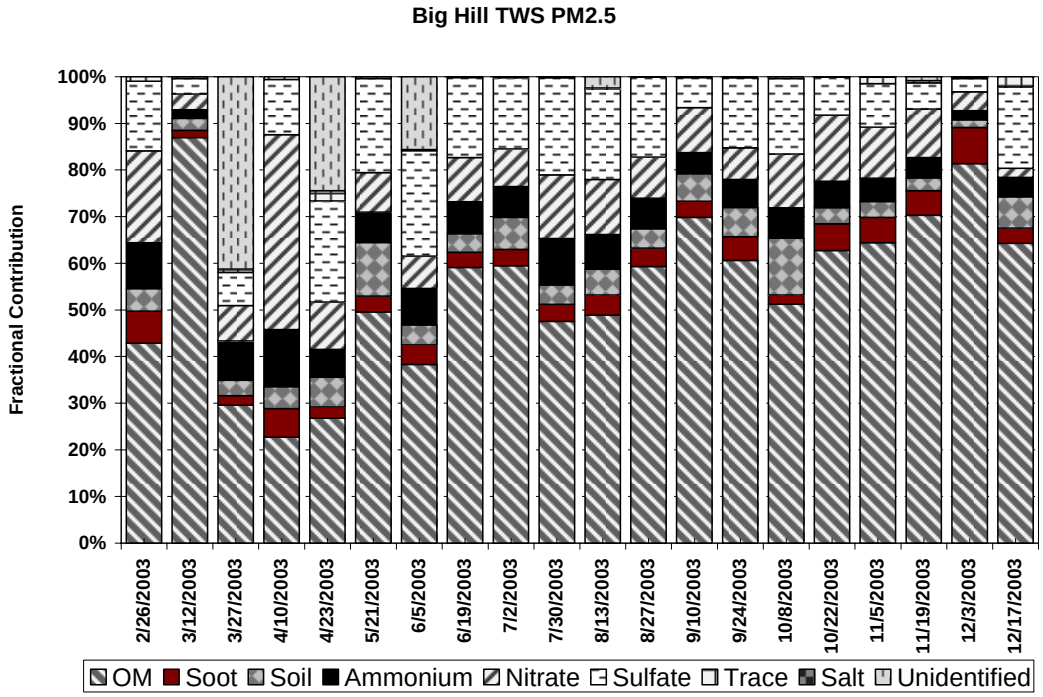

(a)

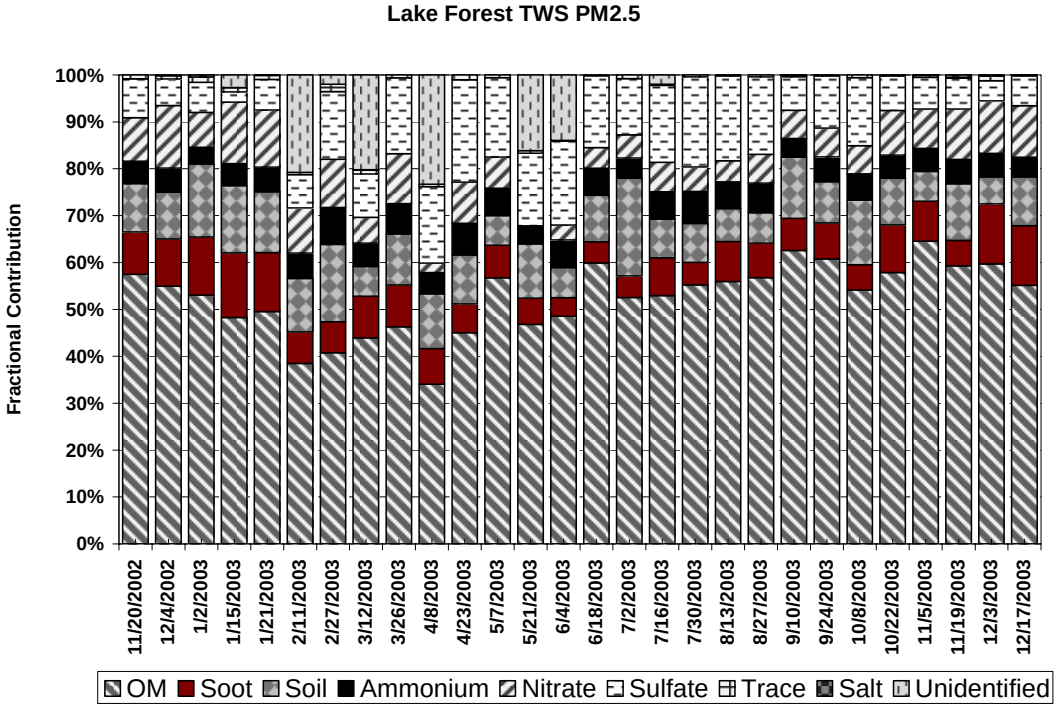

(b)

Figure 4-7. Time series plots of contribution of each major chemical components to fractional $PM_{2.5}$ mass at: a) Big Hill, b) Lake Forest, c) Sandy Way, d) SOLA, and e) Thunderbird.

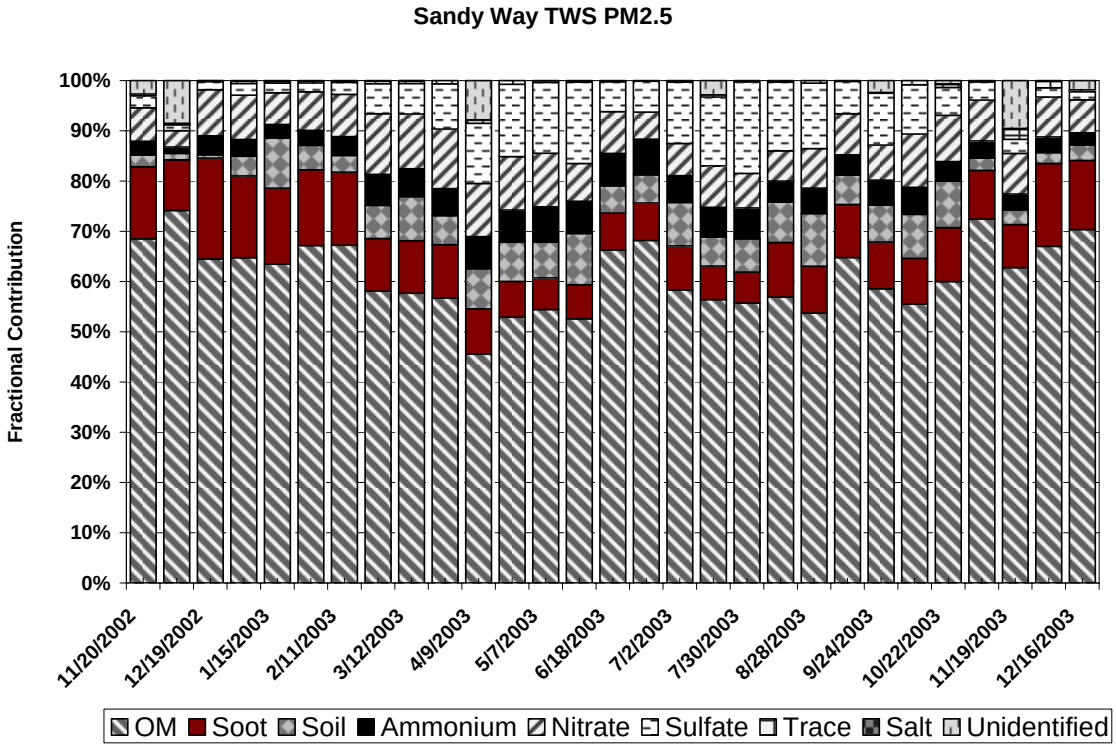

(c)

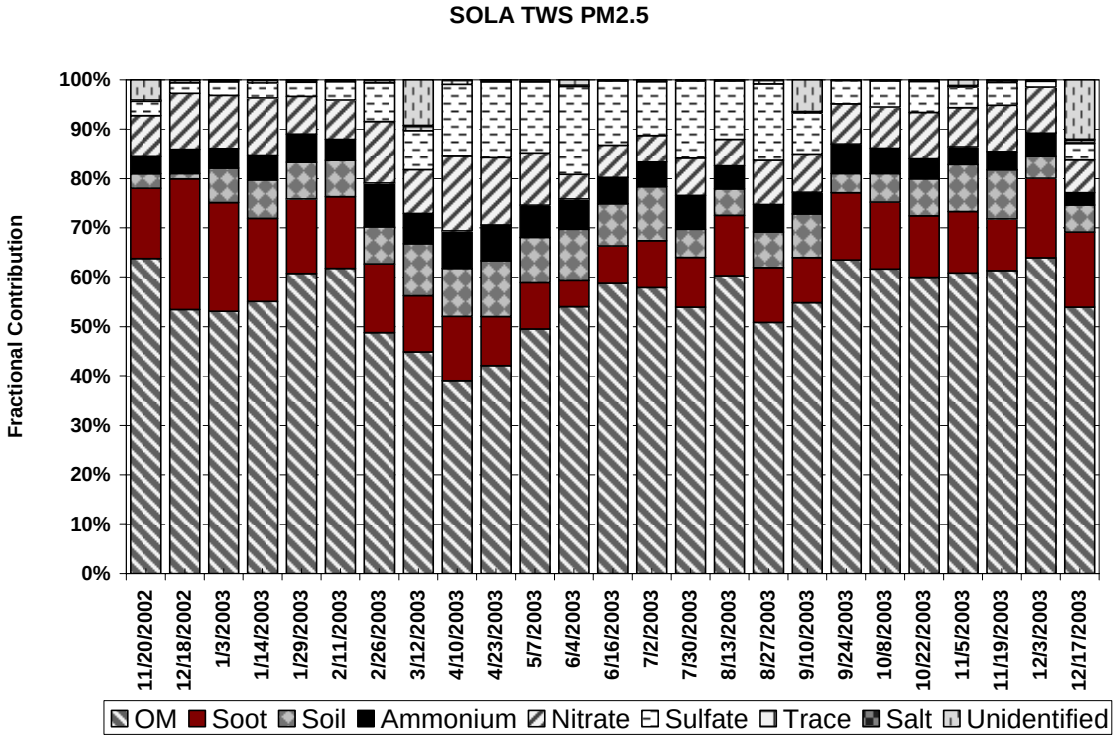

(d)

Figure 4-7, cont'd.

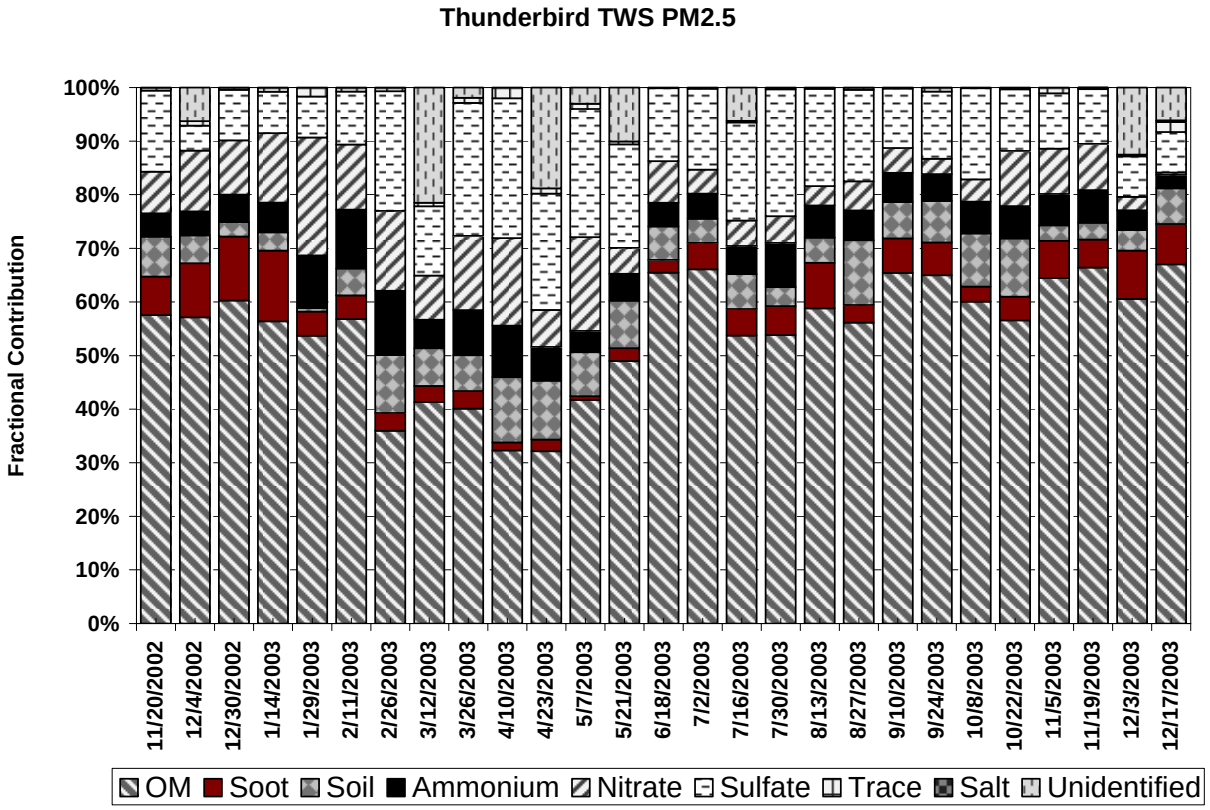

(e)

Figure 4-7, cont'd

5. DISCUSSION AND CONCLUSION

CARB initiated LTADS in 2002 to quantify the contribution of atmospheric deposition to the declining clarity of Lake Tahoe. The initial study design, which included two major components: 1) a monitoring network in the Lake Tahoe Basin and 2) special studies, was described in a June 10, 2002 draft work plan for LTADS.

The monitoring network was designed to provide information on the spatial variations around the lake and upwind of the basin. A total of five sites were selected for a one year monitoring program using TWS. The fives sites selected were: SOLA and SW as sites on each side of Highway 50 in South Lake Tahoe, the most urban environment; LF (near Tahoe City) as a less urban site; TB as a remote background site as a preserved area in the basin; and BH, which represented an upwind site of Lake Tahoe in a wilderness environment. The TWS provided two-week integrated samples of ammonia, nitric acid, TSP, PM_{10}, and $PM_{2.5}$ and served as the backbone of the monitoring plan. The two week sampling duration avoided problems associated with episodic sampling contributed from specific sources. MiniVol samplers were used to measure TSP at remotes sites and were deployed under two different monitoring schemes: buoy MiniVols for TSP (typically 24 hours) and non-buoy MiniVols for TSP (duration and frequency varied).

Field blanks were applied to subtract the passive deposition before, during, and after field sampling; however, field blanks were only collected at SOLA for 10% of the ambient samples and three field blanks were collected for non-buoy MiniVol TSP samples. The limited and site specific field blanks could affect the results of the ambient samples if the blank results were not representative of the range of conditions.

A total of 127, 129, and 128 sets of TWS samples were collected for TSP, PM_{10}, and $PM_{2.5}$, in LTADS, respectively, 36 sets for buoy MiniVol TSP samples, and 160 sets for non-buoy MiniVol TSP. Replicate analyses was performed on 10% of the ambient samples. The chemical data were evaluated for internal consistency by examining the physical consistency and balance of reconstructed mass, based on chemical species versus measured mass. In general, the samples collected met the criteria of internal physical consistency. A few TWS samples were suspected to be outliers yet no field flag was noted for these samples (with the exception of one laboratory flag).

Because the MiniVol samples were poorly correlated temporally, temporal and spatial variations were only examined for TWS samples. The highest annual averages TSP (21.9 $\mu g/m^3$) and PM_{10} (18.8 $\mu g/m^3$) mass concentrations were observed at the SOLA site and the highest annual average $PM_{2.5}$ mass concentration (9.0 $\mu g/m^3$) was observed at the SW site. The lowest TSP, PM_{10}, and $PM_{2.5}$ mass concentration were 6.2, 6.0, and 3.6 $\mu g/m^3$, respectively, observed at the TB site. Similar annual averages of OC, EC, ammonium, and sulfate in TSP, PM_{10}, and $PM_{2.5}$ were observed, suggesting that these species are present mainly in the $PM_{2.5}$ fraction. PM_{10} mass comprised 80-90% of TSP mass and was approximately twice that of $PM_{2.5}$ mass. The most abundant chemical species were OC (16.5-29.8%), silicon (10.8-16.0%), and aluminum (3.9-4.7%) for TSP; OC (16.2-27.8%), silicon (10.0-21.1%), and aluminum (3.5-6.6%) for PM_{10}; and OC (42.1-52.0%), EC (4.9-16.4%), and ammonium (3.1-5.8%) for $PM_{2.5}$.

The lowest TWS TSP, PM_{10}, and $PM_{2.5}$ mass concentrations were observed from March to April 2003 at all five sites. TWS TSP, PM_{10}, and $PM_{2.5}$ mass concentrations observed at the BH, LF, and TB sites from May to October 2003 were twice as high as those observed from November 2002 to February 2003; however, TWS TSP, PM_{10}, and $PM_{2.5}$ mass concentrations were comparable during these two periods at the SW and SOLA sites. The elevated TWS TSP, PM_{10}, and $PM_{2.5}$ mass concentrations at the SW and SOLA sites from November 2002 to February 2003 were due to elevated OC and EC concentrations, which were likely the result of increased traffic, sanding, and wood-burning associated with winter activities in the Lake Tahoe region.

The annual average mass concentrations and chemical species were the highest in TSP and the lowest in $PM_{2.5}$ at each site; however, such physical consistency was not necessarily observed for TWS samples during the same sampling period. For example, PM_{10} mass concentration exceeding TSP was occasionally observed. Such sampling bias can be attributed to the low TWS sampling flow rate of 1.3 liters per minute (LPM), low mass concentration of ambient particulate matter, long sampling duration, and sampling artifacts of semi-volatile species.

The annual average PM_{10} mass concentration comprised more than 80% of the TSP mass concentration. Bounces and penetration of particles larger than 10 μm through the impactor can increase the PM_{10} mass concentration. Particle bounce and penetration efficiency depends on the characteristics of the 50% cutpoint curve and material of impaction substrate. Particle bounce is more pronounced as the sampling time (i.e., particle loading on impaction substrate) increases (Chang, et al, 1999, Tsai, et al, 1995), as well as at low particle concentrations.

The sampling artifacts of semi-volatile species on sampling media can either introduce positive or negative sampling artifacts. The sampling artifacts of semivolatile species depend on ambient sampling temperature, RH, the species' disassociation constant, the ratio of species in particulate and gas phases, and the pressure drop through the sampling media. The positive intercepts in the scatter plots of reconstructed mass, based on chemical species and measured mass, suggest a positive sampling artifact of semi-volatile species, including some OC and ammonium nitrate. Although negative sampling artifacts of nitrate losses can be quantified through the backup filter, it is not clear how adsorption of OC onto the quartz filters impacts the positive sampling artifacts during analysis. As OC is the most abundant species in TWS TSP, PM_{10}, and $PM_{2.5}$, a denuder for volatile organic species and a backup filter should be used in future studies to better assess PM mass and chemical concentrations.

If possible, a higher flow rate for TWS samplers is suggested for future study. The low flow rate of 1.3 LPM used for the TWS can potentially result in significant aerosol measurement uncertainties in LTADS. The impact of a low flow rate can be observed when comparing the sulfate and sulfur slope in TWS $PM_{2.5}$ samples and the phosphate quantified by ion chromatography. The slope comparing sulfate and sulfur concentrations and the average ratios of those in TWS $PM_{2.5}$ samples are less than 3 with medium to low correlation and high standard deviation of the average ratios. The stability of low flow rate is especially critical to reduce the difference in aerosol samples between each set of TWS samplers (quartz-fiber and Teflon-membrane filters). In addition, the random penetration of particles above the cutpoint of the sampling inlet can be significant, if total aerosol loading on filter is low, depending on the distributions of particle mass concentration in the ambient air. Nevertheless, phosphate, one of the most important compounds affecting the clarity of Lake Tahoe, was found to be above the

measurement uncertainty in only two of the 128 TWS $PM_{2.5}$ samples. A higher flow rate in the aerosol samplers is desired if particulate phosphate is to be quantified. Phosphorous quantification on the Teflon-membrane filters by x-ray fluorescence proved problematic due to the energy of the relatively small phosphorous peak falling directly between large silicon and sulfur peaks.

MiniVol samplers were deployed at the satellite sites in LTADS to compliment the TWS samplers. Due to variations in sampling duration for non-buoy MiniVol samplers, it is difficult to characterize horizontal PM variations in conditions or episodic events on the Lake. Consistent MiniVol sampling durations among sites, as well as immediate sample collection (less than 12 hours) after sampling are suggested for future studies to minimize aerosol measurement uncertainties.

6. REFERENCES

Bevington, P.R., (1969). *Data Reduction and Error Analysis for the Physical Sciences*. McGraw Hill, New York, NY.

California Environmental Protection Agency (2005). Air Resources Board Staff Report: Lake Tahoe Atmospheric Deposition Study. Interim Report.

Chang, M.C., Kim, S and Sioutas, C., (1999). "Experimental Studies on particle impaction and bounce; effects of substrate design and material." *Atmospheric Environment*, **15**: 2313-2323.

Chang, M.-C.; Sioutas, C.; Kim, S.; Gong, H. Jr.; and Linn, W.S., (2000). Reduction of nitrate losses from filter and impactor samplers by means of concentration enrichment. *Atmos. Environ.* **34**, 85-98.

Chow, J.C. and Watson, J.G., (1989). Summary of particulate data bases for receptor modeling in the United States. In *Transactions, Receptor Models in Air Resources Management*, Watson, J.G., editor. Air & Waste Management Association, Pittsburgh, PA, pp. 108-133.

Chow, J.C. and Watson, J.G., (1994). Guidelines for PM_{10} sampling and analysis applicable to receptor modeling. Report No. EPA-452/R-94-009. Prepared for U.S. EPA, Office of Air Quality Planning and Standards, Research Triangle Park, NC, by Desert Research Institute, Reno, NV.

Chow, J.C. and Watson, J.G., (1999). Ion chromatography in elemental analysis of airborne particles. In *Elemental Analysis of Airborne Particles, Vol. 1*, Landsberger, S., Creatchman, M., editors. Gordon and Breach Science, Amsterdam, pp. 97-137.

Chow, J.C.; Watson, J.G.; Pritchett, L.C.; Pierson, W.R.; Frazier, C.A.; and Purcell, R.G., (1993). The DRI Thermal/Optical Reflectance carbon analysis system: Description, evaluation and applications in U.S. air quality studies. *Atmospheric Environment* **27A** (8), 1185-1201.

Chow, J.C.; Watson, J.G.; Fujita, E.M.; Lu, Z.; Lawson, D.R.; and Ashbaugh, L.L., (1994). Temporal and spatial variations of $PM_{2.5}$ and PM_{10} aerosol in the Southern California Air Quality Study. *Atmospheric Environment* **28** (12), 2061-2080.

Chow, J.C. Watson, J.G., and Wiener, R.W., (2005) Method No. 508: $PM_{2.5}$ sampling and gravimetric analysis by Federal Reference Method. In *Methods of Air Sampling and Analysis*, Lodge, J.P. Editor. Air and Waste Management Association, Pittsburgh, PA. In preparation

Eatough, D.J.; Aghdaie, N.; Cottam, M.; Gammon, T.; Hansen, L.D.; Lewis, E.A.; and Farber, R.J. (1990) Loss of semi-volatile organic compounds from particles during sampling on filters. In *Transactions, Visibility and Fine Particles*, Mathai, C.V., editor. Air & Waste Management Association, Pittsburgh, PA., pp. 1465-156.

Hidy, G.M., (1985). Jekyll Island meeting report: George Hidy reports on the acquisition of reliable atmospheric data. *Environmental Science & Technology* **19** (11), 1032-1033.

Lioy, P.J.; Mallon, R.P.; and Kneip, T.J., (1980). Long-term trends in total suspended particulates, vanadium, manganese, and lead at near street level and elevated sites in New York City. *Journal of the Air Pollution Control Association* **30** (2), 153-156.

McDow, S.R. and Huntzicker, J.J. (1990). Vapor adsorption artifact in the sampling of organic aerosol: Face velocity effects. *Atmospheric Environment* **24A** (10), 2563-2571.

Pathak, R.K.; Yao, Z.; and Chak, K.C., (2004). Sampling artifacts of acidity and ionic species in $PM_{2.5}$ *Environ. Sci. Technol.* **38**, 254-259.

Stelson, A.W. and Seinfeld, J.H., (1982). Relative humidity and temperature dependence of the ammonium nitrate dissociation constant, *Atmos. Environ.* **16**:983-992.

Tsai, C.J. and Chen, Y.H., (1995). Solid particle collection characteristics on impaction surface of different design. *Aerosol Sci. Technol.* **23**: 96-106

Turpin, B.J.; Huntziker, J.J.; and Hering, S.V., (1994). Investigation of organic aerosol sampling artifacts in the Los Angeles Basin. *Atmospheric Environment* **28(**19), 3061-3071.

Watson, J.G. and Chow, J.C., (1992). Data bases for PM_{10} and $PM_{2.5}$ chemical compositions and source profiles. In *Transactions, PM_{10} Standards and Nontraditional Particulate Source Controls*, Chow, J.C. and Ono, D.M., editors. Air & Waste Management Association, Pittsburgh, PA, pp. 61-91.

Watson, J.G. and Chow, J.C. (2002). A wintertime $PM_{2.5}$ episode at the Fresno, CA, supersite. *Atmos. Environ.* 36(3):465-475.

Watson, J.G.; Lioy, P.J.; and Mueller, P.K., (1989). The measurement process: Precision, accuracy, and validity. In *Air Sampling Instruments for Evaluation of Atmospheric Contaminants, Seventh Edition*, Hering, S.V., editor. American Conference of Governmental Industrial Hygienists, Cincinnati, OH, pp. 51-57.

Watson, J.G.; Lioy, P.J.; and Mueller, P.K., (1995). The measurement process: Precision, accuracy, and validity. In *Air Sampling Instruments for Evaluation of Atmospheric Contaminants*, Cohen, B.S. and Hering, S.V., editors. American Conference of Governmental Industrial Hygienists, Cincinnati, OH, pp. 187-194.

Watson, J.G.; Chow, J.C.; and Frazier, C.A., (1999). X-ray fluorescence analysis of ambient air samples. In *Elemental Analysis of Airborne Particles, Vol. 1*, Landsberger, S. and Creatchman, M., editors. Gordon and Breach Science, Amsterdam, pp. 67-96.

Watson, J.G.; Turpin, B.J.; and Chow, J.C., (2001). The measurement process: Precision, accuracy, and validity. In *Air Sampling Instruments for Evaluation of Atmospheric Contaminants, Ninth Edition*, Cohen, B.S. and McCammon, C.S., Jr., editors. American Conference of Governmental Industrial Hygienists, Cincinnati, OH, pp. 201-216.

Zhang, X. and McMurry, P.H., (1987). Theoretical analysis of evaporative losses from impactor and filter deposits. *Atmos. Environ.* **21**: 1779-1789.

Zhang, X. and McMurry, P.H., (1992). Evaporation losses of fine particulate nitrates during sampling. *Atmos. Environ.* **26A**: 3305-3312.